

Northumbria Research Link

Citation: Asfahan, Hafiz M., Sultan, Muhammad, Miyazaki, Takahiko, Saha, Bidyut B., Askalany, Ahmed A., Shahzad, Muhammad Wakil and Worek, William (2022) Recent development in adsorption desalination: A state of the art review. Applied Energy, 328. p. 120101. ISSN 0306-2619

Published by: Elsevier

URL: <https://doi.org/10.1016/j.apenergy.2022.120101>
<<https://doi.org/10.1016/j.apenergy.2022.120101>>

This version was downloaded from Northumbria Research Link:
<https://nrl.northumbria.ac.uk/id/eprint/51068/>

Northumbria University has developed Northumbria Research Link (NRL) to enable users to access the University's research output. Copyright © and moral rights for items on NRL are retained by the individual author(s) and/or other copyright owners. Single copies of full items can be reproduced, displayed or performed, and given to third parties in any format or medium for personal research or study, educational, or not-for-profit purposes without prior permission or charge, provided the authors, title and full bibliographic details are given, as well as a hyperlink and/or URL to the original metadata page. The content must not be changed in any way. Full items must not be sold commercially in any format or medium without formal permission of the copyright holder. The full policy is available online: <http://nrl.northumbria.ac.uk/policies.html>

This document may differ from the final, published version of the research and has been made available online in accordance with publisher policies. To read and/or cite from the published version of the research, please visit the publisher's website (a subscription may be required.)

Recent development in adsorption desalination: A state of the art review

Hafiz M. Asfahan ^{a,†}, Muhammad Sultan ^{a,†,*}, Takahiko Miyazaki ^{b,c}, Bidyut B. Saha ^{c,d},
Ahmed A. Askalany ^e, Muhammad W. Shahzad ^f, William Worek ^g

^a Department of Agricultural Engineering, Bahauddin Zakariya University,
Multan 60800, Pakistan

^b Department of Advanced Environmental Science and Engineering, Faculty of
Engineering Sciences, Kyushu University, Fukuoka 816-8580, Japan

^c International Institute for Carbon-Neutral Energy Research (WPI-I2CNER),
Kyushu University, 744 Motoooka, Nishi-ku, Fukuoka 819-0395, Japan

^d Mechanical Engineering Science, Kyushu University, 744 Motoooka, Nishi-ku,
Fukuoka-shi, Fukuoka 819-0395, Japan

^e Mechanical Engineering, Faculty of Technology and Education, Sohag
University, Sohag 82524, Egypt

^f Department of Mechanical and Construction Engineering, Northumbria
University, Newcastle Upon Tyne, NE1 8ST, United Kingdom

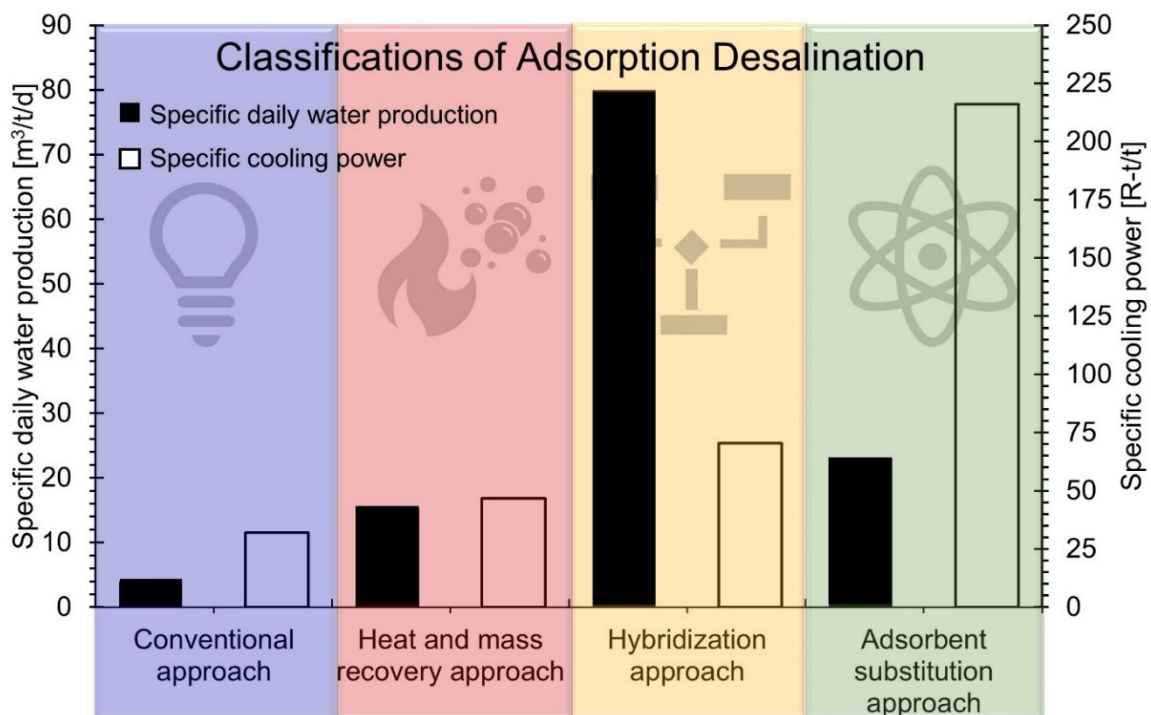
^g Department of Mechanical and Industrial Engineering, Texas A&M University,
Kingsville, TX, 78363, USA

† These authors contributed equally to this work.

* Emails: muhammadsultan@bzu.edu.pk ; sultan@kyudai.jp

Tel: +92-333-610-8888 ; Fax: +92-61-9210298

Graphical abstract



Abstract

Adsorption desalination is prescribed as a promising and eco-friendly solution for mitigating water scarcity, owing to its utilization of low-grade thermal waste and zero liquid brine discharge. The keystones that regulate the performance of the adsorption desalination system (ADS) include nature of adsorbents, system design, and operating conditions. The present study aims to provide a state of the art review on the keystones of ADS. Metal-organic frameworks (MOFs) hold remarkable adsorption capacity and tunable structure. However, hydrothermal instability, high cost, and complex synthesizing procedures are the potential challenges that need to be addressed. The technological advancements in ADS have been classified into: (i) Conventional Approach, (ii) Heat and Mass Recovery Approaches, (iii) Hybridization Approaches, (iv) and Adsorbent Substituting Approach. The study provides critical insight and compares the performance of each approach based on specific daily water production (SDWP), specific cooling power (SCP), and coefficient of performance (COP). The conventional ADS produce SDWP of 4.7 m³/ton/d, however with minimal SCP using payable energy of 1.50 kWh/m³. In heat/mass recovery approaches, pressure equalization-valve delay schemes and master-slave configuration provide ~5% additional water adsorption/desorption on/from silica-gel and reduce ~50% thermal heating load, respectively. Evaporator-condenser amalgamation emphasizes the evaporator temperature of 30-42°C leading towards ~69% higher SDWP with zero SCP. Dual stage, multi evaporators/condensers scheme is found supportive in cogenerating feature of ADS thereby improvising COP to ~0.87. In hybridization approach, ejector integrated ADS produces SDWP of 80 m³/ton and COP of 2.22 using payable energy of 0.92 kWh/m³, however, needs experimental validation. In the adsorbent substituting approach, CPO-27(Ni), Emim-Ac/Syloid 72FP, and composite adsorbent manifest the SDWP to higher levels. The operating conditions are sensitive and need to optimize depending on the configuration of ADS. Possible future research directions may include efficient designing/sizing of evaporators/condensers, minimizing the heat and mass transfer resistances in adsorber/desorber reactor, optimize the thickness of the adsorbent layer in heat exchangers, and investigating wide range of adsorbent classes that can be driven with very low regeneration temperature.

Keywords: Adsorption desalination systems; adsorbent materials; technological advancements and approaches; operating regimes.

Highlights

- State of the art insights are provided for ADS technological advancement
- Thermophysical properties of adsorbents are comprehensively reviewed
- Modification and classification in ADS are explored for optimum performance
- Key factors affecting the system performance parameters are discussed

Table of Contents

Graphical abstract	1
Abstract	2
Highlights	3
List of abbreviations.....	4
1. Introduction.....	6
2. Principle and features of the AD technology.....	15
3. Adsorbents for ADS/ADCS.....	18
3.1 Conventional adsorbents	19
3.2 Metal-organic frameworks	21
4. Classification of ADS based on progressive modifications	23
4.1 Conventional Approaches	24
4.2 Heat and Mass Recovery Approaches.....	29
4.2.1 Pressure equalization and valve delay schemes	30
4.2.2 Master-Slave configuration	34
4.2.3 Evaporator-Condenser amalgamation via heat recovery loop/ integrated vessel 40	
4.2.4 Dual stage, multi evaporators/ condensers scheme	47
4.3 Hybridization Approaches.....	56
4.3.1 Integration with commercialized desalination systems	57
4.3.2 Integration with non-commercialized desalination technologies	62
4.4 Adsorbents Substituting Approaches	68
5. Factors affecting performance parameters.....	75
6. Market aspects, challenges and future perspectives.....	81
7. Summary.....	84
CRedit authorship contribution statement	86
Acknowledgements.....	86
Declaration of Competing Interest	86
References	86

List of abbreviations

AD	adsorption desalination
Ads	adsorption
ADS	adsorption desalination system
ADS-2EJ	ADS assisted with two ejectors
ADS-2EJ-HRL	ADS assisted with two ejectors embedded with heat recovery loop
ADS-EJ	ADS assisted with single ejector
ADS-EJ-HRL	ADS assisted with single ejector embedded with heat recovery loop
COP	coefficient of performance
Des	desorption
E-C	evaporator-condenser
ES	experimental setup
EPA	environmental protection agency
F&C	findings and conclusions
GOR	gross output ratio
HP	high pressure evaporator
HX	heat exchangers
HRL	heat recovery loop
HRL-ADS	heat recovery loop assisted ADS
IL	installation locality
LP	low pressure evaporator
L-V	liquid vapor
P	pressure
PE	pressure equalization
PR	performance ratio
PV	pictorial view
PY	publication year
Ref	references
SCP	specific cooling power
SDWP	specific daily water production
SG	silica gel
SG	silica gel
SR	schematic representation
T	temperature
t	time

$Th_{ads-cycle}$	thermodynamic adsorption cycle
VD	valve delay
VV	vapor-vapor

Subscripts

a	air
ads	adsorption
amb	ambient
c	cool water
ch	chilled water
cond	condenser
des	desorption
evap	evaporator
h-cycle	half cycle
hw	hot water
in	inlet
int-s	inter stage
out	outlet
pe	pressure equalization
red	reduces
reg	regeneration
sw	switching
vd	valve delay
w	water

1. Introduction

Globally, water and energy are interdependent challenges that progressively threaten the survival of both human beings and animals, owing to the rapid growth of population, industrialization, farm mechanization, intensive use of unsustainable technologies, and overexploitation of natural reserves [1–3]. Water scarcity is a natural realistic phenomenon thus far impacting every continent seasonally; however, human involvement exacerbated its amplification and persistently formulated it into a chronic situation [4]. Fig. 1 shows the worldwide seasonal water scarcity index, reproduce here from the World Resource Institute. According to the 2018 edition of the World Water Development Report (WWDR); currently, 3.6 billion people (47% of the world population) have no access to potable water [5]. This reckons exponentially manifested to 5.7 billion by 2050 [5]. Correspondingly, the anticipated freshwater demand sprouted up to 54 billion cubic meters per year (BCM/y) by 2030 and further heightened to 60 BCM/y by 2050 [4,6–9]. Prominently, developing countries are rigorously confronting the freshwater challenges due to the dwelling of a tangible proportion (3/4th) of the world population [10]. Additionally, the available freshwater resources are shrinking because of unsteady overhead withdrawal patterns. Also, the quality of available clean water reservoirs is incessantly declining due to the unruly dumping of wastewater into freshwater bodies. In consequence, aggravates the clean water demand, especially in Africa followed by Asia [5].

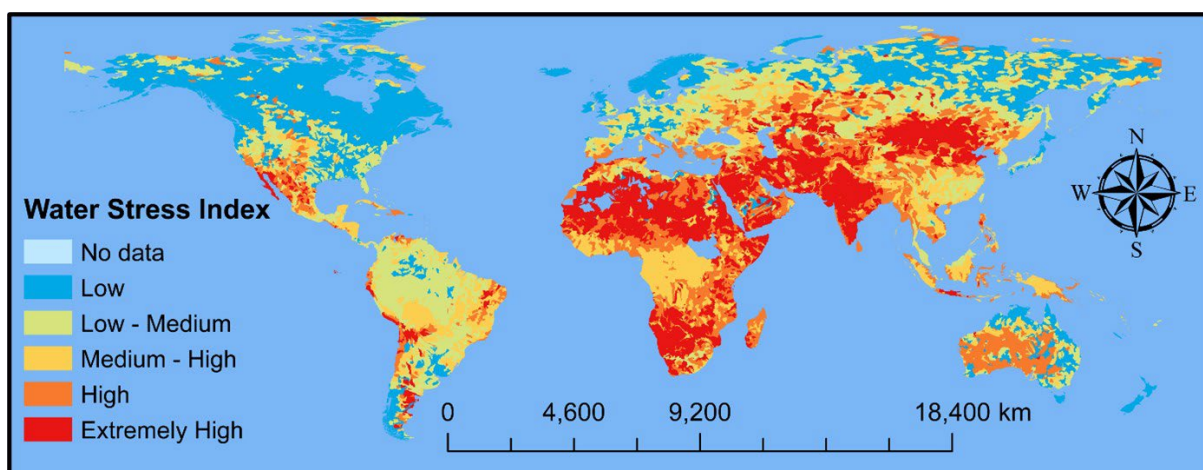


Fig. 1. Water stress index around the globe given by the World Resource Institute, Washington, DC, reproduce from [4,11].

To confront the peaking water demands, desalinization of seawater is prescribed as a remarkable solution and worth adopting, contemplated by researchers. In this regard, various desalination strategies have been patented, documented, and penetrated water markets, aiming

for removing the excessive salts from the amplest quant of seawater [12,13]. Fig. 2 (a), elucidated the spatial distribution of scientific publications, documented on desalination [3]. If consistent with, 2021 International Desalination Association (IDA) statistics, one can know that about 20,000+ desalination plants have been currently installed in 183 different countries, owning gross production capacity of more than 35 billion cubic meters per year (BCM/y) [9,14]. Fig. 2 (b) presents the worldwide geographical distribution of installed desalination localities [15]. This visual presentation reveals that desalination is booming throughout the globe and the nations are solemnly synchronizing the growing water paucity. Additional information which can be extracted from Fig. 2 (b) is that more than half of desalination plants are installed in high-income countries, while low-income countries contribute only 0.1% of the total desalination share due to high capital investments and unsustainable technologies [15].

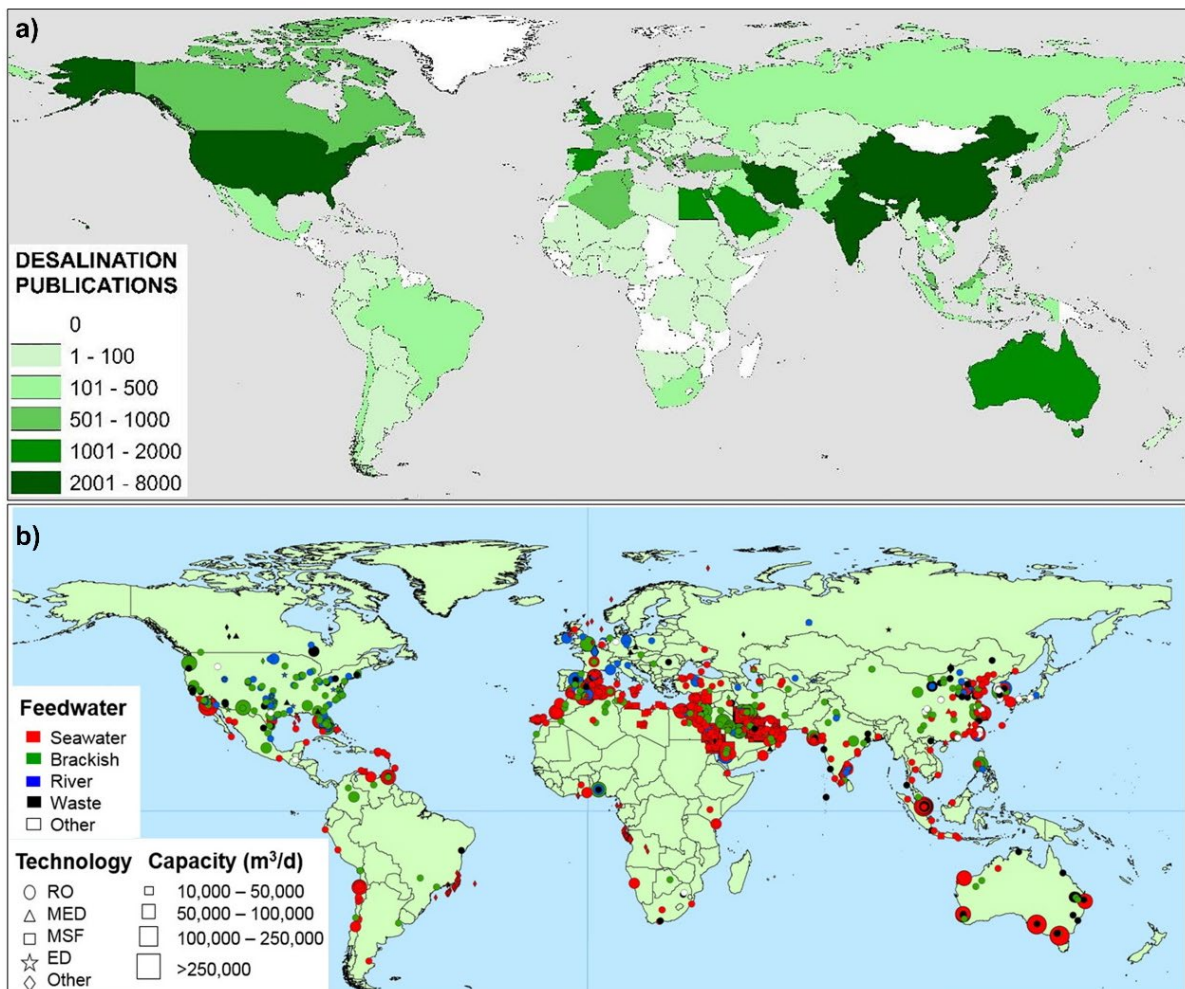


Fig. 2. Worldwide spatial distribution of (a) number of publications on desalination topics from 2000-2020 and (b) installed desalination plants [3,15].

Generally, desalination technologies have been discretized into thermal and non-thermal engineering systems [16]. In thermal systems core concepts like evaporations and condensation are employed, whereas in non-thermal, filtration and crystallization conceptions have been widely investigated [13]. Fig. 3 depicts the classification of thermal and non-thermal desalination systems. As evident from the literature survey it has been identified that, reverse osmosis (RO) [17], multi-stage flash (MSF) [18], and multi-effect desalination (MED) [19] systems retain high market penetration, respectively.

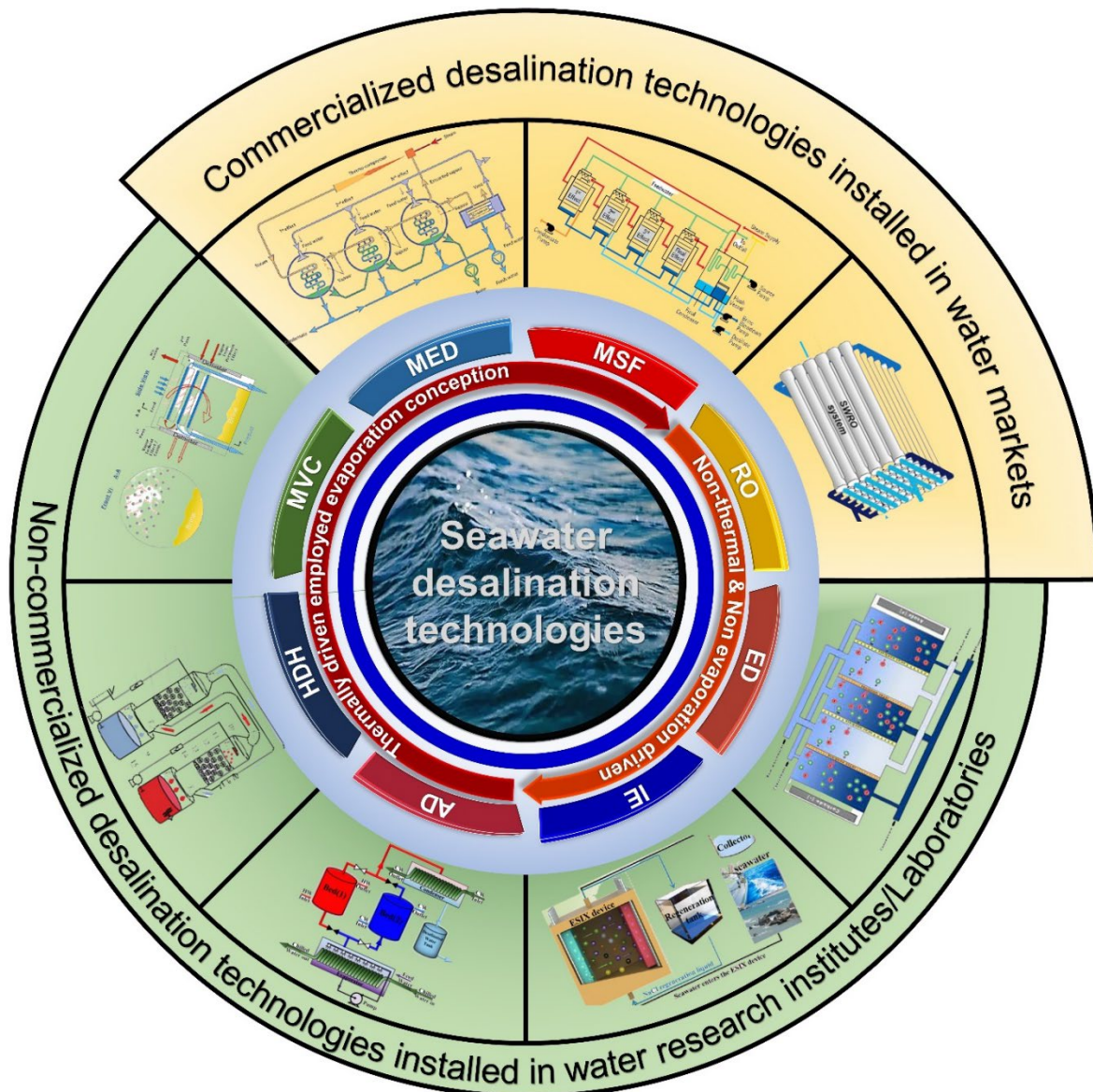


Fig. 3. Classification of desalination technologies: commercialized (abbreviated here as multi-effect (MED), multi-stage flash (MSF), and reverse osmosis (RO)), and emerging (abbreviated here as: mechanical vapor compression (MVC), humidification dehumidification (HDH), adsorption desalination (AD), ion-exchange (IE), and electrodialysis (ED)).

Indeed, desalination quenches the global thirst, and ensures food security and human prosperity. However, hired systems for desalination purposes have some engineering shortcomings which significantly impact the systems' durability and environmental sustainability [20–24]. Fig. 4 illustrates the market status of commercialized desalination technologies associated with engineering shortfalls that need to be surmounted. For instance, commercialized desalination technologies put a huge strain on natural fossil fuel reserves. According to some accounts, nearby, 10 tons of oil is burnt to acquire 1 m³ of desalinated water [25] In addition, due to the high operating temperature of thermally driven systems, corrosion of major components frequently happens which adversely impacts the performance of the system. Similarly, in the case of RO facilities expensive membranes embedded with low cycle stability/ durability and low recovery ratio are some impediments.

On the other hand, contemplating environmental aspects, collectively desalination contributes a massive share of CO₂ and greenhouse gas (GHG) emissions [26]. Insights from UN-WWDR, by the end of 2040, desalination singularly responsible for 0.218 billion tons per year (Bt/y) CO₂ emissions, hence degrading the environmental stability [8,27]. Beyond this, the perilous concentrated brine water received as a by-product from desalination manufactories contiguously mounting the aquatic discrepancies. It has been reported that desalination plants are capable to treat 45-50% of feed water. According to recent statistics, almost 141.5 million cubic meters per year (MCM/y) of brine have been heedlessly dispatched into the aquatic environment [15,28]. Also, the intensive energy consumption for seawater desalination and high cost for unit production, causing economic un-stability or vulnerability especially for developing nations. Although, driving desalination facilities with renewable energy means deemed as worthy footprint towards sustainability. However, high capital investments limit it adaption for low-income countries. In addition, engineering shortcomings in system designing keenly need technological advancements for sustainability point of view defined by UN.

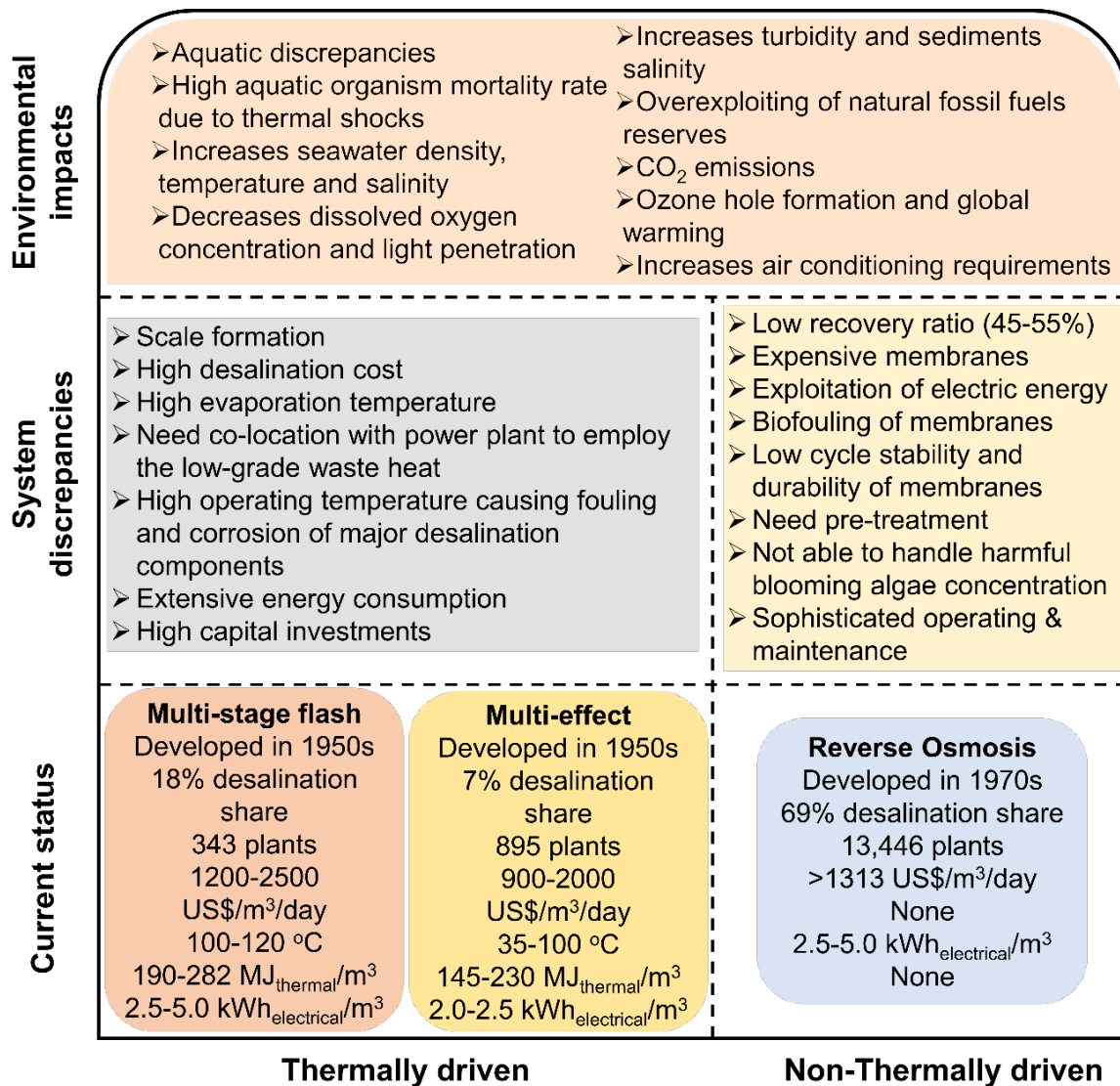


Fig. 4. Current status, system discrepancies and environmental impacts of commercialized desalination technologies. The current status entails the information in sequence as follows: installation year, market share, number of plants installed around the globe, capital investment, operating temperature, thermal energy consumption, and electrical energy consumption.

Emerging desalination technologies are remarkably designed to overcome the engineering shortfalls and for abating the environmental impacts in order to achieve the UN 2030 Sustainable Development Goals (SDGs). In this regard, adsorption desalination (AD), is worthy to mention. The reason is that AD technology possess capability to drive with the low-grade waste heat emitting from industries, steam turbines/engines, and even from automobiles exhaust [29]. Thereby, upscaling its contribution in reduction of fossil fuels dependency, global warming, and additional CO₂ emissions for desalination [30]. In addition, it can be drive or integrate with renewable energy resources such as solar thermal systems, wind energy, natural

gas, biomass etc., thus retrieving the greener globe. On system scale, the technology comprising of no moving parts and perform vacuum evaporation. Consequently, resolving fouling and corrosion issues as exist in the other commercialized desalination technologies. In addition, the technology incorporates low capital investment, entail with low operating and maintenance cost which endorsing its employment. Above all, the cogenerating feature of AD technology, such as producing freshwater along with high-grade cooling, addressing not even the water scarcity problem but also confronting the mounting air conditioning requirements [22,31–33]. In addition, the treated water produce from the AD technology is comparable with the drinking water standards [34]. Extensive research efforts are being endorsed to improve the system productivity. In addition, few review articles were reported to provide a summary of progress reported so far. Table 1 provides the summary of the previous review literatures reported on adsorption desalination system (ADS) including salient features, concluding remarks, and identify the potential review gaps.

Table 1:

Summary of the previous literature reviews on the Adsorption desalination system (ADS).

Title and authors	Year	Salient features	Concluding remarks	Potential review gaps
A state of the art of hybrid adsorption desalination–cooling systems Alsaman et al.[16]	2016	<ul style="list-style-type: none"> • Reviewing the pros and cons of the ADS entail with its co-generating feature • Include experimental and numerical studies • Thermodynamic perspectives 	<ul style="list-style-type: none"> • ADS has a promising future ahead; however, more efforts are required to improve the system productivity 	<ul style="list-style-type: none"> • Summarizing historical research studies from 2004 to 2015
Metal-organic frameworks in cooling and water desalination: Synthesis and application Mohammed et al. [32]	2021	<ul style="list-style-type: none"> • Reviewing the synthesizing aspects/procedures of the metal-organic frameworks (MOFs) • Provide insights on adsorption characteristics of MOFs • Experimental systems that integrate MOFs 	<ul style="list-style-type: none"> • Adsorption properties of a large number of MOF are not explored so, far. Therefore, a massive avenue of research and development is still present prior developed a commercialized cost-effective ADS 	<ul style="list-style-type: none"> • Historical modification and technological advancement in ADS are not explored • Optimum operating regime to drive an ADS are not identified
A review of recent advances in adsorption desalination technologies Riaz et al. [29]	2021	<ul style="list-style-type: none"> • Conduct a comprehensive review on ADS focusing on integrational schemes • Economic aspects of ADS are highlighted 	<ul style="list-style-type: none"> • Solar driven ADS and multi-effect (ME) integrated ADS could be promising configurations • The ADS capable to manage high salinity with payable cost of US\$0.2/m³ 	<ul style="list-style-type: none"> • Technological advancements and system classification • Optimistic operating regimes are not explored
Review on adsorption materials and system configurations of the	2022	<ul style="list-style-type: none"> • Provide an overview on adsorbents including silica gels, zeolites, and MOFs • Review energy-efficient combination schemes of ADS 	<ul style="list-style-type: none"> • Silica-gels and zeolites developed a cost-effective ADS, however, entails with low production capacity • Few experimental test rigs are developed for the validation of the 	<ul style="list-style-type: none"> • Performance of the ADS corresponding to influential operating conditions are not explored

adsorption desalination applications		with other desalination technologies	ADS performance with numerical results	<ul style="list-style-type: none"> • Optimum operational parameters to drive an ADS
Hua et al. [35]				
Adsorption desalination: Advances in porous adsorbents	2022	<ul style="list-style-type: none"> • Provide a comprehensive review of activated carbons, graphenes, zeolites, carbon nanotubes (CNT), MOFs, and covalent organic frameworks (COFs) from the perspectives of exploring their potential in ADS 	<ul style="list-style-type: none"> • Activated carbons and zeolites are cheaper and safer however, not compatible from the viewpoint of its low adsorption equilibrium • Graphenes and CNT possess high adsorption equilibrium, however, their hazardous concerns need to be addressed before their utilization • MOFs hold high versatility due to their tunable structure, however, lagged with thermophysical instability and expensive • COFs have potential due to its versatility, but their research are in the cradle stages 	<ul style="list-style-type: none"> • Technological advancements and progressive improvement in ADS •

The present study aims to provide insights on technological advancements related to ADS and assesses its readiness level for desalination markets. With these perspectives, a state of art review is presented, covering the adsorbents investigated for ADS. In addition, the modifications reported on the ADS are reviewed and classified accordingly into four main approaches. The approaches include (i) Conventional Approaches, (ii) Heat and Mass Recovery Approaches, (iii) Hybridization Approaches, and (iv) Adsorbents Substituting Approaches. Furthermore, performance of the ADS are explored based on the key performance indicators and analyze their response corresponding to varying operating/rating conditions. The optimum operating regimes for driving the ADS are identified for each approach. Lastly the study provides critical insights and identify the future perspectives in order to develop a sustainable, low-cost and commercialize able ADS. Fig. 5 illustrates the footprint entail with the potential aspects that are discussed in the of the present study.

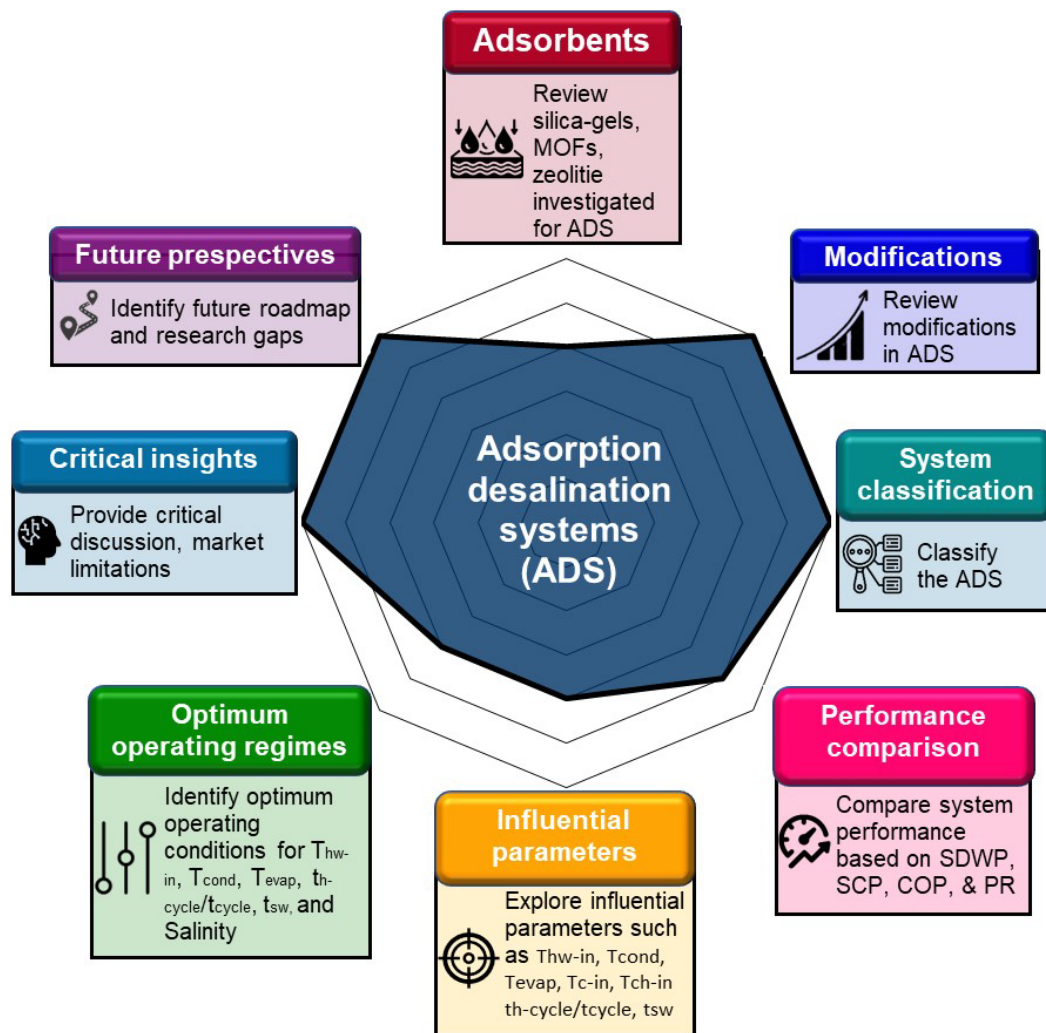


Fig. 5. Potential footprint of the present review paper.

2. Principle and features of the AD technology

The working of the adsorption desalination (AD) technology is similar to the vapor compression cycle except for the mechanical compressor; a thermal compressor has been installed as an alternative to increase the temperature and pressure of the circulating refrigerant [37]. The thermal compressor drive with low-grade waste heat comprising of a reactor/vessel packed with an adsorbent material that has been capable to perform adsorption and desorption processes simultaneously however, by changing the driving conditions (i.e., pressure and temperature) [35]. In AD technology, the thermal compressor equipped with the combination of four thermodynamic processes that has been paired in a manner to follow a cyclic pattern. Fig. 6 describes the thermodynamic processes in sequence for completing a single AD cycle. The adsorbent material possesses high tendency/affinity for the water vapors present in the system. Consequently, the water vapors are attracted and adhere on the surface by developing a van der wall force of attraction. The developed electrostatic forces are weak and are vulnerable to disintegrate when the energy supplied from the external heat source [38–40]. The amount of the water vapors adsorbs on the adsorbent surface depend upon the type of the adsorbent materials and its adsorption capacity [40].

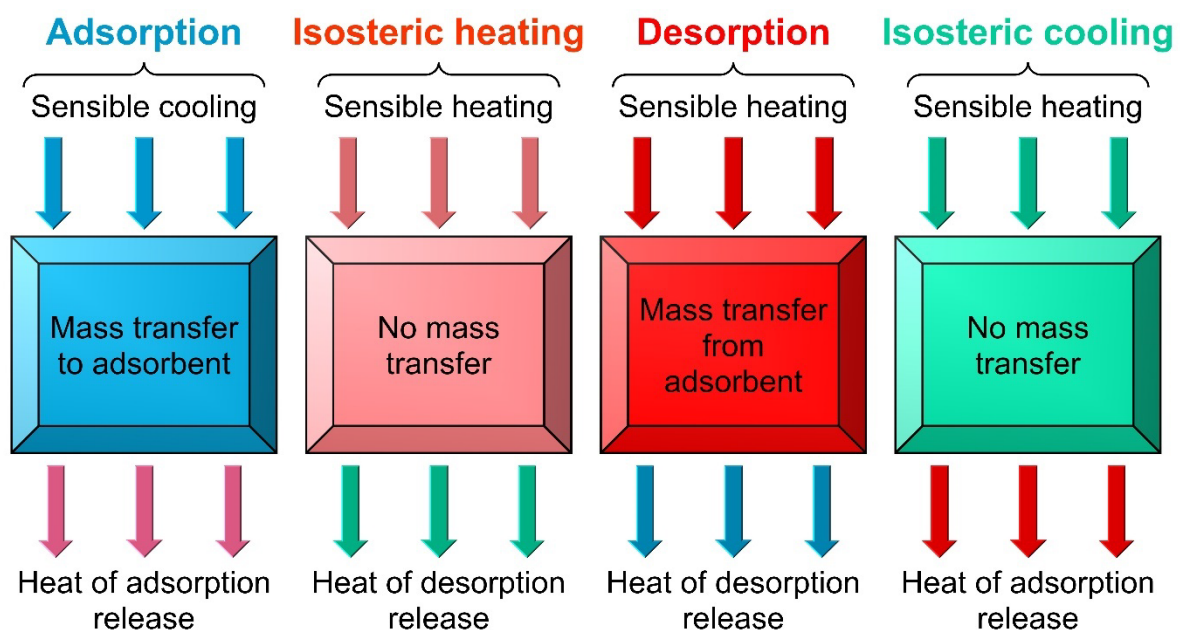


Fig. 6. Thermodynamic processes employed by the thermal compressor to accomplish a single desalination cycle. The blue and red color combinations depict the degree of coldness and hotness of the input/output sensible energy to/from the adsorbent/desorbent beds, respectively.

Fig. 7 (a) illustrate the schematic of 2-bed ADS furnished with additional system accessories such as opening and closing valves, temperature and flow sensors, hot-water and cold-water baths [16]. The 2-bed ADS mainly contains four main chambers/vessels imbedded with heat exchangers (HXs): (i) evaporator for evaporating the saline water, (ii) two adsorbent/desorbent chambers for adsorbing and desorbing the water vapors during their respective cyclic turn, and (iii) condenser for phase transformation (vapors to liquid) [29]. The heat exchangers are employed to maintain the requisite thermal fronts. The ADS initiates the purification process by feeding the untreated seawater into a pre-treatment chamber. Here the seawater filtrated and decrease the concentration of dissolved oxygen. The obtained sweater has been charged into the evaporator via brine feeders at very high pressure. The interconnected vacuum pump creates a suction effect hence significant quant of water vapors are produced at very low temperature ($\leq 35^{\circ}\text{C}$). Due to hydrophilicity of adsorbent material water vapors flash into the adsorption chamber and adsorb on the porous surfaces until the saturation arrives. Initially the adsorption process occurs which triggers the evaporation process occurring in the evaporator. The valve between the evaporator and adsorption bed is open to undergo the adsorption process. Once the bed saturated, the valve between the adsorber bed and evaporator close. Prior to perform the desorption process a switching time is provided to the adsorber bed to isothermally heat it and reaches equivalent to the condenser pressure. Once switching time run out, the desorption process taking place in which the non-payable heat supplied to the bed. During desorption phase the valve between the condenser and desorption bed is open. The water vapors directed to the condenser, where the cool water is circulating in the HX to capture the latent heat of condensation and producing fresh condensate. After desorption process, switching time or isosteric cooling is provided to the desorbent bed to drop the pressure and temperature in order to execute the successive desalination cycle. Fig. 7 (b) presents a typical thermodynamic cycle followed by the AD system. For continuous water production, it is usually suggested to affix at least two adsorbent beds. A typical operating condition of AD system is presented in Table 2. However, these conditions are super sensitive to system throughputs such as specific daily water production (SDWP), coefficient of performance (COP), performance ratio (PR) and specific cooling power (SCP) [36].

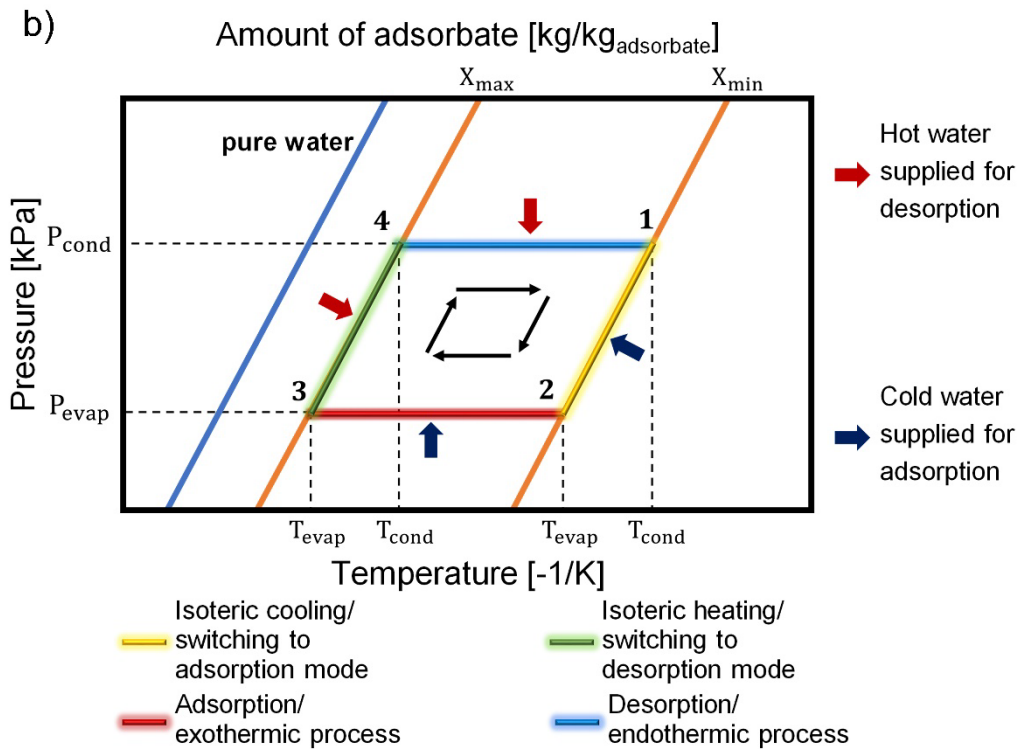
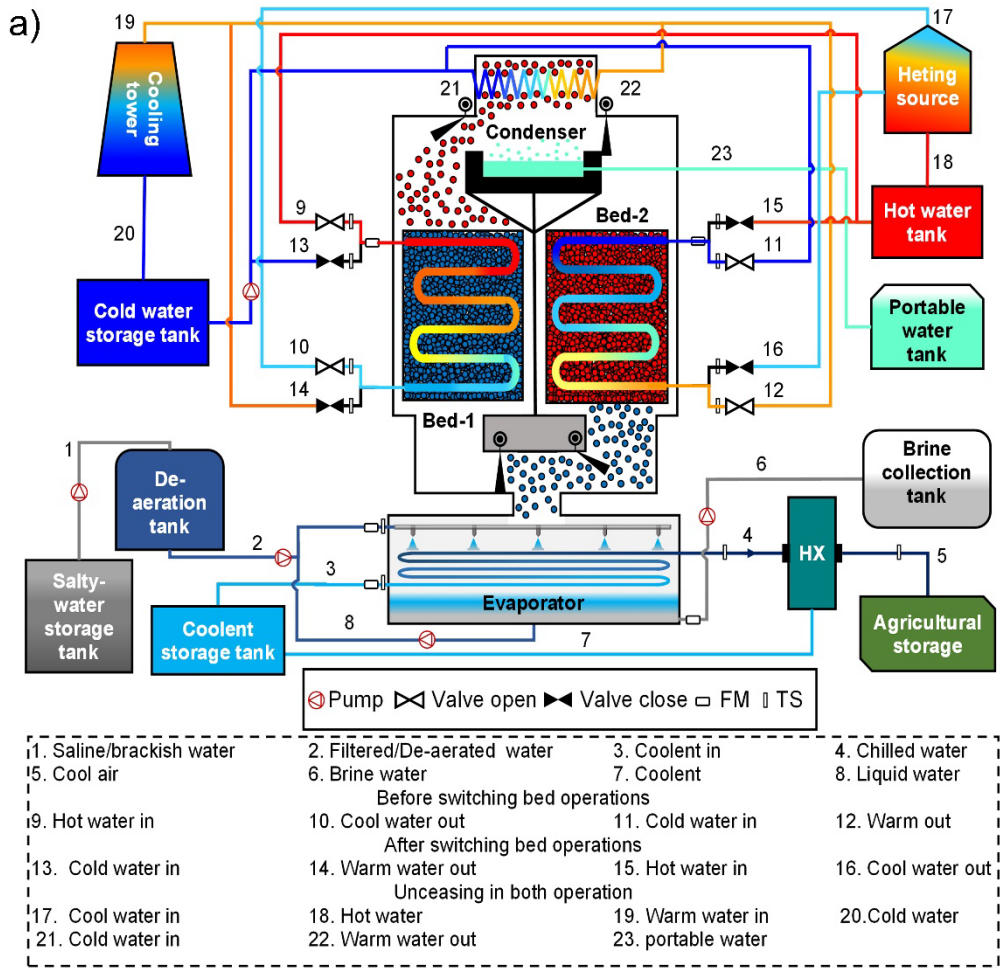


Fig. 7. (a) Schematic of 2-bed AD system, and (b) Dühring diagram (P-T-X) of AD system.

Table 2

Typical operating condition of AD system [41,42].

Parameters	Temperature (°C)	Flow rate (LPM)
Bed-1 hot water inlet	65–85	48
Bed-2 cold water inlet	30.0	48
Condenser cold water inlet	30.0	120
Switching time (s)	20-40	
Spray nozzles pressure (kPa)	175	
Evaporator pressure (kPa)	1.1–2.9	
Chilled water	7–25	
Half cycle time (s)	300–1200	

3. Adsorbents for ADS/ADCS

Prior to deeper dive in technological advancements of AD system, authors, in this section, categorically reviewed sorbents coupled with AD system. Extensive research reveals that sorbents are the most influential constituent of AD system, possessing both hydrophilic and hydrophobic features under controlled thermodynamic parameters (i.e., temperature and pressure) [43]. The porous media or sorbent contains pore spaces in which the adsorbate particles are settled for time being. As the thermodynamic parameters manipulates, porous media dispatched the holding adsorbate particles. The inter/intra particle diffusion kinetics models were used to simulate this process [24,39,44]. Typically, low, and high temperature fronts, respectively generates more hydrophilic and hydrophobic conditions. However, progressive rise in adsorption pressure improves the material sorption capacity, at pre-specified temperature [23,45]. The adsorption isotherms are the graphical depiction of moisture uptake in response of varying adsorption pressure, confined with the information related to material equilibrium uptake and saturation pressure [40]. According to International Union of Pure and Applied Chemistry (IUPAC), the adsorption isotherms followed six moistures up taking responses/ shapes, depending on the thermophysical properties of employed adsorbents. From literature survey the adsorbents are classified in conventional adsorbents and emerging adsorbent i.e., metal organic framework. This section only includes such adsorbents that has been investigated with ADS or ADCS.

3.1 Conventional adsorbents

Silica gel (SG), is an amorphous microporous structured adsorbent, actively used in a variety of adsorption-based applications due to its cost-effectiveness, and ease in local accessibility features [31]. It has a surface area ranging from 586 m²/g (NS-10 type) to about 863.6 m²/g (A⁺⁺ SG) whereas, the pore size lies between 0.28 (A type)–0.489 (A⁺⁺ type) nm. Fig. 8 uniquely showcased the thermophysical properties and adsorption isotherms of SG class adsorbents. According to IUPAC classification, SGs typically followed the type-I and type-II adsorption isotherms. Therefore, it was found suitable in such applications where the sorption occurring at relatively low pressures [33,46].

Zeolites are naturally occurring adsorbents containing microporous crystalline structure [46–48]. However, they can be synthesized on industrial scale for wider application. Typically, zeolites are classified into aluminophosphate (AQSOA-Z series) and ferroaluminophosphate (FAM-Z series) [49]. Considering, pore size distribution AQSOA-Z01/Z05 and FAM-Z01/Z05 belongs to AFI type whereas AQSOA-Z02 and FAM-Z02 are the CHA type zeolites [50–52]. Fig. 9 showcased the thermophysical properties and adsorption uptake with SEM images. The AFI zeotype followed S-shaped whereas, CHA zeotype depicts type-I adsorption isotherm according IUPAC standards.

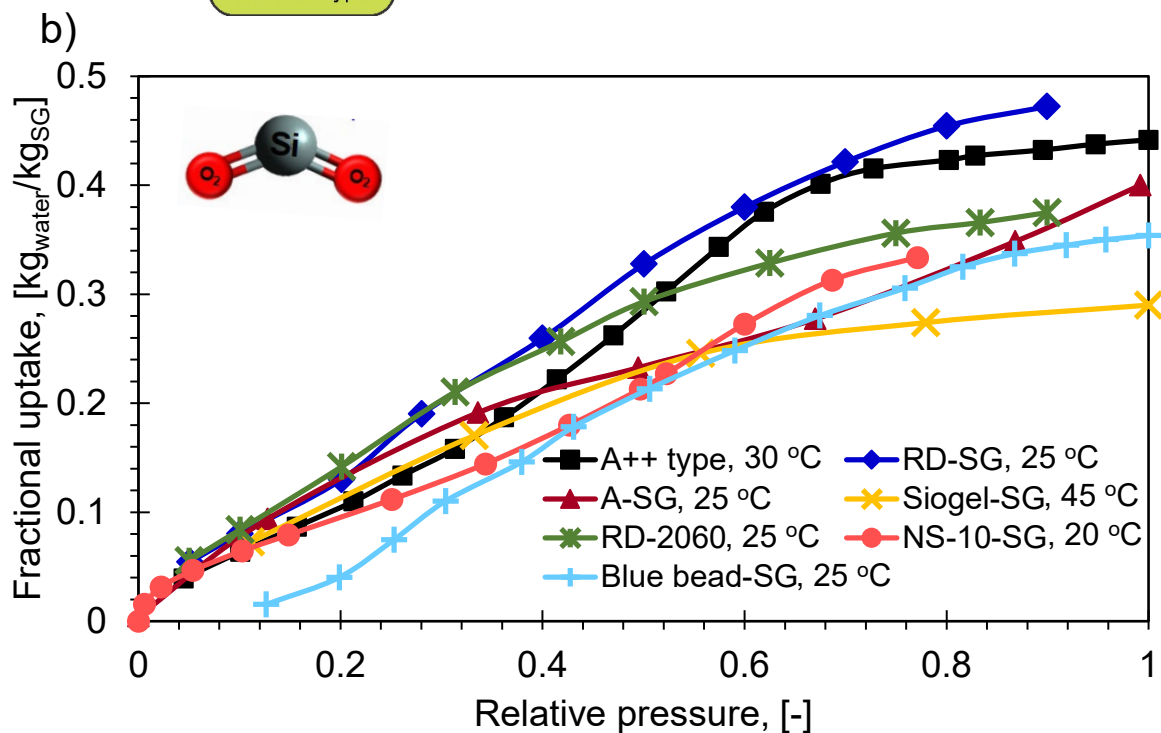
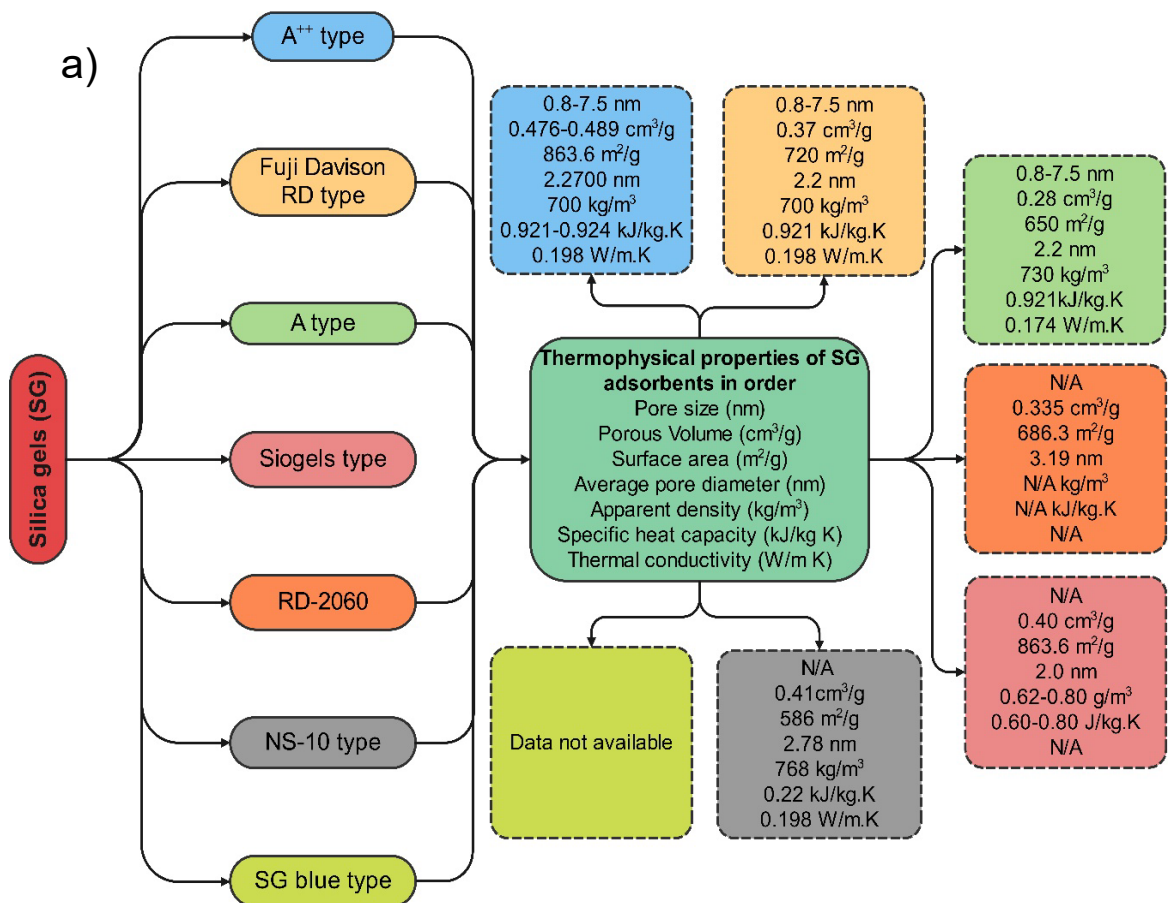
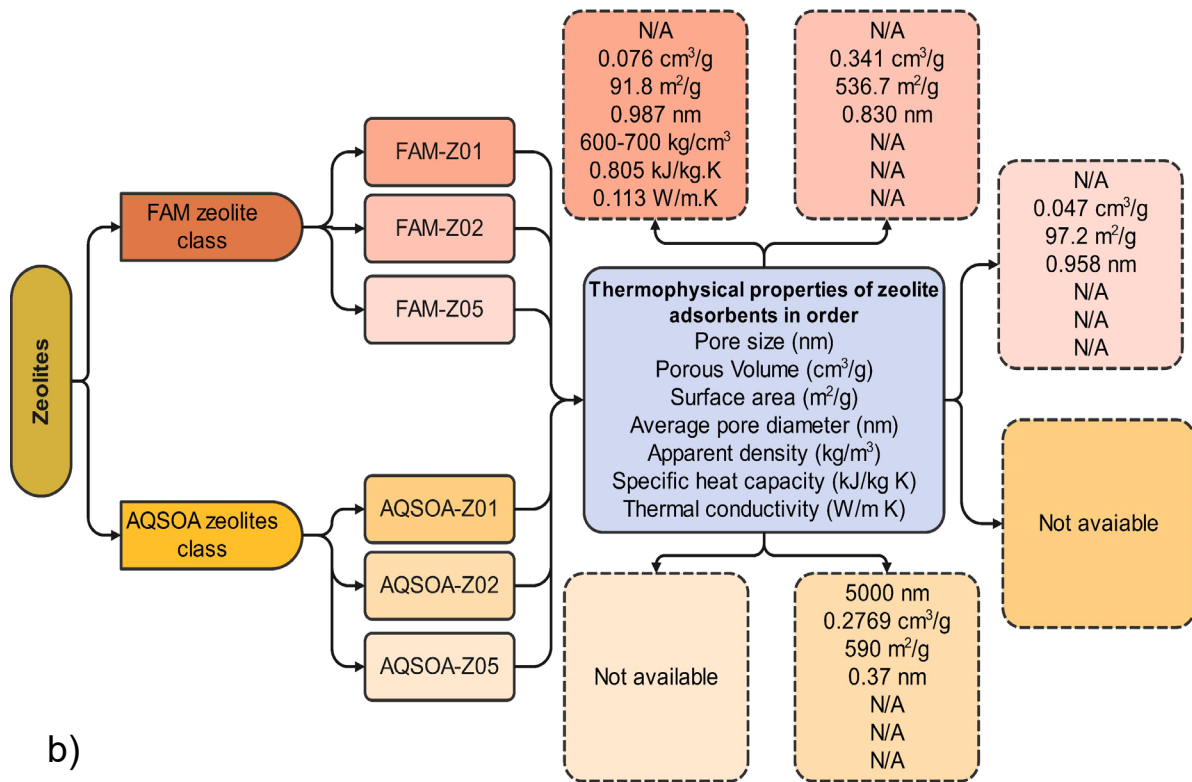


Fig. 8. (a) Thermophysical properties of conventional adsorbents, and (b) adsorption isotherms of SG. The SG has been classified into A⁺⁺ type [42], Fuji Davison RD [53–56] [41,54–62], A type [55,63], siogels [64,65], RD-2060 [66,67], NS-10 [68], Blue type [69].



b)

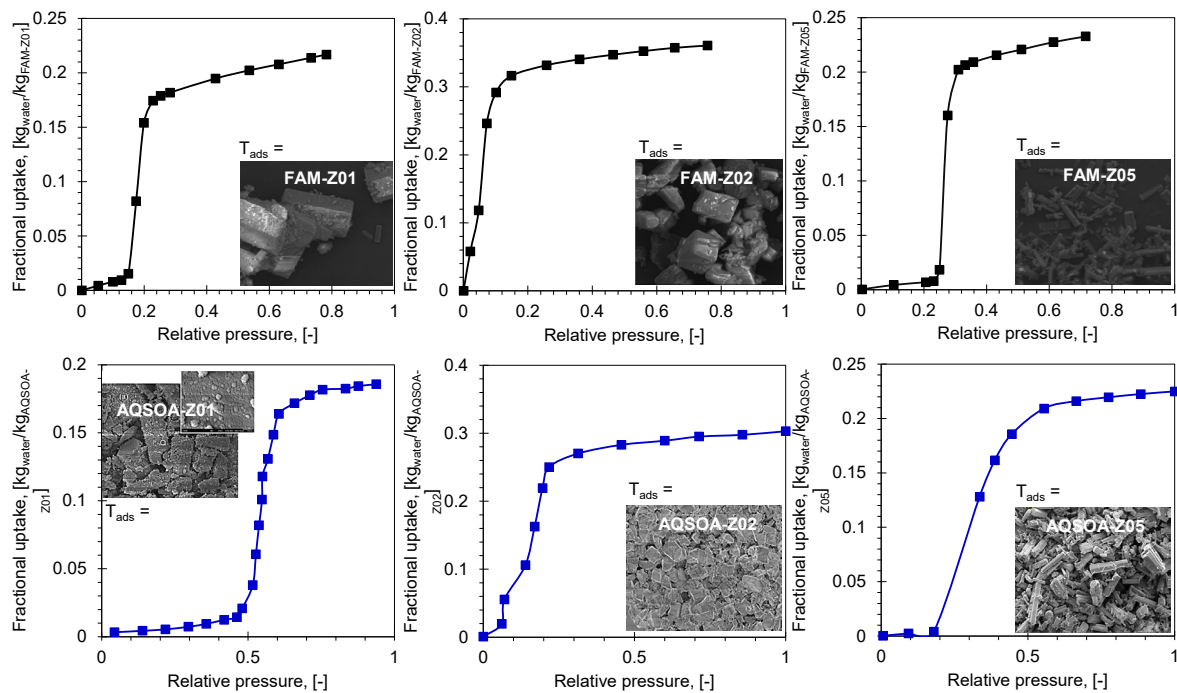


Fig. 9. (a) Thermophysical properties of advance adsorbents and (b) adsorption isotherms of AFI and CHA zeotypes, reproduced from [51,70,71].

3.2 Metal-organic frameworks

Metal-organic frameworks (MOF) are new class of micro and nano-porous group of adsorbents with tunable adsorption properties. The MOF are hybrid adsorbents in which organic linker connect with inorganic metal ion by coordination, metal ions provide more

stability to crystals and enhance their hydrophilic character. Metal nodes in MOFs contribute to increase flexibility, side spaces and provide many ways to synthesis many adsorbents with same organic linker. According to Cambridge database [72], nearly 12,000 MOF structures have been synthesized which are using 102 organic linkers with different metal nodes. Fig. 10 showcased the SEM images, crystal structure and thermophysical properties of MOFs adsorbent used in ADS/ADCS. Similarly, Fig. 11 presents their adsorption isotherms.

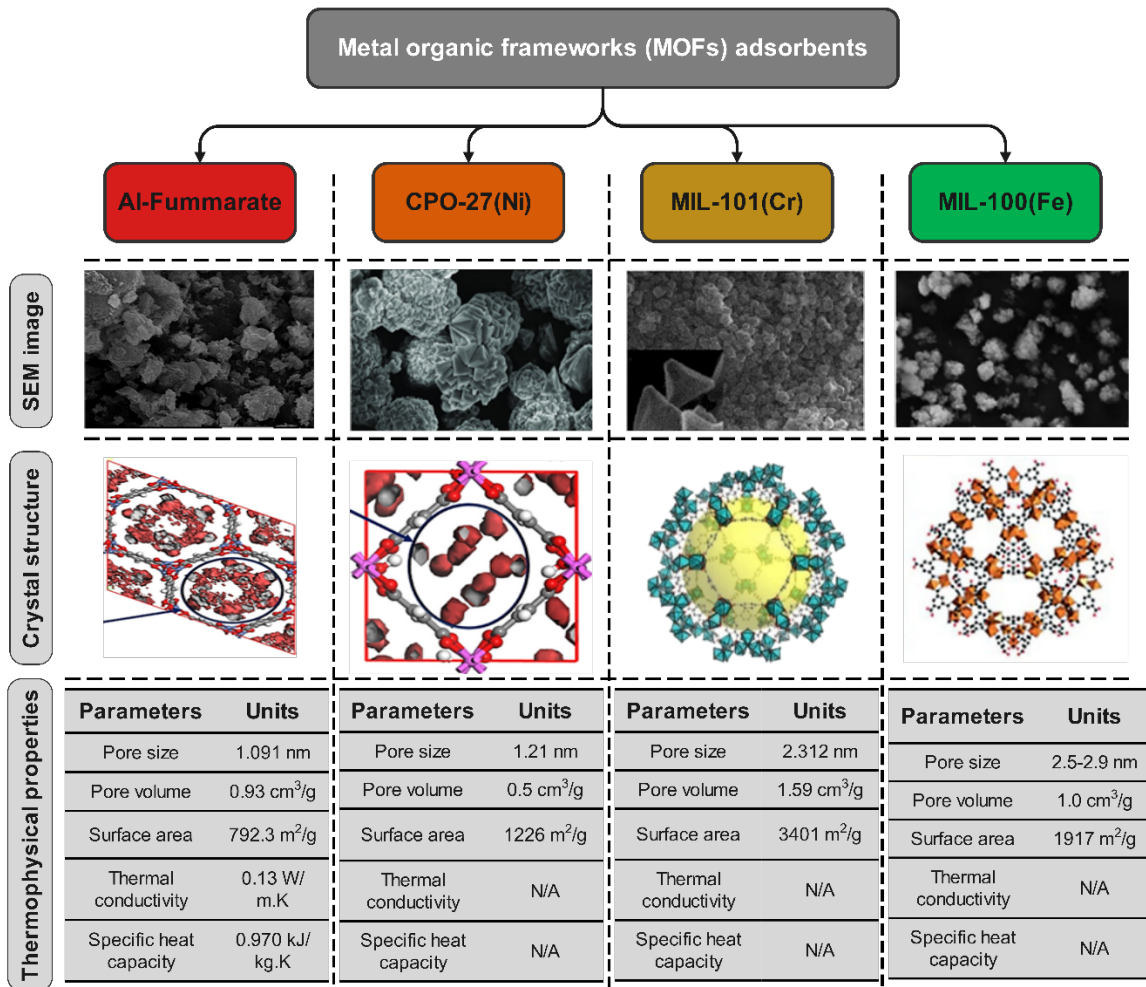


Fig. 10. Thermophysical properties of MOFs adsorbents used in ADS/ADCS. The source of the data are as follows: (i) Al-Fummarate: SEM [10] and crystal structure [73], (ii) CPO-27(Ni): SEM [74] and crystal structure [73], (iii) MIL-101(Cr): SEM [75] and crystal structure [76], and (iv) MIL-100(Fe): SEM image [77] and crystal structure [78].

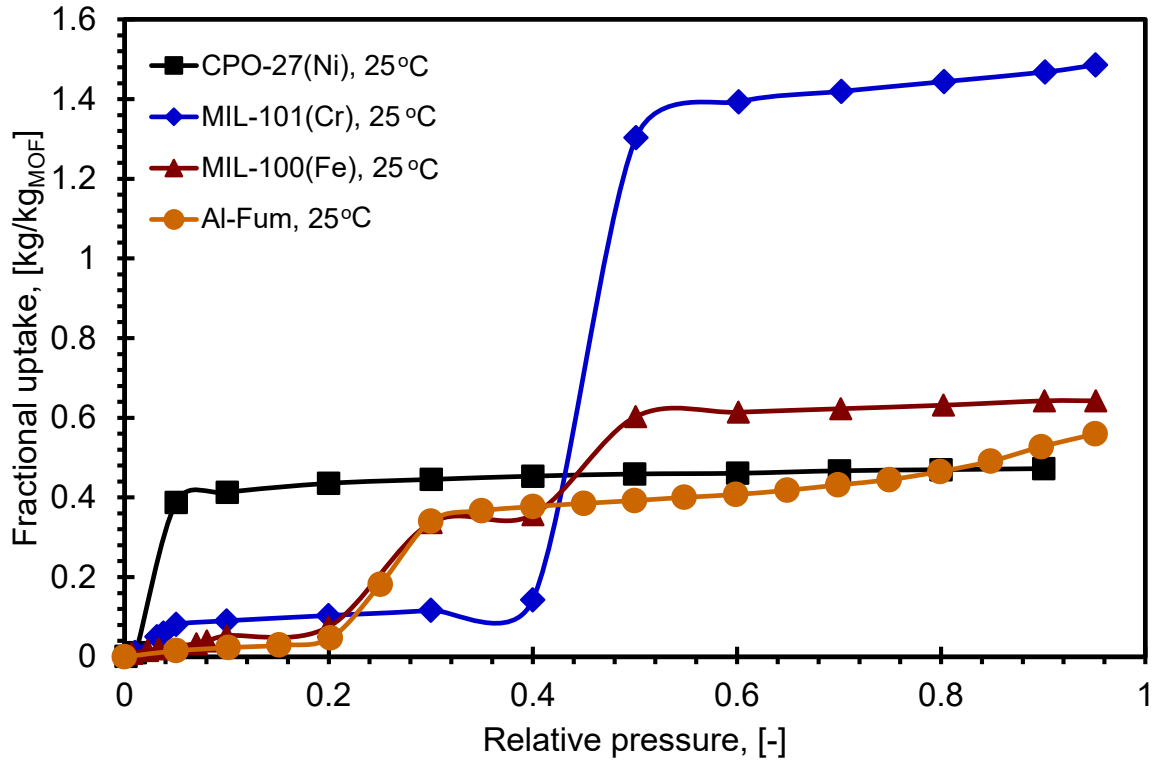


Fig. 11. Adsorption isotherms of MOFs adsorbents, reproduced from [79–81].

4. Classification of ADS based on progressive modifications

The low-grade waste-heat-driven adsorption desalination system (ADS) are receiving much attention in the beginning of 21st century due to its eco-friendly attributes. Despite of their appealing benefits, few downsides were also confronted which need to be surmount. For instance, the productivity and performance efficiency (i.e., SDWP, SCP and COP) of ADS are minimal as compared to commercialized desalination facilities. In order to improvise the co-generating feature of ADS, substantial efforts were endorsed. By tracking the footprints, the progressive advancements/modification of ADS segregates into four main approaches: (i) convectional approach, (ii) heat and mass recovery approach, (iii) hybridization approach and (iv) material substitution approach. Fig. 12 showcase the configurational domains in which ADS has been classified. In upcoming sections detailed insights has been provided uniquely in order to achieve the study objectives.

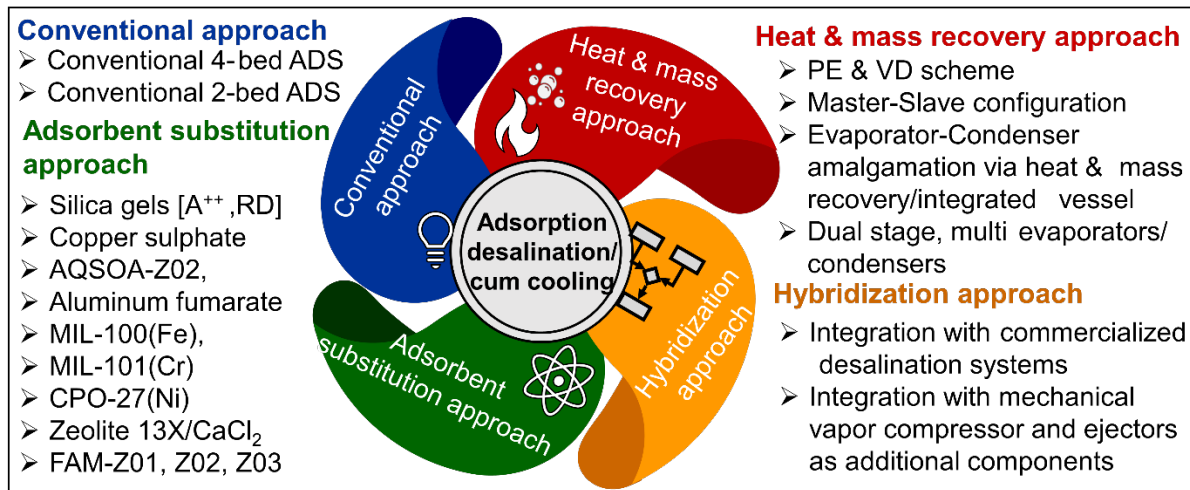


Fig. 12. A specialized illustration representing the configurational approaches in ADS/ADCS.

4.1 Conventional Approaches

The AD Conventional Approach refers to a standalone prototype of silica-gel-based ADS comprising of single stage, 2-bed, or 4-bed configuration which solely eliminates the excessive salts from the seawater without any cooling/refrigeration effect [82]. However, later research, reported that the ADS might produce a cooling effect simultaneously by slight alteration of the evaporator temperature [41,69,83]. In this regard, the relevant studies are also included, which employ the silica-gel as an adsorbent, comprising a different number of adsorber beds, entail with the co-generating feature termed ADCS. In addition, several studies integrate the renewable thermal energy sources (i.e., solar collectors and solar panels etc.) with the ADS in order to acquire the non-payable energy for driving the system. Therefore, the authors include such studies that qualify the criteria of the Conventional Approach, however, irrespective of their free energy source.

Fig. 13 presents the pictorial and flow diagrams of the experimental facilities for reference that meet the defined benchmarks of the Conventional Approach. The working of the 4-bed ADS is similar to the 2-bed configuration as described in Fig. 7 however, the difference is that a pair of beds perform the adsorption and desorption processes in conjunction. Table 3 gives the summary of the studies that investigated the ADS based on the Conventional Approach. The salient features entail the findings and concluding remarks of such studies are presented accordingly in Table 3. Wang and Ng [82] reported that the ADS produces SDWP of 4.7 m³/ton/d along with no biological contamination. However, the co-generation feature of the ADS was not explored. From the relevant literature review as described in Table 3, one can be identified that the experimentally verified SDWP reported in the range between 4 to 4.7

$m^3/\text{ton}/d$ which identified the potential research gaps that need to be surmounted to increase the system productivity.

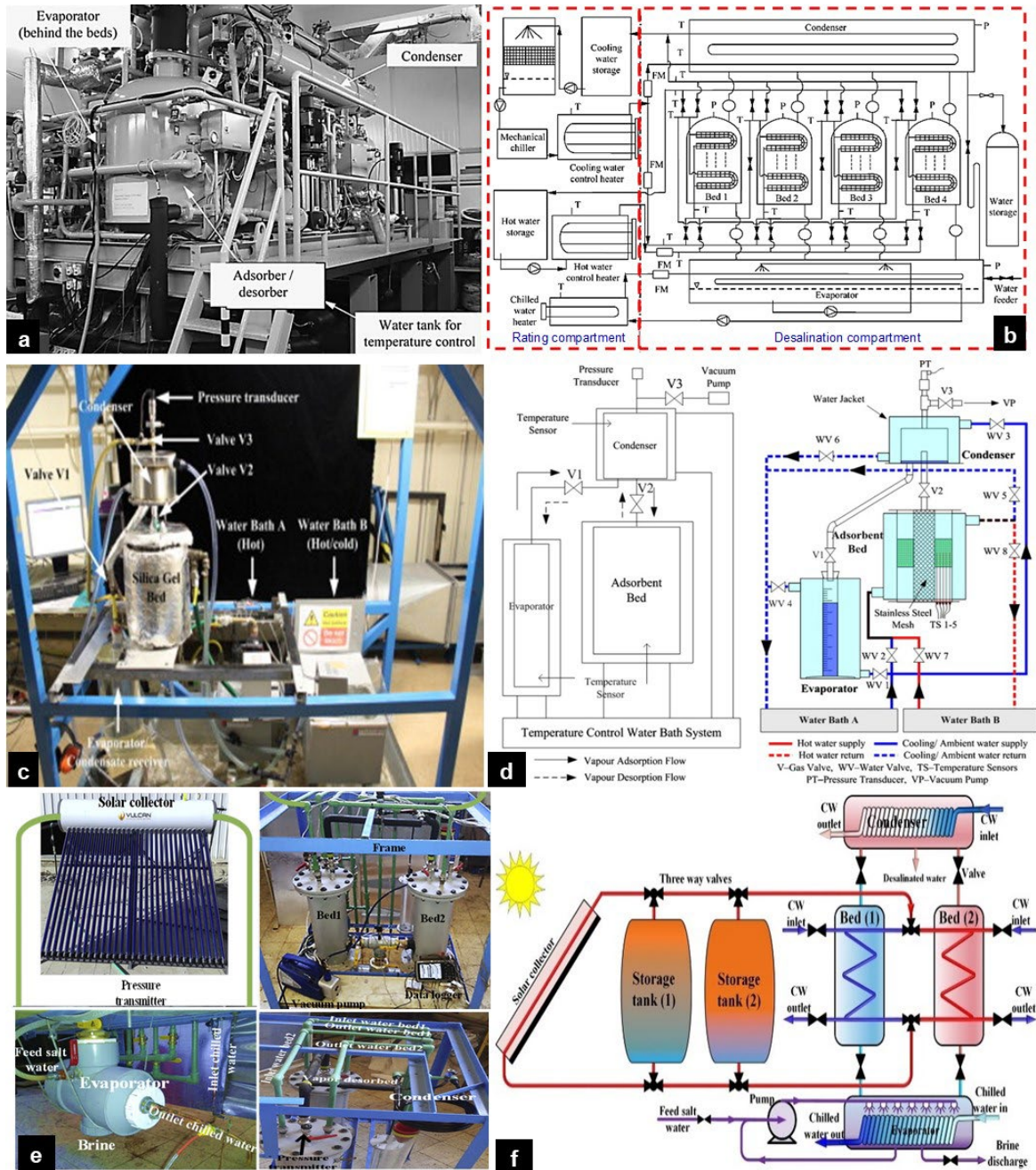


Fig. 13 Experimental facilities working on Convectional Approach: (a) and (b) are the pictorial presentation, and flow schematic of pilot-scale 4-bed ADS installed in National University of Singapore (NUS), Singapore [82], where (c) and (d) are the pictorial, block and flow diagram of the 1-bed ADS installed in The University of Adelaide (UoA), Australia [59], (e) is the pictorial presentation of the lab-scale prototype integrated with the solar collector developed in Sohag University (SU), Egypt [69], and (f) is the flow schematic for the ADS integration with ADS [83].

Table 3

Summarization of the studies reported on ADS/ADCS working on the Conventional Approach.

Year	Methodology	No. of beds	Adsorbent	Operating conditions			SDWP [m ³ /ton/d]	COP -	PR -	SCP [R-ton/ton]	Ref.
				T _{hw-in} [°C]	T _{c-in} [°C]	T _{ch-in} [°C]					
2005	ES	4	SG	85.0	29.4	12.2	4.7	0.24	N/A	N/A	Wang and Ng [82]
	Salient features of the work						Findings and concluding remarks				
<ul style="list-style-type: none"> In this study, previously designed and installed pilot-scale prototype of adsorption chiller in department of mechanical engineering, National University of Singapore (NUS) [84–86] was upgraded into ADS. Furthermore, the study explore the impact of rating conditions such as T_{hw-in}, T_{c-in}, t_{h-cycle}, and t_{sw} on the SDWP, and COP. 						<ul style="list-style-type: none"> Optimum t_{sw} was reported 40s. Small t_{h-cycle} leads towards maximum SDWP and minimum COP and vice versa for high t_{h-cycle}. High T_{hw-in} entail more SDWP and COP. 1.6°C drop and 1.8°C rise in T_{c-in} and T_{ch-in} contribute 10% additional SDWP, respectively. SDWP could be boosted up if T_{ch-in}>15 °C and T_{cw-in}<25 °C. ADS is functional at T_{hw-in} even low at 65 °C. 					
2012	ES+M	1	RD-SG	60-80	M I-III*	N/A	N/A	N/A	N/A	N/A	Wu et al. [59]
	<ul style="list-style-type: none"> An experimental test rig was developed for evaluating the three different thermodynamic cycles as proposed by Wu et al. [87]. The criteria for evaluating ther thermodynamic cycles are as follows: <ul style="list-style-type: none"> Mode I: T_{evap} < T_{cw-in} = T_{cond} (13 °C < 20 °C,) Mode II: T_{evap} = T_{cw-in} = T_{cond} = 20 °C or P_{evap} = P_{cond} Mode III: T_{evap} > T_{cw-in} = T_{cond} (30 °C > 20 °C) 						<ul style="list-style-type: none"> The water production was reported 59.7 ± 2.3 ml, 60.0 ± 4.0 ml, and 61.3 ± 4.7 ml, from mode-I, mode-II, and mode-III, respectively. Mode-II, and mode-III favored the desalination due to high T_{evap} The t_{h-cycle} was reported 24 hr. Condensation of the water vapors in the piping network was also identified which drop down the true value of water production. 				
2017	ES+M+Sim	2	Blue-bead-SG	85	25	25	4	0.45	N/A	112**	Alsaman et al. [69]
	<ul style="list-style-type: none"> Novelty in the study was experimentally investigating the ADCS in communication with the solar collector in accordance with Egyptian climatic scenario. In addition, the effect of rating conditions and ideal cycle thermodynamic response of ADCS were realized. 						<ul style="list-style-type: none"> Optimum t_{h-cycle} was computed 650s. T_{hw-in} = 85°C found suitable, further increment will drop COP which reflects high heat loss and less cooling potential. Lower T_{c-in} circulation to adsorber and condenser HX's reveals high system throughput (SDWP, COP, and SCP) and maxima measured at 15°C. In response to seawater evaporation, T_{ch-out} observed low as 17.5°C. 				

In this context, Wu et al. [88] developed a steady-state thermodynamic model for analyzing the system productivity assuming silica-gel as an adsorption/desorption media. In addition, the impact of $T_{\text{cw-in}}$ and $T_{\text{hw-in}}$ on SDWP and the energy required to produce per kg of desalinated water were investigated. It was reported that ADS consumes 3200 kJ/kg energy to produce 0.2 kg/cycle of freshwater at $T_{\text{cw-in}} = 20 \text{ }^\circ\text{C}$ and $T_{\text{hw-in}} = 90 \text{ }^\circ\text{C}$. Later, the authors realized the influence of the evaporator temperature (T_{evap}) on the system performance. In this regard, three thermodynamic cycles were theoretically analyzed corresponding to varying the T_{evap} and later experimentally verified by developing a small test rig [59,89]. Fig. 14 shows a comparison between the thermodynamic cycles working on the Conventional Approach. From Fig. 14 (a) a sudden pressure drift was observed which was mainly due to high T_{evap} during the switching period. Fig. 14 (b) depicts that, the thermodynamic cycle of the ADS that could be accomplished in two stages: (i) isobaric desorption (1-2), and (ii) isobaric adsorption (2-3). Similarly, Fig. 14 (c) presented another thermodynamic cycle for ADS proposed by Wu et al. [59,89]. The cycle comprising of two desorption processes such as processes 1-2 (isothermal) and 2-3 (isobaric). On the other hand, the adsorption process is taking place in isothermal conditions where the $T_{\text{cw-in}} < T_{\text{eva}}$. This temperature difference creates a pressure drift which allows the water vapors to adsorb at a constant temperature. In addition, it was reported that the isothermal adsorption process is faster compared to the isobaric adsorption process due to the availability of more pressure gradient between the evaporator and adsorber bed [59]. The thermodynamic cycles presented in Fig. 14 (b) and (c) limit the co-generating feature of the ADS by maximizing the water production and could acquire more the $\text{the}_{\text{-cycle}}$. Therefore, the studies on such thermodynamic cyclic configurations are suppressed. Wu et al. [90] developed a dynamic model based on governing heat and mass balance equations entailing the thermodynamic concept in which the $T_{\text{evap}} < T_{\text{cw-in}}$ and validated it with developed experimental results obtained from the prototype. The study identified the SDWP of $0.68 \text{ m}^3/\text{ton/d}$ could produce the capacity to complete four cycles/day [90].

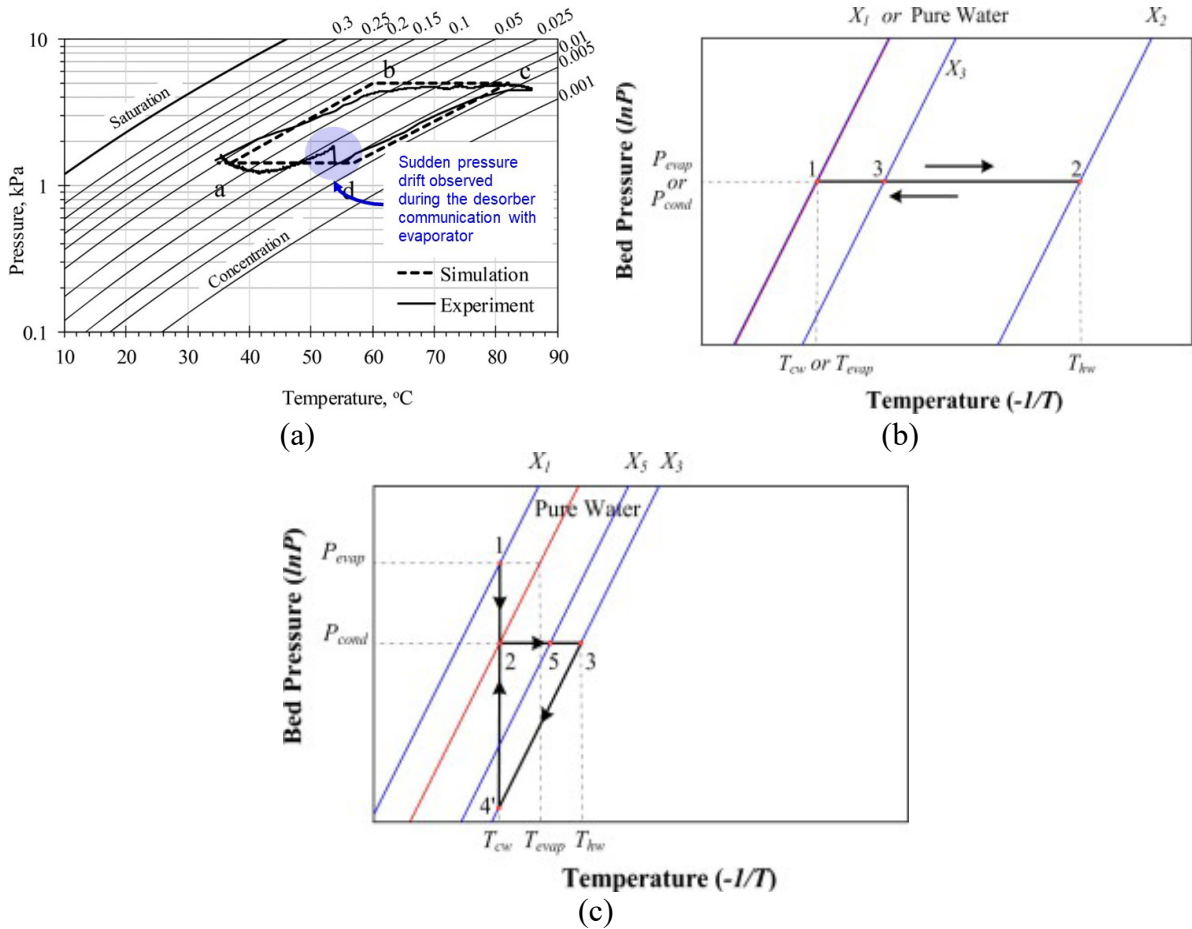


Fig. 14. P-T-X diagram of the ADS working on the Conventional Approach: (a) $T_{evap} < T_{cw-in}$ [69], (b) $T_{evap} = T_{cw-in} = T_{cond}$, and (c) $T_{evap} > T_{cw-in}$.

The conventional ADS equipped with low production capacity entail the producing high thermal wastes that has been dumped into the relevant water baths. Consequently, significant quantity of supplied waste heat not being utilized for desalination. In addition, the conventional ADS are over designed that need to be compacted. However, the mentioned downsides/research gaps are addresses by the researchers later. For instance, developing a small scale desalinators capable to produce relatively high SDWP as compared to conventional ADS [91]. In addition, several heat mass recovery schemes are implemented in the conventional ADS to improve the system productivity which has been described in detail in the subsequent sections.

4.2 Heat and Mass Recovery Approaches

The AD Heat and Mass Recovery Approach refers to various heat/mass recovery strategies aiming to make the ADS energy-efficient entail with maximum SDWP. So far, the following heat/mass recovery approaches are identified from the literature survey:

4.2.1 Pressure equalization and valve delay schemes

The pressure equalization (PE) and valve delay (VD) schemes refer to the mass and heat recovery schemes, respectively that used the conventional ADS along with PE valve and a controlling mechanism that supports in opening/closing of the relevant heating/cooling bath valves with a second of delay [60,92–94]. In PE scheme, a PE valve needs to be installed between adsorber (bed-1) and desorber (bed-2) as shown in Fig. 15 (a). As the bed-2 completes its desorption phase, the PE valve is turned ON for a shorter period of time. Due to pressure gradient/drift between adsorber bed (low pressure) and desorber bed (high pressure) additional water vapors were desorbed from bed-2 and adsorbed on bed-1. The phenomenon termed as pressure swing desorption/ adsorption [95]. Fig. 15 (b) shows the ideal cycle improvement in ADS due to installation of PE valve. From Fig. 15 (b) it has been realized that PE scheme significantly improves the saturation and unsaturation limits of adsorbent material.

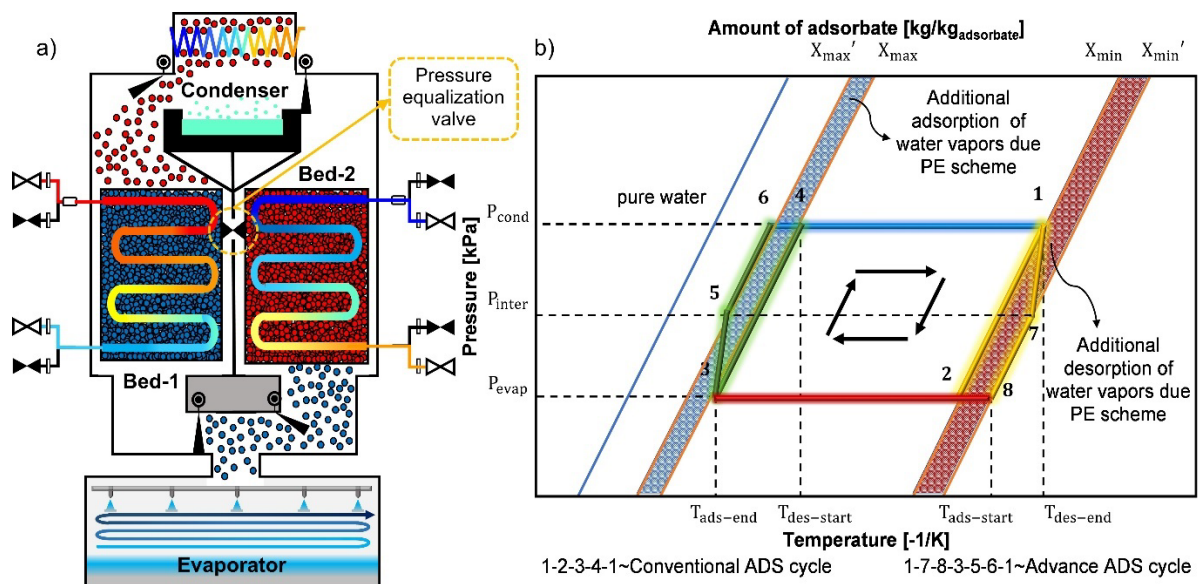


Fig. 15. (a) schematic illustration, and (b) theoretical improvement improvisation in ideal cycle of the ADS coupled with PE valve reproduce here from [92].

However, in order to accomplish adsorption and desorption processes effectively, the development of thermal fronts is necessary mainly developed via heat exchangers; that implanted in the sorbent beds. In this regard, significant amount of coolant with specific mass flow rates are needed to be circulated in tubes of HX. The discrepancies arise in ADS as the unfavorable coolant (resident in piping circuit) enters into erroneous path due to instant/simultaneous opening or closing of inlet or outlet valve during isosteric heating or isosteric cooling, respectively. The problem is addressed simply by introducing VD opening scheme that provides additional time to remove the inhabitant coolant from HX tubes, prior to

execute the subsequent phase. For PE and VD, 30s and 70s were found effective [92]. Later, experimental investigation believes that 10s is adequate for PE [60,93]. Table 4 contains the summary of publications reported on PE and VD schemes. From the relevant literature review it has been realized that the optimum PE duration must be short (10s) from the perspectives of obtaining high SDWP and PR from the pilot scale ADS due to completing additional number of desalination cycles/day. On the other hand, the cited study reported that, for small scale ADS, the PE valve is ineffectual and do not create significant pressure drift, due to operating evaporator and condenser approximately at same pressure values. [91].

Table 4

Summarization of the studies reported on ADS working on the Heat and Mass Recovery Approach: pressure equalization and valve delay schemes.

Year	Methodology	No. of beds	Adsorbent	Rating conditions			SDWP [m ³ /ton/d]	COP [-]	PR [-]	SCP [R-ton/ton]	Ref.
				T _{hw-in} [°C]	T _{c-in} [°C]	T _{ch-in} [°C]					
2007	ES	2	SG	85.0	29.4	12.2	4	N/A	0.32	N/A	Wang et al. [92]
	Salient features of the work				Findings and concluding remarks						
<ul style="list-style-type: none"> The study advances theoretical knowledge conduct experiments and make comparison with and without PE and VD schemes. Optimum PE time (t_{pe}) and VD time (t_{vd}) were identified based on the key performance indicators i.e., SDWP and PR. 				<ul style="list-style-type: none"> Optimum t_{vd}, t_{pe}, t_{h-cycle} and t_{sw} time was reported 70s, 30s, 480s and 40s, respectively. Revisiting of PE and VD schemes contributes 15.7% and 42.5% rise in SDWP and PR, respectively. 							
2007	ES	4	SG	85	29.5	30	8.2	N/A	0.55	N/A	El-Sharkawy et al. [93]
	<ul style="list-style-type: none"> The study focused to investigate the t_{pe} by operating evaporator at relatively high temperature; consequently, producing high cooling flux which was managed by increasing T_{ch-in}~25 °C. The impact on key performance indicators are analyzed by varying the T_{ch-in}, T_{hw-in} and t_{pe}. 				<ul style="list-style-type: none"> The t_{h-cycle} and t_{sw} were opted 360s and 40s, respectively. SDWP and PR of the ADS drops as t_{pe} increases 10-35s, due to drop-in mass transfer rates, low production cycles. Optimal t_{pe} was reported 10s for 4-bed ADS having 22% improvement in SDWP with 1.5 kWh/m³ electrical energy consumption. 						
2020	M+Sim	2	SG	95	30	30	9.58	0.58	N/A	N/A	Amirfakhraei et al. [94]
	<ul style="list-style-type: none"> The study focused to investigate the PE scheme for mass recovery and communicate HXs of adsorption/desorption beds (depicting Master-Slave configuration described in section 4.2.2), and HXs of evaporator, and condenser (depicting Evaporator-Condenser amalgamation via heat recovery loop described in the section 4.2.3) as a heat recovery schemes. 				<ul style="list-style-type: none"> t_{h-cycle}, t_{pe} and t_{hr} was set 600s, 30s, and 20s, respectively. In comparison with conventional 2-bed ADS, cumulative improvement in SDWP was recorded 66% due to high evaporator temperature. No cooling effect was reported due to high T_{evap}, responding T_{ch-out} 27.5 °C to 33.5 °C. 						

From Table 4 it has been concluded that, the PE and VD schemes mounting the SDWP ~ 2 folds as compared to the conventional ADS. The authors reported that, the PE time and (t_{pe}) and valve delay time (t_{vd}) are the influential aspects of PE and VD schemes integrated ADS [93]. Fig. 16 presents the impact of t_{pe} on SDWP and PR. According to the Wang et al. [92] increase in t_{pe} responds to increase in SDWP and PR due to availability of more time to transfer moisture from high pressure bed to low pressure bed. In addition, high pressure emphasizes the hydrophilicity of adsorbent material thereby more water vapors will adsorb on the adsorbent material. Contrastingly, El-Sharkawy et al. [93] analyzed that, an optimum time frame or point for the opening of the PE where the performance of the ADS found maximum beyond this point the SDWP and SCP dramatically decreases due to drop-in mass transfer rate. In addition, it could be reason that, high t_{pe} retards the number of desalination cycles completed per day.

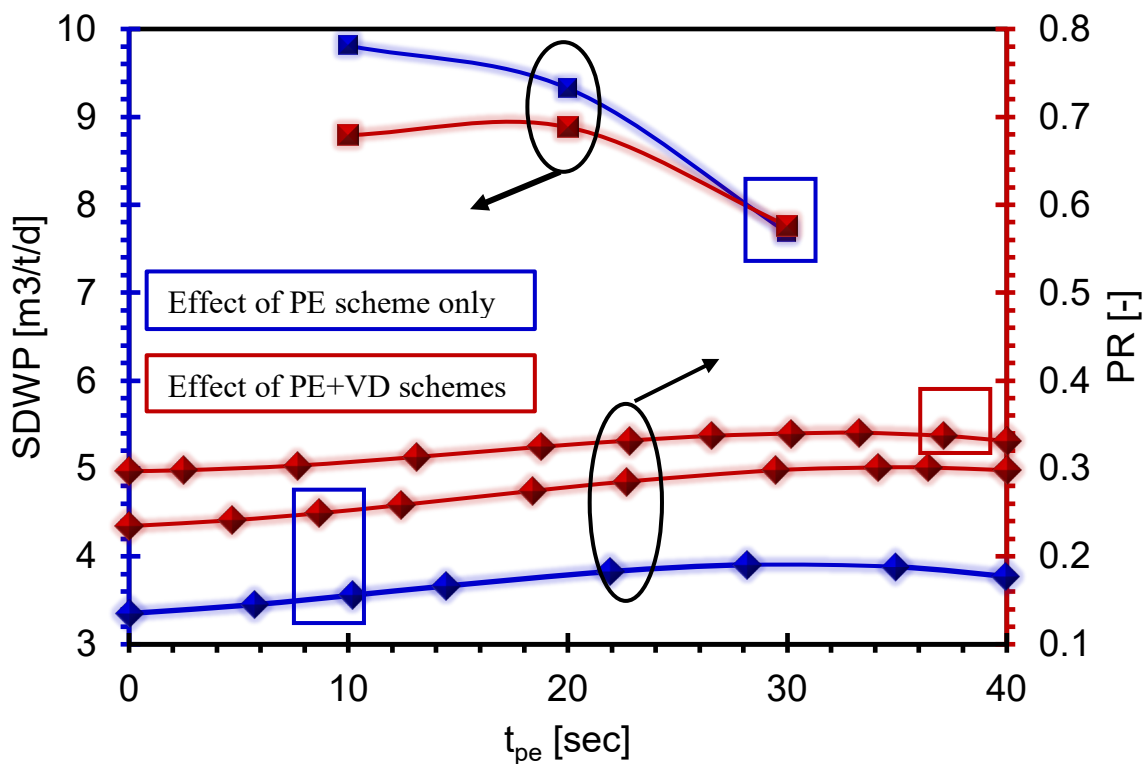


Fig. 16. Effect of pressure equalization (PE) time on SDWP and PR reproduce here form [92,93].

4.2.2 Master-Slave configuration

Master-Slave configuration refers to the heat recovery approach that has been incorporated to capture the heating/cooling loads coming out from the desorber/adsorber beds which has been previously dumped into the heating/cooling water baths, respectively. The residential coolant circulating in HXs marginally losses its temperature when its passes through the adsorber and desorber heat. The coolant can be potentially re-utilized during the antecedent processes such as isosteric heating and isosteric cooling, respectively as show in Fig. 17 [94].

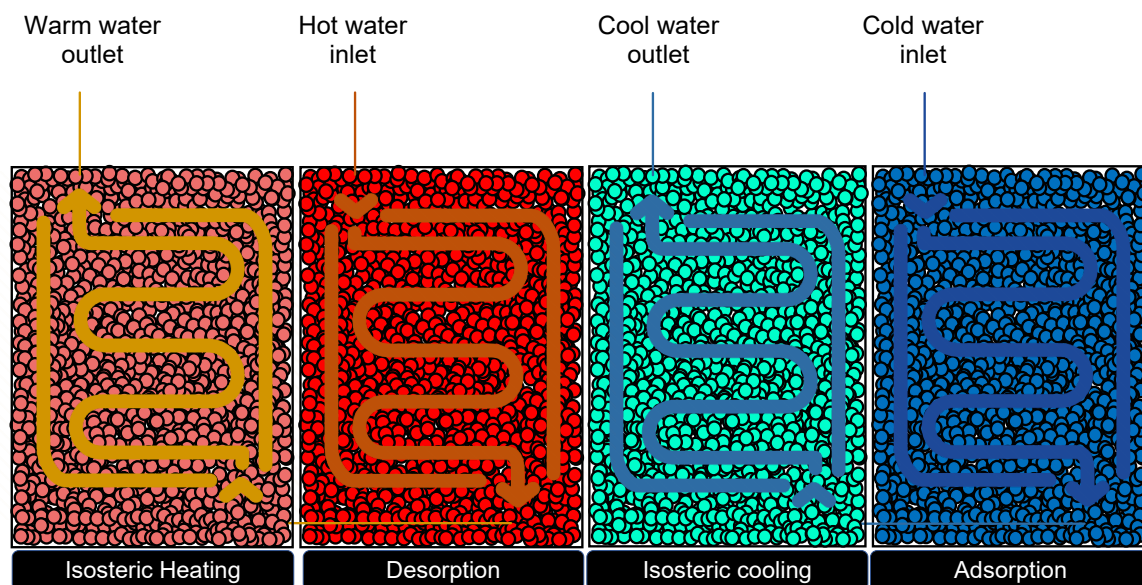


Fig. 17. Adsorption and desorption bed heat utilization scheme.

However, in Master-Slave configuration two beds are operating in similar modes which has been differentiated into Master-adsorption bed and Slave-adsorption bed. The Master-adsorption bed is the bed where the actual adsorption process takes place and after that isosteric heating process executes whereas the Slave-adsorption bed is the bed where the non-actual adsorption process takes place and after that actual adsorption process occurs. The retrofitting between HXs of adsorber and desorber beds are imperative to implicate the Master-Slave configuration. Fig. 18 shows the operational strategy of ADS employing the Master-Slave scheme. For instance, during first cycle bed-1 and bed-4 performs desorption, thereby both linked with each other and serve as Master and Slave beds, respectively. Whereas bed-2 and bed-3 performs adsorption and correspondingly serve as Slave and Master bed. The outlet hot water from the Master-desorption bed supplied to the Slave-desorption whereas the outlet water from the Master-adsorption bed directed to Slave-adsorption. Prior to initiate the second cycle, t_{sw} has been provided in which the bed-1 and bed-3 was needed to pre-cool and pre-heat, respectively. On the other hand, bed-2 and bed-4 previously serve as Slave mode switch to

Master mode for adsorbing and desorbing more water vapors, respectively. Similar pattern will follow-up for rest of cycles by changing the beds modes to get the high SDWP with minimum energy consumption.

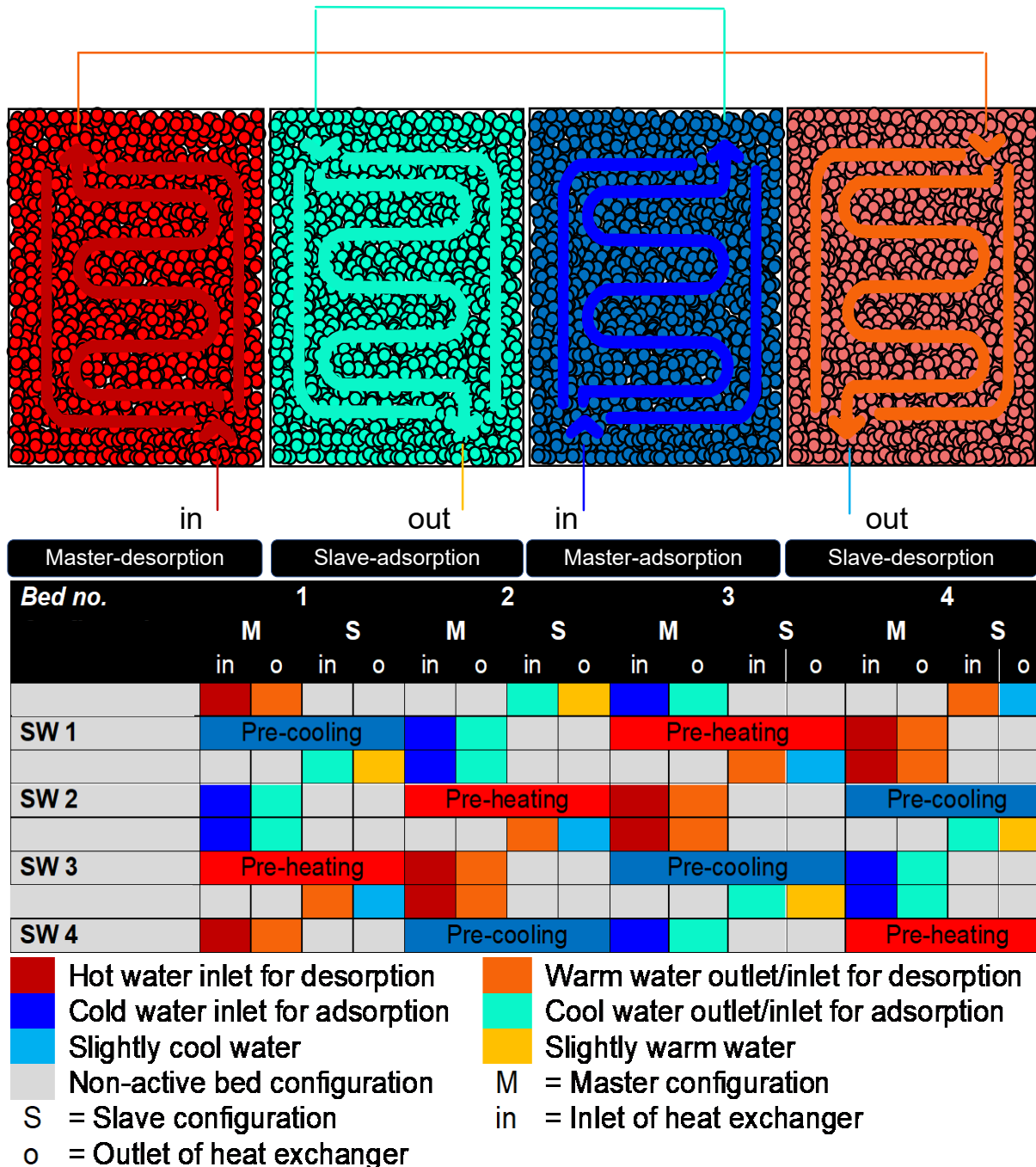


Fig. 18. Operational strategy of ADS incorporating Master-Slave scheme.

Fig. 19 shows the pilot-scale experimental facilities and lab-scale prototypes working on Master-Slave configuration. The cited studies experimentally investigate the Master-Slave fashion as the heat recovery approach coupled with ADS [41,60] and ADCS [41]. A test rig

has been developed having series connection for coolant circulation between HX's of adsorber and desorber beds [91,96]. Prominent findings regarding the cited studies are furnished in Table 5.

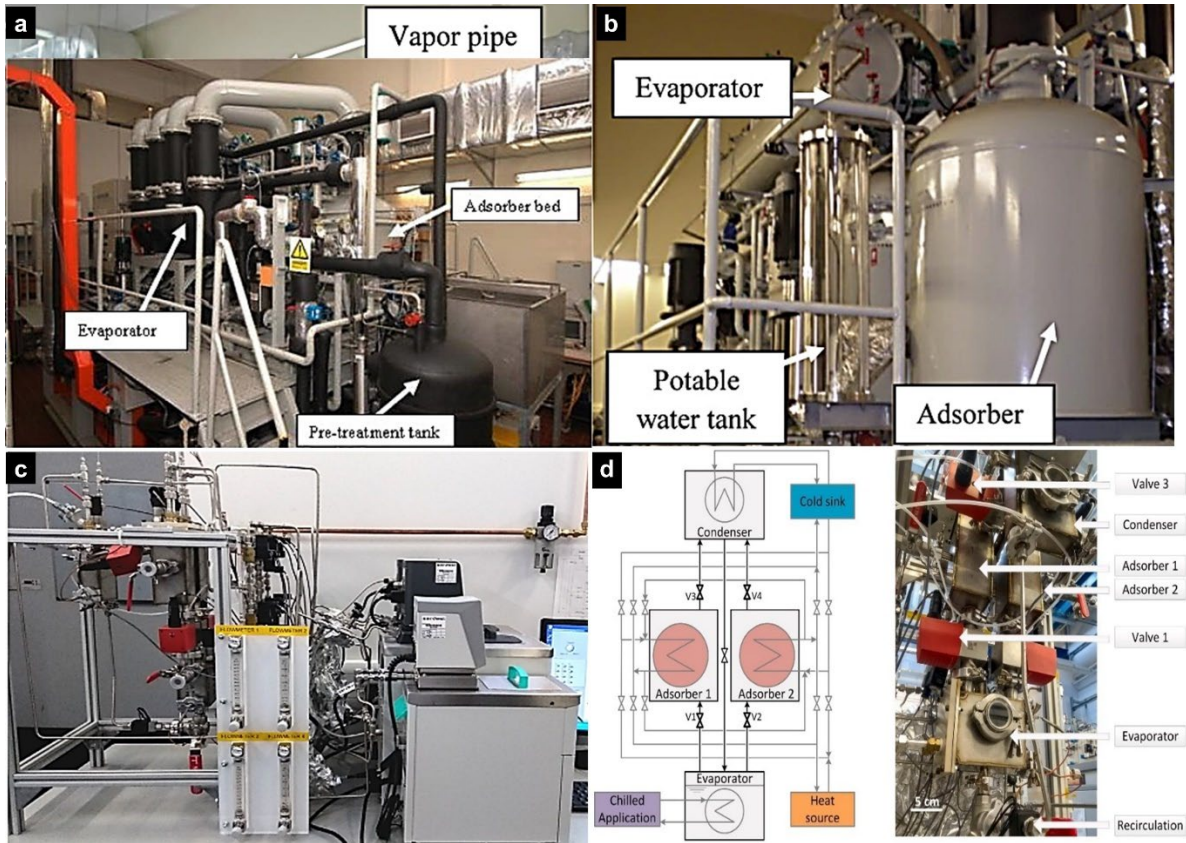


Fig. 19. Experimental facilities reported in literature working on Master-Slave configuration: a) and b) NUS, Singapore [41,60], c) and d) The University of Edinburgh, Scotland, UK [91,97].

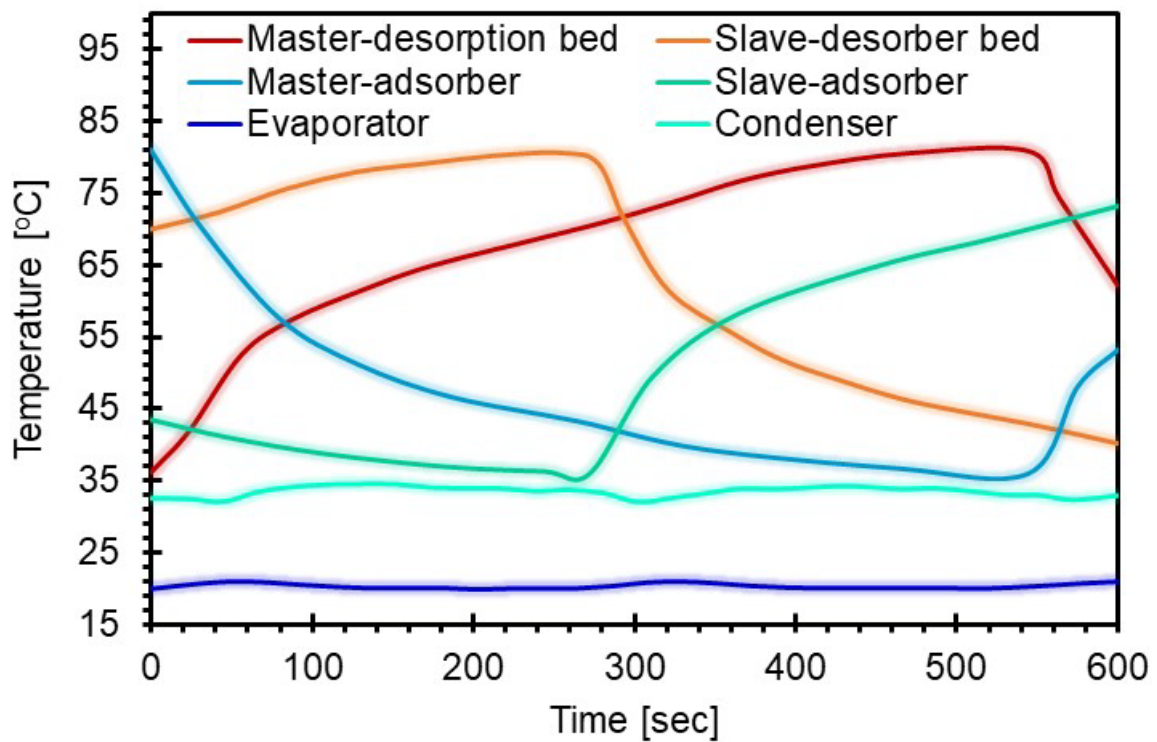
Table 5

Summarization of the studies reported on ADS/ADCS working on the Heat and Mass Recovery Approach: Master-Slave configuration.

Year	Methodology	No. of beds	Adsorbent	Rating conditions			SDWP [m ³ /ton/d]	COP [-]	PR [-]	SCP [R-ton/ton]	Ref.
				T _{hw-in} [°C]	T _{c-in} [°C]	T _{ch-in} [°C]					
2009	ES	2, 4	RD-SG	85	30	N/A	8.79, 10	N/A	0.57, 0.61	N/A	Thu et al. [60]
	Salient features of the work				Findings and concluding remarks						
<ul style="list-style-type: none"> The cited study investigates Master-Slave configuration for both 2-bed mode and 4-bed mode of ADS. Impact of T_{hw-in} on the t_{cycle} was analyzed. 				<ul style="list-style-type: none"> It was determined that, for both 2-bed and 4-bed modes of ADS, the T_{hw-in} should be higher ≥ 70 °C, otherwise Slave-desorber bed will not operate able due to low T_{hw-out}. High T_{hw-in} shortens the t_{cycle}, due to increase the water vapor desorption rate and vice versa. The t_{pe}/t_{sw} opted 10s/40s, respectively. 							
2012	ES+M+Sim	4	RD-SG	65–85	29.5	30	8	N/A	N/A	51.6	Ng et al. [41]
	<ul style="list-style-type: none"> The cited study initially explores the ADCS with Master-Slave heat recovery scheme from the viewpoints of acquiring and improvising the cogeneration advantages. In addition, numerical model was developed and validated it with experimental outcomes. 				<ul style="list-style-type: none"> t_{h-cycle}/t_{sw} was opted 960/40sec, respectively. T_{ch-in} was found sensitive to T_{ch-out}, SDWP and SCP. Lower T_{ch-in} (30-10°C) leads to produce lower T_{ch-out} (25-7°C), having lower SCP (51.60-23.05 R-ton/ton) and SDWP (8.0-3.56 m³/ton/d) at T_{hw-in}=85°C. 41.25% increment in SDWP is recorded as compared to conventional ADS [82]. 						
2019	ES	2	SG	80	30	30	7.7	N/A	0.6	N/A	Olkis et al. [91]
	<ul style="list-style-type: none"> The motivation of the cited study was developing a compacted ADS in order to assess the different adsorbent material. The study performs blank experimentation by not incorporating SG adsorbent in the system. 				<ul style="list-style-type: none"> t_{h-cycle} opted 600s. PR limit to 0.48 without Master-Slave scheme. 25% increment in PR was recorded with Master-Slave scheme. The scheme is suitable with high t_{h-cycle}, thus leads to slight drop in SDWP. Approximately half of the total input energy was used by system components (i.e., heating or cooling of metallic elements). 400g SG requires, 3770kJ energy for producing 1kg of water. 						

						<ul style="list-style-type: none"> • Peak heating demand was cut in half due to the Master-slave scheme. 				
	ES	2	Siogel-SG	80	23.5	31.9	10.9	0.83	0.35	45.6
	SR					F&C				
2019	<ul style="list-style-type: none"> • The cited study experimentally computes the thermodynamic cycle of the ADCS coupled with Master-Slave configuration. • Impact of operational parameters on thermodynamic cycle was explored and compared with ideal cycle. • Cogenerating feature of ADCS were critically analyzed. 					<ul style="list-style-type: none"> • Distorted/flatter shape of $T_{h_{ads-cycle}}$ was observed in realistic conditions, as shown in Fig. 20 (b). • 41% increment in SDWP was recorded if $P_{evap} \approx P_{cond}$ which could be obtained when $T_{evap} \approx T_{cond}$. • For high grade cooling T_{evap} should be lower. • 60% reduction in performance during cogeneration, thereby concluded that SG not a suitable candidate for multipurpose. 				
	Olkis et al. [97]									

The studies report 43.8% and 9.83% improvement in PR for both 2-bed and 4-bed ADS, respectively [92,93]. Fig. 20 (a) presents the outlet temperature profiles of ADS employing Master-Slave configuration. Fig. 20 (b) gives the P-T-X presentation of ADS employing the imitation of Master-Slave scheme at assorted cycle times. The shorter cycle time bounds to achieve the ideal saturation limit of adsorbent material. The distorted shape is merely due to condensation of water vapors on adsorber vessel walls during isosteric heating (1-2) and again adsorb on porous media during isosteric cooling (3-4) [97]. To conclude the section, Master-Slave arrangement further added 18% increment in SDWP, and 9.8% in PR, and halves the input heating load, as compared to PE and VD approach [91,93] and thereby, proven its implementation as energy efficient heat recovery solution for both ADS and ADCS.



(a)

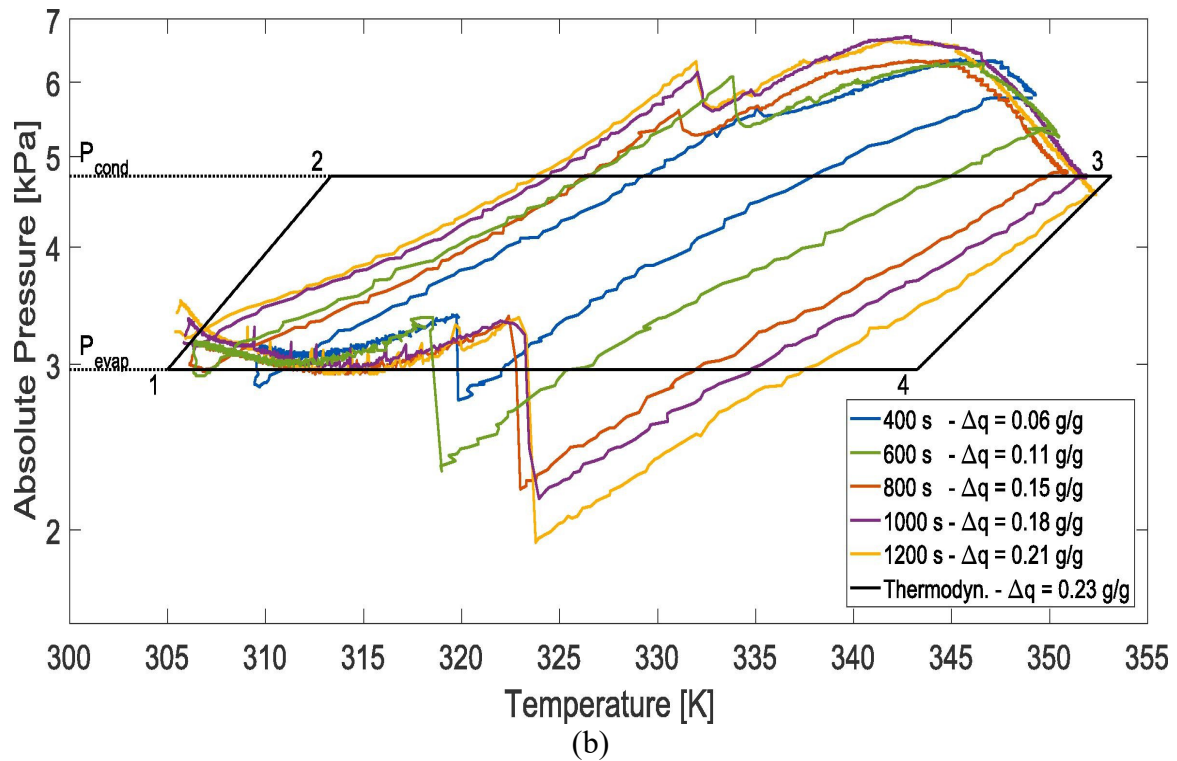


Fig. 20. (a) Outlet temperature profiles of circulating/residential coolant based on Master-Slave configuration reproduce here from [41], (b) P-T-X presentation of ADS employing Master-Slave scheme [97].

4.2.3 Evaporator-Condenser amalgamation via heat recovery loop/ integrated vessel

From the perspectives of developing energy-efficient ADS, copious investigation was conducted, considering the retrofitting in conventional ADS in a manner of integrating evaporator and condenser (E-C). The motif was to capture the latent heat of evaporation/condensation or waste heat from respective chambers and directly utilize it to uplifts the quantum of SDWP by decreasing/increasing, condenser/evaporator temperature, respectively. In this regard, to ensure adequate heat transferring between E-C, two trails were proposed, namely, (i) heat recovery loop (HRL) and (ii) encapsulated E-C vessel/device. The employed retrofitting enables to: (i) retrieve regeneration heat for sea water evaporation, (ii) increase evaporator temperature, which contributes more evaporation, (iii) create pressurization effect which enhances adsorption process, (iv) drop condenser operating temperature, which produces more condensate. Fig. 21 presents the pictorials of the experimental facilities that were modified by integrating HRL between E-C and encapsulated E-C device along with flow diagrams. The experimental [42] and numerical investigation [53,98] were made by developing a piping circuit between E-C. The developed numerical model accounts for the reverse adsorption/desorption problem, which mainly happens due to

un-appropriate t_{sw} and pressure swing. Consequently, water vapors condensed in evaporator. Also, encapsulated E-C device was numerically investigated [99,100]. The salient features and prominent findings are showcased in Table 6.

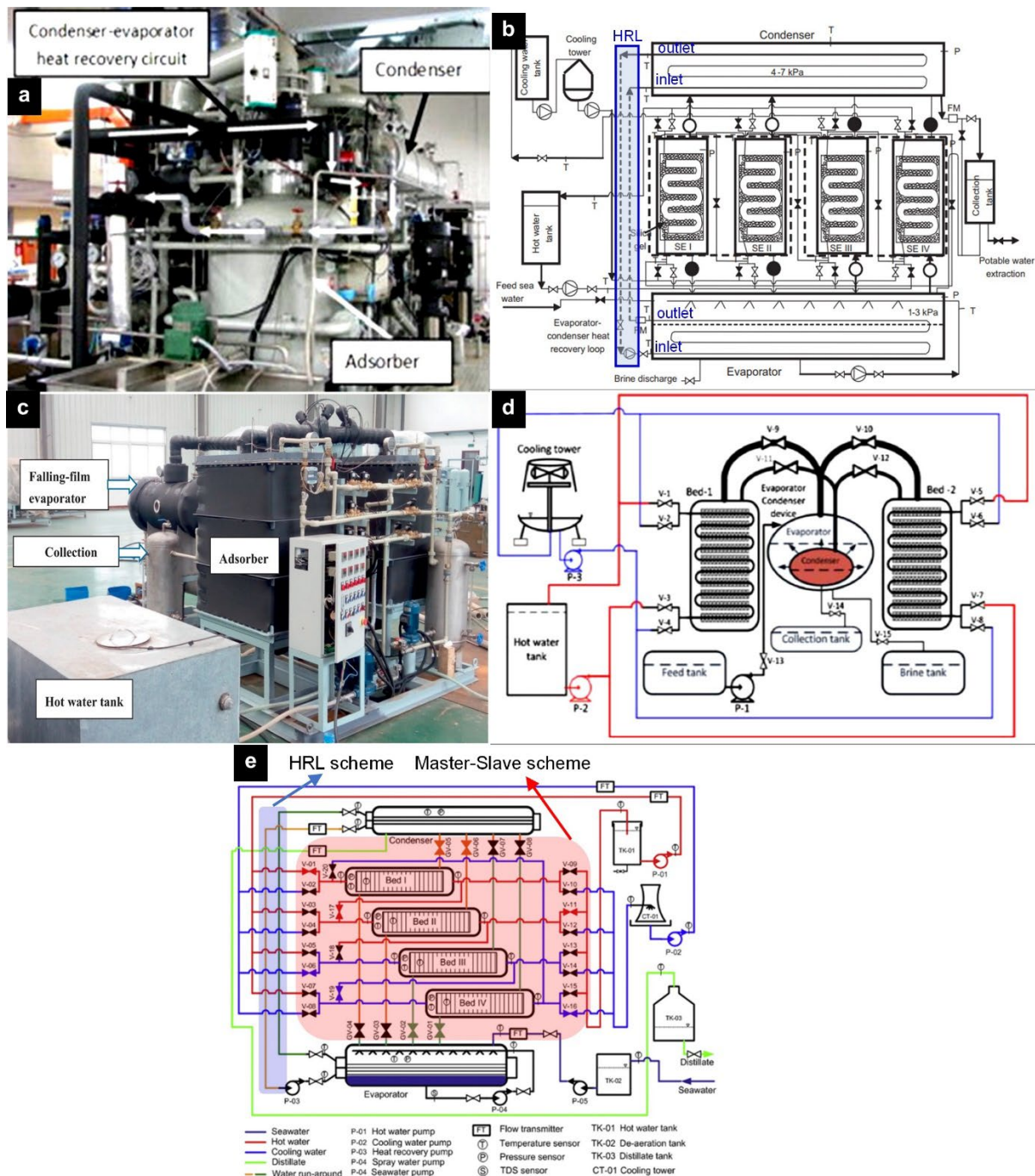


Fig. 21. Experimental facilities and corresponding flow diagrams working on Evaporator-Condenser amalgamation via heat recovery loop/ integrated vessels: (a) pictorial view of ADS+HRL installed in NUS, Singapore [98], (b) flow diagram of the ADS+HRL system [53], (c) pictorial view of integrated evaporator-vessel device installed in Tianjin University, China [63], (d) flow diagram and conception of integrated evaporator-condenser device [100], and (e) flow diagram of the ADS working on fused heat recovery schemes [98].

Table 6

Summarization of the studies reported on ADS/ADCS working on the Heat and Mass Recovery Approach: Evaporator-Condenser amalgamation via heat recovery loop/ integrated vessel.

Year	Methodology	No. of beds	Adsorbent	Rating conditions			SDWP [m ³ /ton/d]	COP [-]	PR [-]	SCP [R-ton/ton]	Ref.
				T _{hw-in} [°C]	T _{c-in} [°C]	T _{ch-in} [°C]					
2011	ES+M+Sim	4	SG	50-85	30	N/A	5.2-13.5	N/A	0.77	N/A	Thu et al. [53]
	Salient features of the work						Findings and concluding remarks				
<ul style="list-style-type: none"> The cited was focused to develop a run-around circuit or heat recovery loop (HRL) between evaporator and condenser. In addition, the effect of rating conditions on key performance parameters were explored and compared with conventional ADS. 						<ul style="list-style-type: none"> Due to HRL in ADS, negligent temperature difference was recorded between condenser outlet/inlet and evaporator inlet/outlet, respectively, reflecting high quality insolation. t_{h-cycle}/t_{sw} opted 600/40s, respectively. HRL make ADS functional even at 50°C. In addition, the scheme improves the SDWP by two folds. 					
2013	ES	4	A ⁺⁺ SG	85	30	N/A	15	N/A	0.746	N/A	Thu et al. [42]
	<ul style="list-style-type: none"> The cited study was focused to conduct the performance analysis on ADS+HRL and compute the improvement in ideal thermodynamic cycle. Lowest possible T_{hw-in} was identified to operate the ADS+HRL and compared with conventional ADS. 						<ul style="list-style-type: none"> Due to HRL, 2°C rise in T_{evap} (32°C) and 4°C drop in T_{cond} (26°C) was recorded which facilitate additional evaporation and condensation, respectively. Operating pressure in ADS+HRL was found 3-7kPa. ~28% additional heat has been scavenged, from the condenser which previously wasted consequently, ~1/5th times more vapors uptake by adsorbent. ADS+HRL produce equivalent SDWP (4.7 m³/ton/d) on 50°C T_{hw-in}, as reported by Wang et al. [130] on 85°C T_{hw-in}. 50% reduction in t_{sw} (40s to 20s) were observed due to HRL [82]. 				
2017	ES+M+Sim	2	SG	85	30	30	8	N/A	N/A	N/A	Alsaman et
	<ul style="list-style-type: none"> The cited study was incorporated the solar collector with ADS+HRL in order to acquire the non-payable heat for adsorbent bed regeneration. 						<ul style="list-style-type: none"> t_{h-cycle} opted 650s. Due to HRL, T_{evap} was increases from 15°C to 32°C, which reflects more evaporation and pressurized adsorption, consequently more SDWP. 				

	<ul style="list-style-type: none"> The study also compared the ADS+HRL performance with conventional ADS. 					<ul style="list-style-type: none"> The SDWP of ADS+HRL increases by two folds as compared to conventional ADS 					
2013	M+Sim	2	A ⁺⁺ SG	85	30	N/A	26	N/A	0.710	N/A	Thu et al. [99,100]
	<ul style="list-style-type: none"> The cited studies were narrowly targeted to mutually investigate the compatibility of HRL and integrated evaporator-condenser device in ADS. The validated numerical models were developed to implicate the effect of HRL and encapsulated evaporator-condenser device on performance of ADS. 					<ul style="list-style-type: none"> Owing to vessels integration (E-C), 42°C T_{evap} was recorded, which incurred more evaporation and SDWP. Operating pressure of the adsorption bed was found 9-12 kPa, which earned 4% additional vapors uptake. t_{h-cycle}/t_{sw} drop to 300s/20s, respectively Energy utilization was reduced to 1.38 kWh/m³ with an overall heat transfer coefficient of 2,300 W/m².K at the highest/lowest T_{reg-in}(85°C)/t_{c-in}(25°C), respectively. 					
2017	ES+M+Sim	4	A ⁺⁺ SG	70	27.6	N/A	10	N/A	0.79	N/A	Thu et al. [98]
	<ul style="list-style-type: none"> The cited study was focused to develop an improved numerical model capable for simulating the reverse adsorption/desorption process. In addition, the effect of HRL and Master-Slave configuration were mutually investigated. The effect of rating conditions on the system key performance indicators were also analyzed. 					<ul style="list-style-type: none"> t_{h-cycle}/t_{sw} opted 360/20s, respectively. T_{evap}/T_{cond} was noted 27.5°C/32.5°C, respectively. Present configuration omits the additional heating/cooling water baths for evaporator/condenser due to equivalent energy utilization profile. Frequent heating and cooling fronts are required at shorter t_{h-cycle}. The cycle found capable to operate low as 50°C. High-grade cooling was not acquired due to high T_{evap}. 					
2018	ES	2	A-SG	83±1	27	N/A	4.69	N/A	0.76	N/A	Ma et al. [63]
	<ul style="list-style-type: none"> The cited study focused to evaluate falling film evaporator, capable to perform evaporation (shell side) and condensation (tube side), jointly. For heat recovery adsorption/desorption beds and evaporator/condenser are configured. For mass recovery PE scheme was coupled in the ADS. 					<ul style="list-style-type: none"> Due to HRL condensation heat captured effectively for seawater evaporation. t_{h-cycle} is opted as 900s out of which 90s and 30s are for heat and mass recuperating, respectively. Study found that, heat recovery scheme not directly improve the SDWP, however, it is able to use the input energy efficiently. 					

Fig. 22 gives a comparison of temperature-time profiles among the conventional ADS, integrated E-C device and ADS+HRL reproduce here in order to analyze the increment in drop down of T_{evap} and T_{cond} . The solid and dotted line indicate the T_{evap} and T_{cond} , respectively. From the Fig. 22 it has been realized that, the T_{evap} of conventional ADS drop by 2-3 °C during each successive cycle due to the cool down of the circulating $T_{\text{ch-in}}$. Overall, the T_{evap} and T_{cond} ranges between 15-30 °C and 30-34 °C, respectively in case of ADS having no heat recovery scheme [101]. The HRL between E-C and integrated E-C schemes increases the T_{evap} even up to 45°C, based on the numerical modeling, however the experimental validation was recorded around 30 to 35 °C . [101][63]. The increase in T_{evap} produces maximum water vapor mass with high evaporation rate, consequently, magnifies the SDWP. On the other hand, the T_{cond} recorded even up to 48 °C which could not be beneficial in sense of capturing less latent heat of condensation [99]. If compared between integrated E-C and HRL scheme it has been realized that former scheme is more efficient because of onsite utilization of condensation heat for evaporation. However, in case of HRL well insulation will potentially utilized to capture the maximum heat of condensation due to significant losses in the piping network.

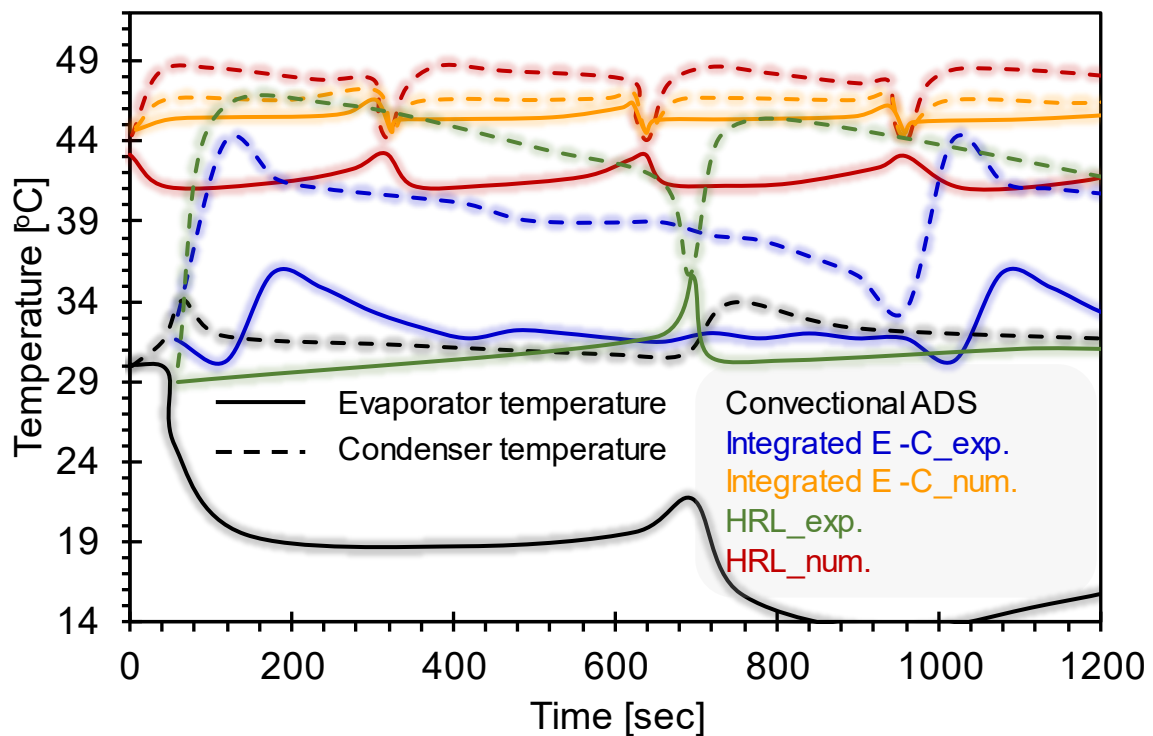


Fig. 22. Temperature-time profiles of evaporator and condenser in response of employing: heat recovery circuit, and integrated evaporator condenser device. The data has been reproduced here from cited reference [63,99–101] for comparison.

Fig. 23 illustrates thermodynamic adsorption cycle comparison between conventional and advance ADS employing E-C integration schemes, i.e., (top) HRL and (bottom) E-C device. From Fig. 23. it can be observed that the retrofiting dramatically improves the SDWP. It was merely due to increase in T_{evap} which consequently uplifts the P_{ads} . Overall, 33%/18.23% increment in SDWP/PR was recorded [42] in advance ADS assisted with HRL than conventional ADS employing Master-Slave scheme [60]. In comparison, a quantum jump in SDWP was attained by the integral E-C vessel/device. Fig. 23 (bottom) shows the significant improvement in saturation limit of adsorbent material employed in ADS equipped with E-C device. Approximately 1.3°C temperature difference was recorded between condenser-evaporator, which depicts more heat harvesting from condenser for seawater evaporation [99,100]. As a result, 42% rise in SDWP was measured as compared to HRL assisted ADS. However, it is highlighted here that, integration of evaporator and condenser is not suitable for acquiring multi-benefits due to high evaporator temperature. For high-grade cooling the T_{evap} should be higher than the T_{cond} which is not possible in such scheme. Therefore, the proposed scheme give quantum jump to SDWP with zero cooling effect. However, the integration proves to be energy efficient and allows the ADS to operate even at 50°C $T_{\text{reg-in}}$ which hitherto not possible for conventional ADS.

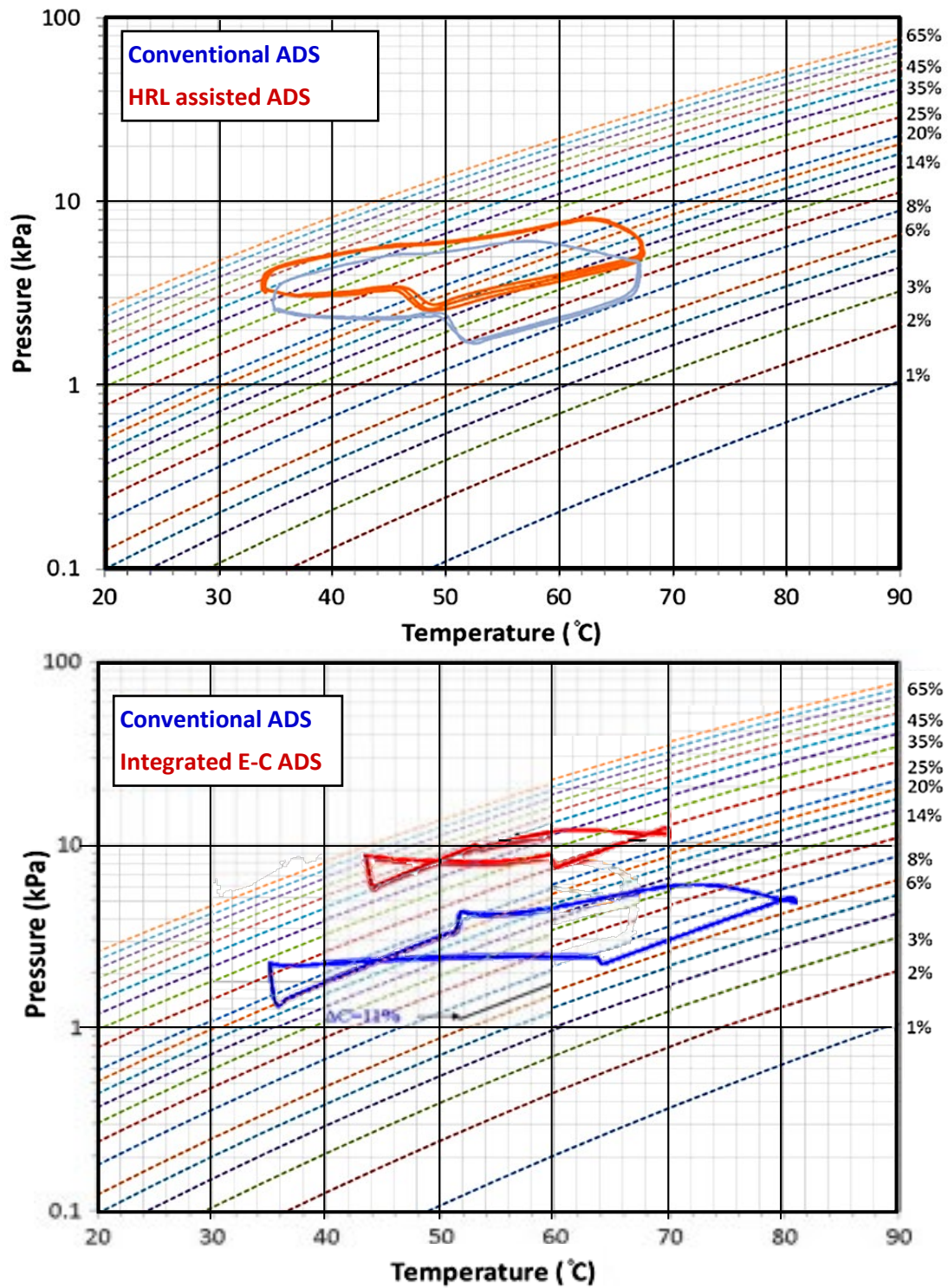


Fig. 23. Thermodynamic adsorption cycle comparison of conventional ADS with advance ADS employed (top) heat recovery loop, and (bottom) integrated evaporator condenser device [42,100].

4.2.4 Dual stage, multi evaporators/ condensers scheme

Apart from integrating evaporator-condenser trails, dual-stage, multi evaporators/condensers were also widely investigated as an alternative approach with the viewpoints of lowering the driving source temperature and acquiring substantial quantum of associated benefits. A collection of studies of types instrumentation [102], experimentation [58,103,104], and thermodynamic modeling [105,106] are made for air-driven dual-stage ADCS. The configuration was enforcing dual adsorption by connecting the stage-1 and stage-2 adsorber beds in a manner of compelling the desorb water vapors from stage-1 beds to again adsorb on stage-2 beds. The plenum was interlocked between the active stages; also prior to condenser for preventing any pressure fluctuations which could be emerge due to differential adsorption and desorption kinetics among the different stages. The schematic illustration and pictorial view of experimental facility is presented in Table 7. The core objectives of the studies were: (i) determination of optimum inter-stage pressure (P_{int-s}) [105] (reported as a crucial entity in two-stage configuration which is the difference between the operating pressures of stage-2 and stage-1 adsorbers), (ii) comparison study among single-stage and dual-stage configuration supporting with the impediments of single-stage [103], (iii) performance investigation on 2/ 3-bed mode [104], and estimate the lowest possible driving source temperature that could be efficient for air-driven ADCS [58]. Regarding, single-stage impediments, it was identified that air-driven desalination facility is inevitable due to thermal inventories and reverse flow problem of adsorb/desorb vapors [104,107]. Longer switching period could be the solution [103]; however it was found inevitable due to necessitate of additional driving heat and faster switching kinetics in comparison with adsorption/desorption processes [108,109]. Thereby, dual-stage configuration was proposed as pragmatic solution to address the underlined problem, especially for air-cooled ADCS. Similarly, dual-stage ADCS [110] was investigated which was embedded with both trails of evaporator-condenser amalgamation. Prominent findings are showcased in Table 7. Fig. 24 presents the relevant dual stage, multi evaporators/condensers schemes reported in the literature.

Governing wide research on adsorption science, it was identified that desorption process owns faster kinetics as compared to adsorption [111,112]. In addition, low pressure adsorption left unsaturation in adsorbent material, affecting the overall system productivity [113]. Therefore, it was the intended need to introduce an intelligent configuration. With this mind set, cited study formulate additional adsorption period functional at HP evaporator [114]. Similarly publications relevant to pressurized adsorption conception were also available [113,115]. In addition, longer adsorption period was assigned, comparative to desorption period; to accomplish the sorbent equilibrium capacity [115]. The configuration confers improvement in SCP and SDWP by 26% and 45%, respectively as compared to conventional ADCS [30,41,116]. The numerical investigation on combined physical/ chemical sorption mechanism were also investigated by employing SG and CuSO₄, respectively [117]. The SG beds communicated with both LP and HP evaporators while CuSO₄ solely interlock with HP evaporator. Configuration improvised SCP and SDWP up to 55% and 56%, respectively [117]. The cited study [118], extend the findings of integrated E-C device [99,100] and multi-stage configuration by employing water driven HX's which was ignored in previous investigation [103–105]. Contrary to prior works, two different brine feeding mechanisms for evaporator (i.e., (i) perforated plate and (ii) tray embedded with spray nozzles) were investigated. Study recommended the assembling of pressurized spray nozzles due to production of fine droplets which degrade heat resistance and promote mist specific surface area; in turn rapid evaporation in shorter residency period [68,119–121]. Fig. 25 shows the progressive modification in Dühring's diagram in response of various configuration, evident from the cited literature.

Table 7

Summarization of the studies reported on ADS/ADCS working on the Heat and Mass Recovery Approach: M dual-stage, multi evaporators/condensers.

Year	Methodology	No. of beds	Adsorbent	Rating conditions			SDWP [m ³ /ton/d]	COP [-]	PR [-]	SCP [R-ton/ton]	Ref.
				T _{reg-in} [°C]	T _{c-in} [°C]	T _{ch-in} [°C]					
2014	M+Sim	8	RD-SG	85	30	N/A	0.94	0.16	N/A	7.3	Mitra et al. [105]
	Salient features of the work						Findings and concluding remarks				
<ul style="list-style-type: none"> The cited study conducted numerical simulation in order to evaluate the efficacy of the dual stage adsorber bed configuration. In addition, the effect of inter stage pressure (P_{int-s}) was analyzed and identify its optimum range. Furthermore, the effect of t_{cycle} for air-cooled ADCS were evaluated from the perspectives of obtaining maximum throughput. 						<ul style="list-style-type: none"> Optimum P_{int-s} might be in between 4-5kPa. Beyond the optimum of P_{int-s}, 30% reduction in SDWP, and 20% reduction in COP could be confronted. t_{h-cycle} and t_{sw} opted 300s for simplifying the complexities in respective valve operation. Longer t_{sw} closer the beds to requisite regeneration and adsorption temperatures. 					
2015	ES+M+Sim	4	RD-SG	85	41	N/A	N/A	0.18		400**	Mitra et al. [103]
	<ul style="list-style-type: none"> The study proposed dual stage air-driven ADCS owing to address backflow of water vapors in single-stage air driven ADCS which reflects abrupt rise/drop of bed pressure on communicating with condenser/evaporator, respectively due to inappropriate t_{sw}. In addition, different switching time were investigated to address the backflow problem. 						<ul style="list-style-type: none"> Longer t_{sw} (600s) could address the backflow problem; however, it confers shorter sorption time and quantum drop of SDWP cycles per day. In dual-stage, the backflow phenomenon resolves due to P_{int-s} and dual adsorption (LP-stage-1 and HP-stage-2) process. The t_{sw} decreases with the increase in P_{evap}. Maximum COP was recorded 0.25 at t_{h-cycle} of 1800 s, while t_{sw} of 100 s. 				
2015	ES	6	RD-SG	85	42		0.68	0.235	N/A	670**	Mitra et al.
	<ul style="list-style-type: none"> The study conducts an experimental investigation on air cooled dual stage multi-evaporator configuration of ADCS. In addition, designing pros and cons and constructional elements were described in-depth. 						<ul style="list-style-type: none"> t_{h-cycle}/t_{sw} was deliberated 1800/200s. For stage-1 and stage2, P_{ads}/P_{des} were recorded 1/3kPa and 3/6.7kPa, respectively causes water vapors reflux due to small t_{sw}. 				

	<ul style="list-style-type: none"> Experimentally analyze the impact of influential parameters on the overall system productivity. 					<ul style="list-style-type: none"> 3-bed mode configure ~50% more specific throughputs comparative to 2-bed mode. High P_{evap} (1.7kPa) confers additional seawater evaporation. 						
2017	M+Sim	4	RD-SG	85	42	24	0.9	0.24	N/A	8.8	Mitra et al. [58]	
	<ul style="list-style-type: none"> The cited work determined the realistic minimum $T_{\text{hw-in}}$ in order to drive dual stage air cooled ADCS. In addition, the effect of rating conditions and influence of inter-stage pressure on the key performance indicators were analyzed. 					<ul style="list-style-type: none"> Adapted from linear extrapolation, it was reported that, for air-cooled ADCS, nadir $T_{\text{hw-in}}$ could be range between 46-52°C, depending upon the $T_{\text{ch-in}}$ (24-11.5°C). Optimum $t_{\text{h-cycle}}$ found 1800 s when $T_{\text{hw-in}} = 85$ °C, however mounted to 3000 s as the $T_{\text{hw-in}}$ drop 65 °C. High $T_{\text{ch-in}}$ compels high P_{evap}, governing more adsorption, and low-pressure drift ($P_{\text{cond}}-P_{\text{evap}}$), props system throughput. Owing to degrading the $T_{\text{hw-in}}$, steer to an increase in optimum $t_{\text{h-cycle}}$, response lowering the system-specific outcomes. 						
2016	M + Sim	4	AQSOA-Z02	85	30	N/A	15.4	N/A	N/A	46.6	Youssef et al. [110]	
	<ul style="list-style-type: none"> The cited work investigates dual stage configuration for communicating the ADS with integrated E-C device. The difference in the operating modes and relevant findings are given below: 											
	Mode A			Mode B			Mode C					
<ul style="list-style-type: none"> Ceased chilled water circulation in integrated E-C device. $T_{\text{evap}}/T_{\text{cond}}$ achieves 10/23°C, having net fractional uptake 0.18kg/kg_{AQSOA-Z02}. Maximal SDWP and SCP observed, 6.64 m³/ton/d and 46.6 R-ton/ton, respectively. 1.17 kW/m³ and 0.0061 kW/R-t energy consumption was estimated for SDWP and SCP, respectively. 0.169 US\$/m³ and 0.021 US\$/R-ton/d cost is estimated for SDWP and SCP, respectively. 			<ul style="list-style-type: none"> Unceased chilled water circulation in integrated E-C device, implicated with HRL. $T_{\text{evap}}/T_{\text{cond}}$ achieves 10/15°C, having net fractional uptake 0.250kg/kg_{AQSOA-Z02}. Maximal SDWP and SCP observed, 12.4 m³/ton/d and 32.4 R-ton/ton, respectively. 1.06 kW/m³ and 0.0055 kW/R-ton energy consumption was estimated for SDWP and SCP, respectively. 			<ul style="list-style-type: none"> Ceased chilled water circulation in integrated E-C device, implicated with HRL. $T_{\text{evap}}/T_{\text{cond}}$ achieves 3/9°C, having net fractional uptake 0.259kg/kg_{AQSOA-Z02}. Maximal SDWP and SCP observed, 15.4 m³/ton/d and 0.0 R-ton/ton, respectively. 0.94 kW/m³ and 0.0 kW/R-ton energy consumption was estimated for SDWP and SCP, respectively. 0.136 US\$/m³ and 0.0 US\$/R-ton/d cost is estimated for SDWP and SCP, respectively. 						

						<ul style="list-style-type: none"> • 0.154 US\$/m³ and 0.018 US\$/R-ton/d cost is estimated for SDWP and SCP, respectively. 					
2016	M+Sim	3	A ⁺⁺ SG	85	30	12.5/17.3	6.5	0.84	0.67	592**	Thu et al. [114]
	<ul style="list-style-type: none"> • The cited study investigated 3-beds employment with two evaporators operating at HP (2–3 kPa) and LP (0.6-1.2 kPa) following merry-go-round operational scheme. After LP_{evap} adsorption the bed switch to HP_{evap} in order to completely saturate the adsorbent material. 						<ul style="list-style-type: none"> • 2/3rd of t_{cycle} allocate for adsorption (1/3rd for LP_{ads} and 1/3rd for HP_{ads}) and rest for desorption. • t_{cycle}/t_{sw} opted 780/40s. • T_{ch-out} from LP_{evap}/HP_{evap} recorded 7.5/17.3 °C having capability to produce 7.1/10.8 kW cooling, respectively. • HP_{ads} uplifts ~44% saturation limit of A⁺⁺SG.LO09 • Promotes high T_{evap}, which steer more seawater evaporation and thereby pressurized adsorption. 				
2016	M+Sim	4	AQSOA-Z02+SG	85	30	14.8	15.76	0.53	0.52	47.8	Ali et al. [113]
	<ul style="list-style-type: none"> • The cited work proposed dual stage ADCS, comprising of two AQSOA-Z02-based adsorber beds for stage-1 and two SG-based adsorber beds for stage 2 interconnected with LP_{evaqp} and HP_{evap}, respectively. • In addition, HRL between HP_{evap} and condenser were installed to upscale the evaporation rate in stage-2 						<ul style="list-style-type: none"> • Stage-1 mutually produce, however low SDWP and high SCP, due to employment AQSOA-ZO2 while in stage-2 only desalinated water produce due housing of SG entail with HRL. • t_{h-cycle} for stage-1/2 were opted 400/300s. • T_{evap} and P_{evap} of stage-1 was recorded 9°C and 1kPa; respond more cooling due to high hydrophilic drift of AQSOA-Z02 at such conditions. • Due to HRL, T_{evap}/T_{cond} reach 33.5/24°C, responded more evaporation and condensation in respective vessels. 				
2	M+Sim	4	SG	85	30	30	8.01	0.87	0.55	66.88	A

					<ul style="list-style-type: none"> The study focused to evaluate the effect of longer adsorption time and shorter desorption time for the multi-bed, dual evaporator configuration in which evaporator operating at HP and LP, respectively. The HP_{evap} merely responsible for desalination while LP_{evap} produce high grade cooling. 	<ul style="list-style-type: none"> Authors reported that, due to faster desorption kinetics and slower adsorption kinetics assigning equal periods for both processes are not justifiable. For both HP_{evap} and LP_{evap} adsorption period of 1240 s are adequate, half for each while for desorption period 440 s found optimum. HP_{evap} and LP_{evap} capable to produce high-grade and low-grade cooling having T_{ch-out} of 18-20 °C and 8-11 °C, respectively. Configuration ensures 45% additional SDWP comparative to conventional ADS. 					
2020	M+Sim	3	RD-SG+CuSO ₄	85	25	25	12	N/A	0.67	450**	Ali et al. [117]
	<ul style="list-style-type: none"> The cited work contributed in a manner of integrating physical sorption (RD-SG) and chemical sorption (CuSO₄) processes for emphasizing the overall ADS productivity. 					<ul style="list-style-type: none"> HP_{evap}/LP_{evap} operated at 2.25/1 kPa, respectively. 30g/80g water vapor mass were adsorbed by RD-SG at LP_{evap}/HP_{evap}, respectively. From this configuration the SDWP, SCP and COP were manifested by 56%, 55% and 25%, respectively. Higher T_{hw-in} contribute more SDWP and SCP with minute drop in COP. Configuration allow to drive the ADCS even at 55°C with SDWP of 8m³/ton/d and SCP of 420R-ton/ton 					
2019	ES	2	N10-SG	75	20	20	6.76	N/A	N/A	37.05	Woo et al. [68]
	<ul style="list-style-type: none"> The cited study focused to evaluate the effectiveness of the perforated plates and spray nozzles as brine feeding mechanisms for the AD evaporator. In addition, the study analyzed the thermophysical properties of the N10-SG and determine its adsorption equilibrium profiles. Furthermore, effect of the brine salinity and operating pressures on the performance of the ADS were explored corresponding to varying the rating conditions. 					<ul style="list-style-type: none"> Authors reported that, automizer assisted AD evaporator capable to produce 14% to 25% more SDWP and 12% to 30% additional SCP which uprising the recovery ratio $\geq 83\%$. In addition, optimal $t_{h-cycle}$ decreases by 50 s due to incorporating spray nozzles. High T_{ch-in} mounting the evaporator pressure which accentuate the adsorption kinetics and upsurge the evaporation rate. The quality of produce water is comparable with deionized water. 					

2020	M+Sim	8	SG	85	25	25	9.6	0.76	N/A	49	Naeimi et al. [118]
	<ul style="list-style-type: none"> The cited work numerically analyzed the potential of the double-stage multi-bed, dual-evaporator with integrated E-C device. The low-pressure evaporator (LP_{evap}) and high-pressure evaporator (HP_{evap}) were installed to produce high grade cooling and maximize SDWP, respectively while integrated E-C device for capturing the latent heat of condensation. In addition, the study focused to evaluate the optimal cycle time for HP adsorption ($t_{LP,ads}$) and LP adsorption ($t_{HP,ads}$). 					<ul style="list-style-type: none"> For first stage, the temperature for HP_{evap}/LP_{evap} was recorded 20/10°C, responsible for low/high grade cooling, respectively. Temperature regime of integrated E-C device was observed between 25-31°C, which configure faster evaporation. $t_{LP,ads}$ and $t_{HP,ads}$ were allotted 660s each, while t_{sw} was 40s. Longer $t_{LP,ads}$ conducive for high-grade cooling due to extension of evaporation period, whilst reduce the hydrophilic gradient against HP_{ads}; thereby respond low-grade cooling from HP_{evap}. High/Low T_{ch-in}/T_{cond} for HX of $HP_{evap}/condenser$ were recommended to acquire maximum throughput, respectively. 					

Note:- **W/kg

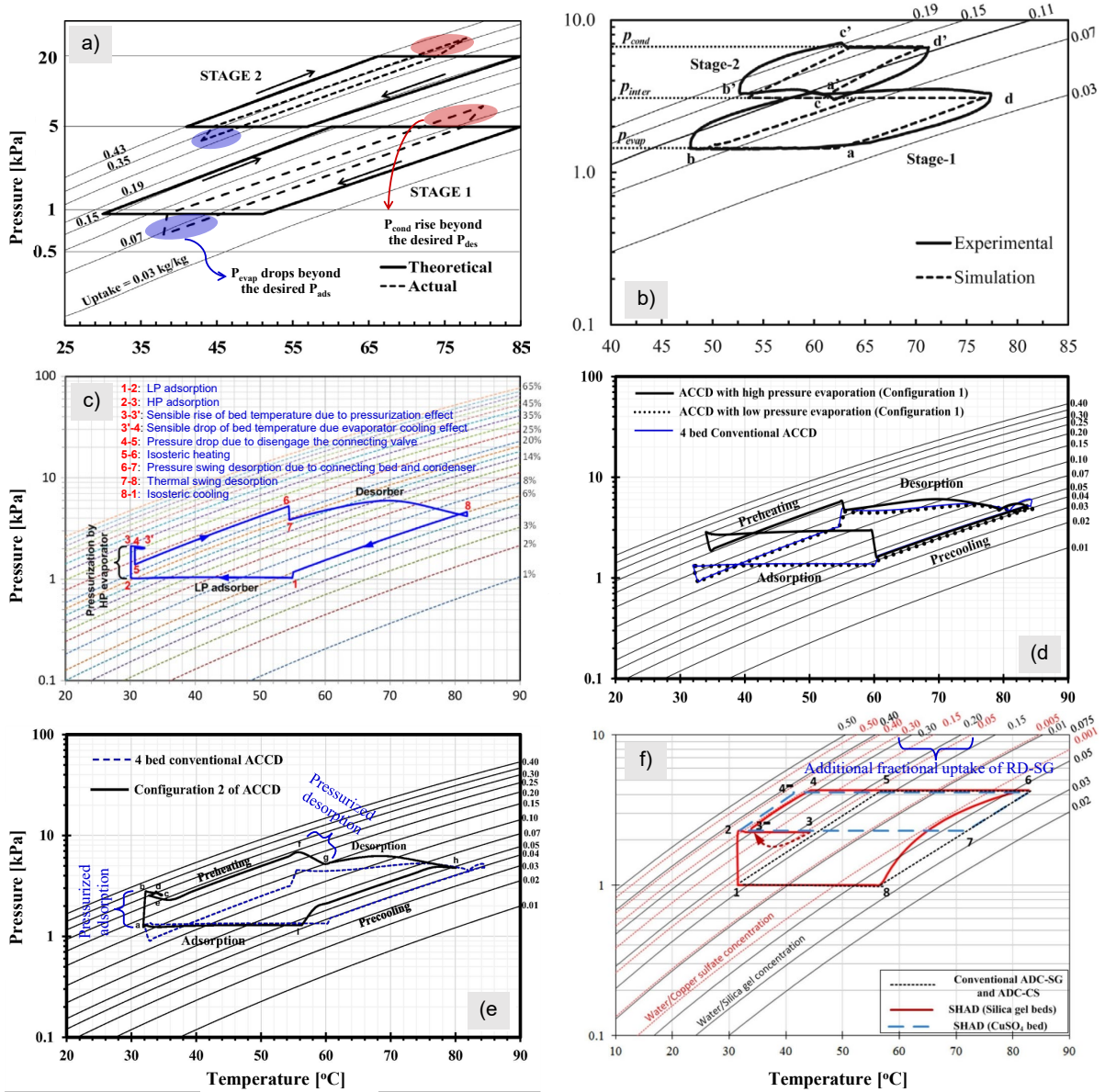


Fig. 25. Dühring diagrams acquired in response of progressive modification in ADCS. Here (a) and (b) are the cyclic response of air-driven ADCS with longer and shorter switching periods, respectively [103,105]. From (a) It was identified that longer switching period lowering/increasing evaporator/condenser operating pressure, accordingly which respond significant drop of SDWP and SCP. Whereas (b) highlights that shorter or optimum switching period allow the dual-stage configuration to operate at pre-designed operating pressures. (c), (d) and (e) depicts the impact of introducing HP evaporator which results instant pressurized adsorption and instant depressurized desorption, hence approximately double the fractional uptake of the same sorbent material [114,115,117].

Recently, few advance strategies were reported focusing on adsorbent porosity distribution [122], along with heat transferring kinetics, and geometry of embedded fined tube heat exchangers [123,124]. Proper fin spacing is crucial parameter and found sensitive to porosity distribution [122]. Having the fin size of 5mm and D3-F shaped porosity distribution,

determine 16.2% improvement in combined system performance. In addition, fork-row placement of fined tube heat exchangers in adsorber bed was recommended as compared to in-line placement [123]. Moreover, 6mm fin diameter assure high thermal conductivity which entail higher uptake. Similarly, retarding fin diameter (18.0mm-8.0mm), fin height (17.5mm-5.0mm), and fin spacing (11.6mm-3.6mm) uplifts the overall system productivity [124]. To conclude the section, it has been realized that, so far no optimistic heat exchanger has been designed/investigated for the ADS that ensue the minimal heat and mass transfer resistance. In addition, thickness of the adsorbent coating on the HXs are yet to be investigated in order to saturate and utilized the maximum number of pores spaces available for capturing the water vapors.

4.3 Hybridization Approaches

The Hybridization Approach refers to integrating the ADS/ADCS with commercialized and non-commercialized desalination technologies from the perspective of confronting the engineering shortcomings in both categories. So far, multi-effect desalination (MED), multi-stage flash (MSF), and reverse osmosis (RO) desalination technologies are highly permeated in the water markets. However, these technologies are equipped with environmental, and system level discrepancies; prominently low recovery ratio, and massive thermal and electrical energy consumption that need to be addressed at the best time. Otherwise, dramatic consequences happen which not even suffer the environment but also become problematic for the aquatic life. Owing to the waste-heat driven feature of ADS/ADCS, multiple commercialized and non-commercialized desalination facilities could be hybridized simultaneously with ADS/ADCS. In response, several studies are reported in the literature that integrates the ADS/ADCS with the commercialized desalination technologies which include MED+AD or MEDAD, RO+AD, and MEDAD+RO, etc. On the other hand, few studies relevant to the integration of the ADS/ADCS are also reported. For instance, integration of mechanical vapor compressor, and hybridization with humidification-dehumidification desalination cycle with ADS/ADCS are reported in extent. Another approach that is also viable to discuss in this section is termed as the integration of the ejectors (EJ) with ADS/ADCS. In the subsequent subsections, former hybridization approaches are discussed and compared based on their key performance indicators.

4.3.1 Integration with commercialized desalination systems

As formerly indicate that, the hybridization schemes proposed as a remedy to confront the drawbacks of commercialized desalination systems owing to develop an energy efficient seawater desalinator that produces high yield. The integration of the MSF desalination with ADS could possible. However few studies reported that the employment of the MSF system for desalination purpose is thermally, environmentally, and economically un-sustainable [125–129]. Therefore, no trace of such configuration was identified during literature survey. Fig. 26 gives the pictorial views of the experimental facilities and flow diagrams of MED and RO desalination system that were integrated with the ADS [130–134]. In MEDAD hybridization approach, the lower brine temperature (LBT) effect/stage communicated with the AD evaporator [125]. Due to hydrophilicity of the adsorbent material a cooling effect produces in the AD evaporator, which conveyed to the entire train of MED evaporators [127]. Consequently, noticeable drop in MED effects/stages operating temperature was identified which allow to interlock more evaporation stages/effects in MEDAD as presented in Fig. 27 [135,136]. Table 8 presents the findings and conclusions of the relevant studies that investigate the MEDAD configuration entail with HRL between AD condenser and TBT effect, both experimentally and thermodynamically.

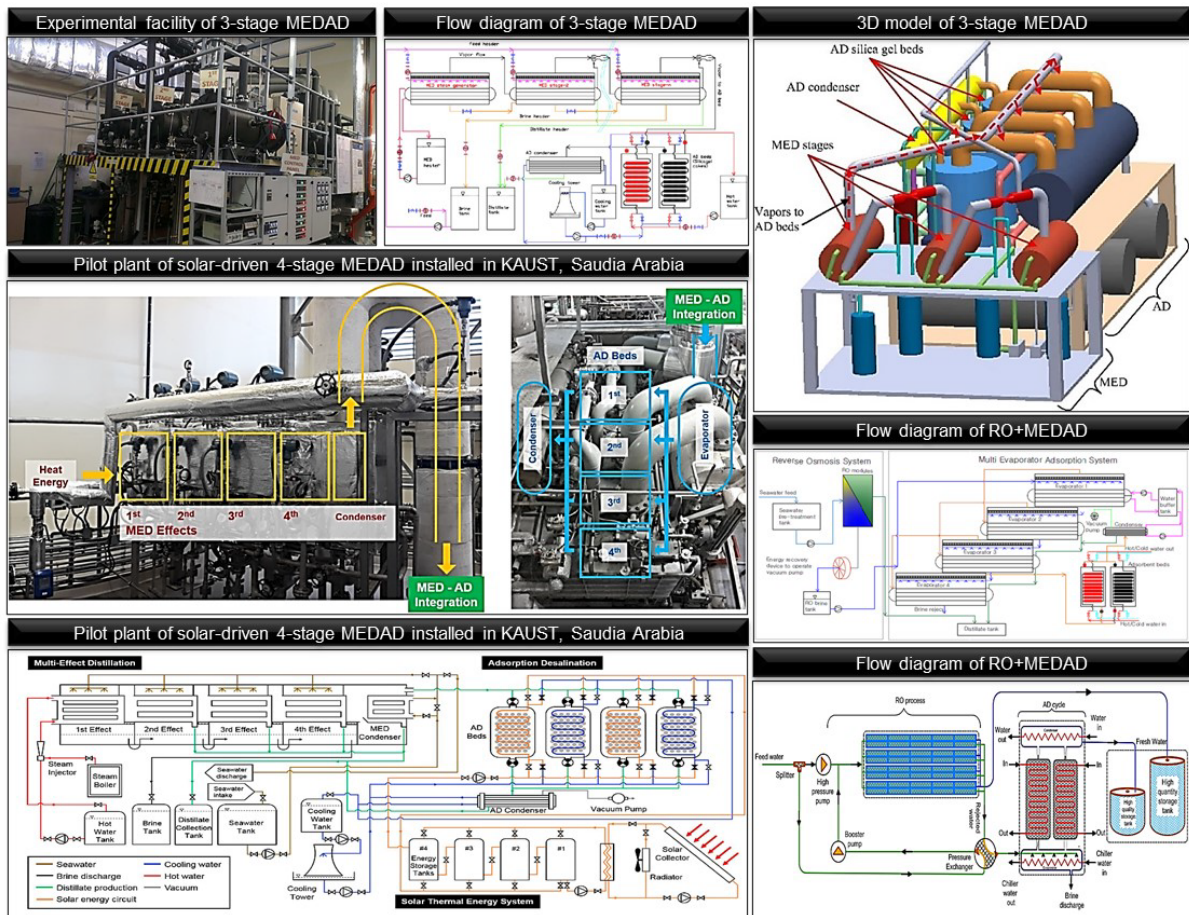


Fig. 26. Pictorial views and flow diagrams relevant to integration of the commercialized desalination technologies with ADS [130–134].

Similar to MEDAD, numerical studies were reported in the literature relevant to RO module hybridization with both ADS and MEDAD system, respectively. The RO module consumes massive electrically energy to create high pressure on one side of the membrane. Consequently, pressurized brine produced which was directed to TBT effect/stage of MEDAD system where latent heat of condensation captured from the AD condenser utilized to produce water vapors [133]. In some cases, a pressure exchanging module/device has been used to transmit the energy to the AD evaporator [134]. The flow diagrams of RO integration with the ADS and MEDAD is presented in Fig. 26. Table 8 presents the summary of relevant studies that theoretically analyzed the RO+MEDAD and RO+ADS.

Table 8

Summarization of the studies reported on ADS/ADCS working on the Hybridization Approach: Commercialized desalination systems.

Year	Methodology	No. of effects/stages	No. of beds	Operating conditions			Adsorbent	GOR [-]	WPR [kg/s]	PR [-]	Ref.
				T _{reg} °C	TBT °C	LBT °C					
2013	M+Sim	8	4	65–90	85	N/A	A ⁺⁺ SG	4.67	0.346	5.96	Thu et al. [125]
	Salient features of the work				Findings and concluding remarks						
<ul style="list-style-type: none"> The cited work numerical investigate the MEDAD system from the perspectives of operating the MED system beyond its thermodynamic restriction. In addition, the study incorporates 8 MED effects with the ADS and explore desalinated water production potential corresponding to different rating conditions. 				<ul style="list-style-type: none"> MEDAD stages were found functional even below 30°C. The cooling impact due to adsorption, propagated to all stages, resulting in lowering the evaporation temperature. 12-18 additional stages/effects could be connectable with the MED due to establishing low pressure by ADS in the last effect. The integration approach could revitalize the MED system, significantly increase the WPR and minimize the desalination cost. 							
2014	M+Sim	8	N/A	N/A	65	5	A ⁺⁺ SG	N/A	0.083	7.3	Shahzad et al. [130]
	<ul style="list-style-type: none"> The cited work reported another simulation-based study on MEDAD system that provide insights on the primary energy used. In addition, the study identifies the operatable thermodynamic boundary for the LBT. 				<ul style="list-style-type: none"> The MEDAD system reduce the LBT up to 5 °C as compared to 40 °C in MED system. Interstage-temperature difference in MEDAD was recorded 2-3°C as compared to 1 °C in MED system. The WPR of MEDAD system manifested by 3 folds at the same TBT if compared to standalone MED system. The maximum payable energy was reported 28 kWh. 						
2014	M+Sim	12	4	85	90	9.82	A ⁺⁺ SG	8.8	0.8	9.19	Thu et al. [127]
	<ul style="list-style-type: none"> The cited work published a numerical analysis that explored the viability and impact of using various MED effects or phases in conjunction with the ADS. The performance was analyzed based on the transient response of MED effect temperatures, WPR and GOR. 				<ul style="list-style-type: none"> In conventional MED system, additional 4 stages surely integrate able that operating below 20°C. Additionally, there is a room to recover the condensation heat, reutilize in intermediate stages and interlock additional stages, for decreasing the LBT (up to 5°C). 40% improvement in GOR and 122% in WPR could be achievable with MEDAD configuration using 12 MED effects/stages. 						
2	ES	3	3	55-85	38	30	A ⁺⁺ SG	N/A	0.033	N/A	S

						<ul style="list-style-type: none"> • The cited work experimentally analyzed the MEDAD configuration at assorted primary heat source (15 to 70 °C). • In addition, freshwater production potential was determined and compared with the standalone MED system. 	<ul style="list-style-type: none"> • Due to hydrophilicity of the adsorbent material the operating temperature of the MED effects/stages decreases by 3 °C to 4 °C. • WPR boosted by 2.5 to 3 folds in relation to MED system. • The primary energy was recorded 14.5 kWh/m³ that can be comparable with RO plants. • The MEDAD configuration can be stretchable even up to 18 effects having WPR of 0.0945 kg/s with LBT of 8 °C, vis-à-vis to 10 effects/stages for MED system with LBT of 40 °C. 					
2015	M+Sim	7	4	85	<35		8	A ⁺⁺ SG	5.1	0.41	6.3	Thu et al. [137]
	<ul style="list-style-type: none"> • The cited aimed to further improvised the performance of the MEDAD by developing HRL between TBT effect/stage to the AD condenser. The capture heat during the condensation process was utilized to operate the effects/stages from 1st to last. No additional heat was supplied to the effects. • In addition, the study developed an ideal close cycle (P-T-w) diagram for MEDAD system. 						<ul style="list-style-type: none"> • All the MED effects operated below 35 °C with an average temperature difference range between 5 °C to 10 °C. In LBT effect the temperature was recorded 8 °C. • The MED effects/stages were driven with condensation heat, resulting in an oscillating cyclic pattern of WPR. • Higher T_{reg} and shorter sorption time increase the MEDAD throughput capacity. • For each set of T_{hw-in}, optimum t_{h-cycle} and number of MEDAD stages varies and need to be selected intelligently from Ref [60]. 					
2020	ES+M+Sim	4	4	60	49.4		19.0	A ⁺⁺ SG	N/A	0.1157	60*	Son et al. [132]
	<ul style="list-style-type: none"> • The cited work perform experimentation on solar-driven MEDAD system using red seawater. • In addition, thermodynamic model was developed that incorporate the film-boiling evaporative model and flash evaporation mechanism which were not investigated in previous synergetic models. 						<ul style="list-style-type: none"> • WPR boomed; 3-5 folds due to engaging flash evaporation. • Only 0.68kW payable energy has been consumed by MEDAD, whereas non-payable energy has been scavenged from ambient via solar thermal system. • 44% and 56% evaporation produce from thermal heating and flash phenomenon, respectively. 					
2017	M+Sim	4	2	85	35		<10	SG	N/A	0.025	N/A	Shahzad et al.
	<ul style="list-style-type: none"> • The cited work integrates the commercialized RO desalination system with MEDAD by developing a numerical model for investigating the feasibility and provide insights on its various influential aspects. 						<ul style="list-style-type: none"> • AE90 membrane has been equipped in RO module having 30% recovery ratio, emitting 50,000 ppm retentate which later directed to 1st effect. • The effect has been driving with 35°C heat source, recovered its major portion from latent heat of condensation. 					

						<ul style="list-style-type: none"> • Inter-stage temperature difference noticed 5-6°C. • the MED effects/stages operated below 28 °C. with LBT of 12 °C. • The average WPR from MEDAD recorded 0.025 kg/s whereas RO module produced 0.0142 kg/s. • Overall, the tri-synergetic approach proves 81% water recovery, consuming 1.76 kWh_{elec}/m³. 				
2018	M+Sim	7	2	85	64.2	48.9	A ⁺⁺ SG	16	110.45	N/A
	<ul style="list-style-type: none"> • In cited work, authors, optimize WPR, water cost (C_w) and energy destruction (d_e) of tri-hybrid system (MEDAD+RO) using genetic algorithms. 					<ul style="list-style-type: none"> • 82% of total supplied energy, destructed by MED, whereas RO and AD contributes 3% and 15% share, respectively. • Thermal desalination necessitates precise system insulation and specialized HX material, for least energy destruction during heat transfer. • WPR, C_w and d_e were optimized to 176.4 kg/s, 0.88 \$/m³ and 7494 kW by manipulating specific parameters mention in Ref. [136]. 				
2018	M+	NR	2	85	NR	NR	RD-SG	N/A	277.84	N/A
	<ul style="list-style-type: none"> • The cited work explores RO+ADS configuration from the perspectives of re-capturing the pressurized energy and improvised the overall recovery ratio. • In addition, the study explores the economic feasibility of the proposed configuration. 					<ul style="list-style-type: none"> • AD evaporator found insensitive to fed high saline concentrations. • High temperature and saline concentration put adverse impact of RO module. • Configuration capable to produce 24,000 m³/day low grade water and 6 m³/ton/d high grade potable water adjacent with 75 R-ton/ton cooling potential. • Minimum energy required for receiving mentioned attributes were stated 0.8 kWh/m³. 				

*Universal performance ratio defined in the cited work [138–140], NR~Not required, N/A~Not Available

Fig. 27 (left) presents the generalized conception of the MED integration with ADS and highlight the relevant benefits. The MEDAD configuration found operational even below ambient temperature (5 °C), however experimentally validated up to 8 °C [137]. The study recommends the interconnection of 12 additional effect/stages which gearing 90% improvement in WPR [127]. Furthermore, heat recovery loop between ADS condenser and 1st effect of MED were put noteworthy improvement in GOR, PR and WPR [137,141]. Fig. 27 (right) presents the P-T-w diagram of the MEDAD configuration which employing the seven MED effects/stages. It can be realized that, with seven stage/effect MEDAD, the LBT reached upto 10 °C having 100% saturation. On the other hand, RO+MEDAD configuration was reported as promising solution which pushing the recovery ratio to higher levels ~81% [133].

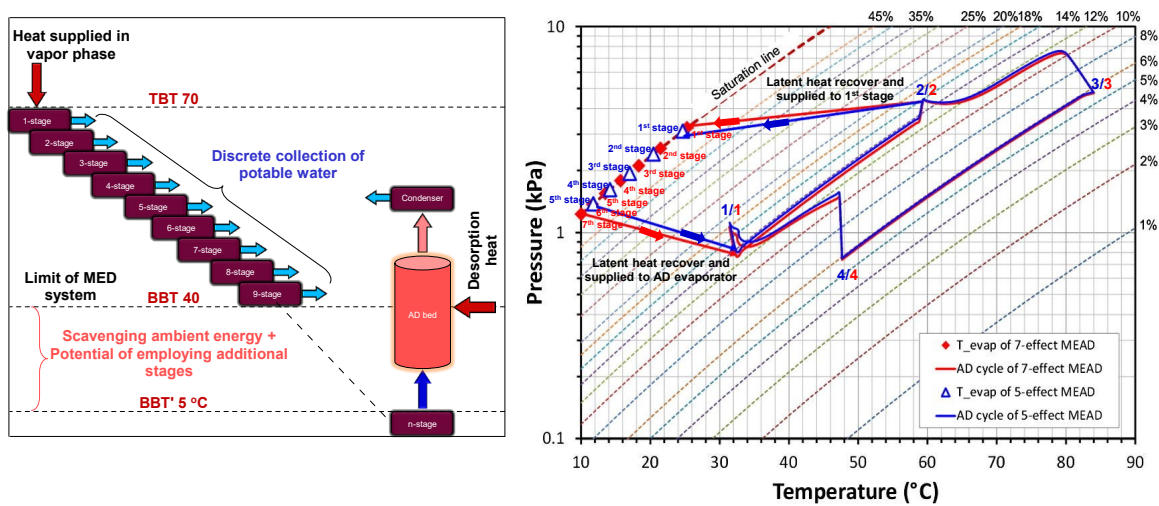


Fig. 27. Generalized conception of MEDAD configuration (left) and P-T-X diagram of 5-stage and 7-stage MEDAD system (right). From the P-T-X diagram it has been observed that all the stages/effects are operating closer to saturation limit of adsorbent material [135,142].

4.3.2 Integration with non-commercialized desalination technologies

From literature review various studies were identified and explored which mainly integrates the non-commercialized desalination systems with ADS/ADCS. The motivation of such studies was to increase the performance and improvised the system productivity in a sense of manufacturing a sustainable, highly productive, and energy efficient, desalination technology. In this context, few studies are cited and discussed in the section for the completeness.

Askalany et al. [143] reported a novel configuration for adsorption cycle that integrates the mechanical vapor compressor (MVC) with the conventional ADS (MVC+ADS). The ideal communication locality for the compressor was proposed between the condenser and

desorption bed as shown in Fig. 28 (a). If compared to conventional ADS, the MVC+ADS completes one desalination cycle in six phases as shown in Fig. 28 (b). The six-phase operational scheme allows the MVC+ADS to increase the adsorption capacity of the adsorbent material and provided ease for phase transition of the desorbed water molecules in the condenser via mounting the saturation pressure and temperature during compression [143]. Fig. 28 c) gives the P-T-w of the MVC+ADS in comparison with conventional ADS. One can identified that, the configuration significantly drops the P_{cond} and increase the adsorption capacity upto few folds.

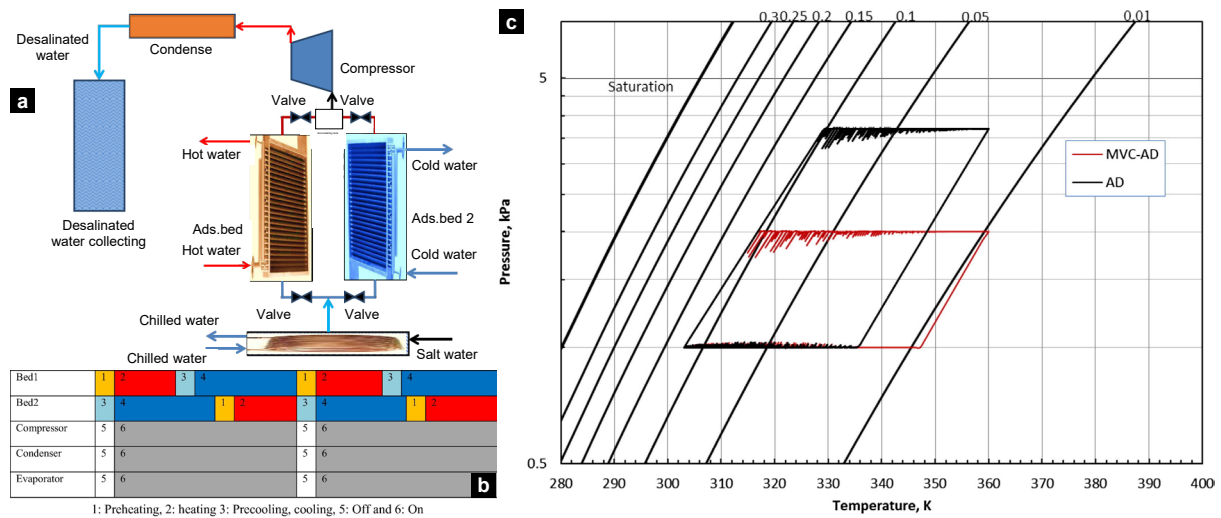


Fig. 28. a) Flow diagram of the MVC+ADS, b) operating scheme of the MVC+ADS, and c) P-T-w diagram of the MVC+ADS in comparison to conventional ADS [143].

Similarly, several studies reported ejectors (EJ) integration with the conventional AD cycle from the viewpoints of achieving maximum increasing the desalinated water production rate. Generally, the ejectors contain two inlet nozzles: (i) primary nozzle, (ii) secondary nozzle and one outlet nozzle [144]. The primary nozzle is connected with the pressurized compartment which is the desorption bed in case of ADS, and secondary nozzle connected with evaporation. In response of pressurized flow from the desorption bed, a vacuum or pressure drift is created in the secondary nozzle, consequently, additional water vapors are scavenged from the evaporator. The outlet of ejector is than connected to the condenser which produces condensate to acquire the freshwater [145] Fig. 29 presents the different arrangements of both single and double stage entail with single and multiple ejectors. One can find the additional details and performance of EJ integration with adsorption cooling system and refrigeration cycles from the cited references [146–149]. Table 9 contains the salient features of relevant work entail with their findings and conclusions.

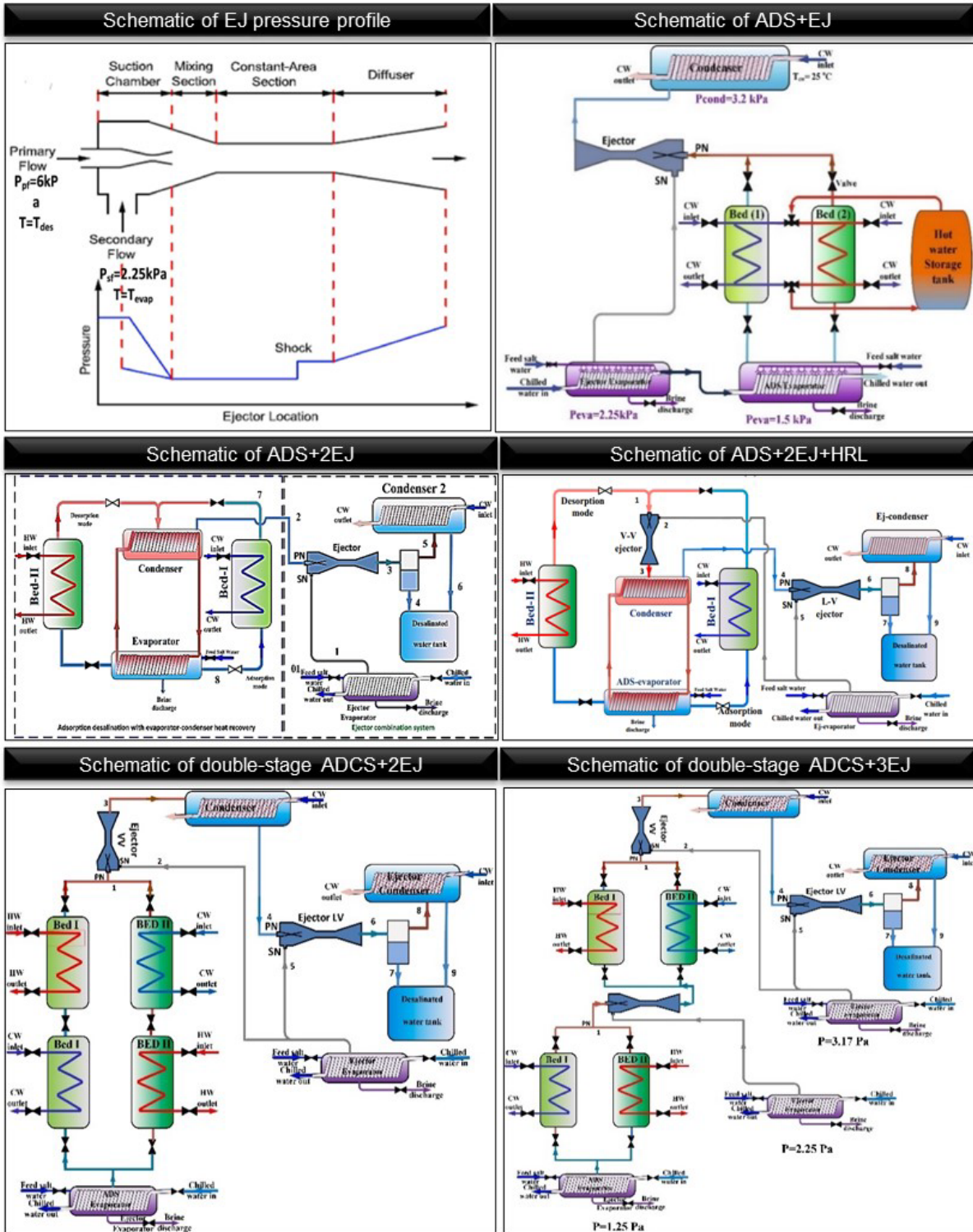


Fig. 29. Different arrangements of ejector integration with ADS reported in literature [143,145,150]

Table 9

Summarization of the studies reported on ADS/ADCS working on the Hybridization Approach: Non-commercialized desalination systems.

Year	Methodology	No. of beds	Adsorbent	Operating conditions			SDWP m ³ /ton/d	COP -	PR -	SCP W/kg	Ref.
				T _{h-in} °C	T _{c-in} °C	T _{ch-in} °C					
2016	M+Sim	2	SG	90	27	27	14	0.6	N/A	210	Askalany et al. [143]
	Salient features of the work						Findings and concluding remarks				
<ul style="list-style-type: none"> The cited work proposed and investigates MVC+ADS as a trial for increasing the freshwater productivity. In addition, an ideal thermodynamic response of the MVC+ADS was analyzed and compared with the P-T-w diagram of the conventional ADS. In addition, the impact of rating conditions on the key performance indicators were computed based on developing numerical model. 						<ul style="list-style-type: none"> In comparison to a standalone AD system, MVC synergy allowed more desalination cycles per day entail with high operational adsorption capacity. In MVC+ADS cycle the operating pressure of condenser was found 4 kPa significantly lower from the P_{cond} of conventional ADS. Similar increasing pattern of SDWP, COP and SCP were noticed, with slightly higher pace, corresponding to varying T_{hw-in}, as observed in conventional ADS. 					
2020	M+Sim	2	SG	95	N/A	25	25 ^a /40 ^b	0.78 ^a /1.1 ^b	N/A	N/A	Askalany et al. [145]
	<ul style="list-style-type: none"> The cited study first time proposed and analyzed the novel ADS+EJ^a and ADS+EJ+HRL^b. Effect of T_{hw-in} on ER were analyzed. In addition, the optimum CR value for ejector was explored. Furthermore, the study developed numerical model for estimating the SDWP and COP of the proposed hybrid desalination system. 						<ul style="list-style-type: none"> Average ER and CR were acquired 0.5 and 1.42, respectively. Optimum entrainment pressure for ADS+EJ and ADS+EJ+HRL opted 2.25 and 4.2 kPa, respectively. ER stated insensitive to T_{hw-in}. Optimum throughput with and without HRL determined at t_{h-cycle} of 400s 				
2020	M+Sim	2	SG	95	25	25	52.67	N/A	1.47	250	Ali et al. [61]
	<ul style="list-style-type: none"> The reference study proposed two configurational schemes for integrating the EJ with ADS and ACS which can be acronym as; (i) ADS+EJ+HRL and (ii) ACS+EJ. A hybrid numerical model was developed and validated with the standalone AD and EJ models for theoretically analyzing both configurations. 						<ul style="list-style-type: none"> Authors found average percentage error in acceptable range with value of 2.65%, 3.34%, and 3.90% in COP, SCP and SDWP, respectively. ADS-evaporator and EJ-evaporator driving temperature values were simulated 20°C and 22°C, respectively. At least 55°C T_{hw-in} found efficient to drive the proposed ADS+EJ+HRL configuration. 				

2020	M+Sim	2	SG	95	25	25	23.0 ^a /79.4 ^b	1.64 ^a /2.2 ^b	N/A	N/A	Askalany et al. [151]
	<ul style="list-style-type: none"> The cited work proposed two distinct arrangements for integrating the 2-EJ with ADS: (i) ADS+2E^a, and (ii) ADS+2EJ+HRL^b. The performance of both configurations were theoretically analyzed and compared in terms of SDWP and COP corresponding to varying the operating conditions. 					<ul style="list-style-type: none"> Longer $t_{h-cycle}$ reduce SDWP, due to reduction in entering of desorb water vapors in EJ primary nozzle. For both configurations, optimum $t_{h-cycle}$ was found 400 s. SDWP of ADS+2EJ measured 3.0 times higher comparative to standalone ADS and could be drive at 65°C. ADS-2EJ-HRL configuration could be drive as low T_{reg} (55°C) with significantly high SDWP comparative to conventional ADS. 					
2021				85	30	25	24.6 ^a /34.1 ^b	1.0 ^a /1.8 ^b	N/A	N/A ^a /290 ^b	Ali et al. [150]
	<ul style="list-style-type: none"> The cited work proposed dual stage (2S) with multiple EJ integration with ADCS. Two configurations were analyzed varying with number of EJ and their positions in the AD cycle. The configuration acronym as (i) 2S+ADCS+2EJ^a, and (ii) 2S+ADCS+3EJ^b. In addition, the key performance indicators were analyzed corresponding to varying the rating conditions. 					<ul style="list-style-type: none"> Authors reported, both configurations were operatable even at 45 °C, however with minimal SDWP (2.34 to 3.0 m³/ton/d), and COP (0.54 to 0.70). In terms of acquiring cogenerating features, 2S+ADCS+2EJ outperformed as compared to 2S+ADCS+3EJ due to high evaporator pressure. 					

The entrainment ratio (ER) and compression ratio (CR) was reported as the most influential features in EJ driven ADS. Higher ER configure more SDWP. The configuration proves 61% improvement in SDWP [145]. The maximum SDWP that could be acquired from ejector driven ADS is 80 m³/ton/d [151]. The idea of employing the ejector within the adsorption desalination cycle has proved its worth in a sense of increasing the daily water productivity by 51% [145]. Fig. 30 presents a comparison between the different ejector integrated ADS based on the SDWP and COP. Among all the reported ejectors driven ADS, one can realized that, ADS+EJ+HRL configuration can produce maximum SDWP (80 m³/ton/d) with COP greater than 2.0.

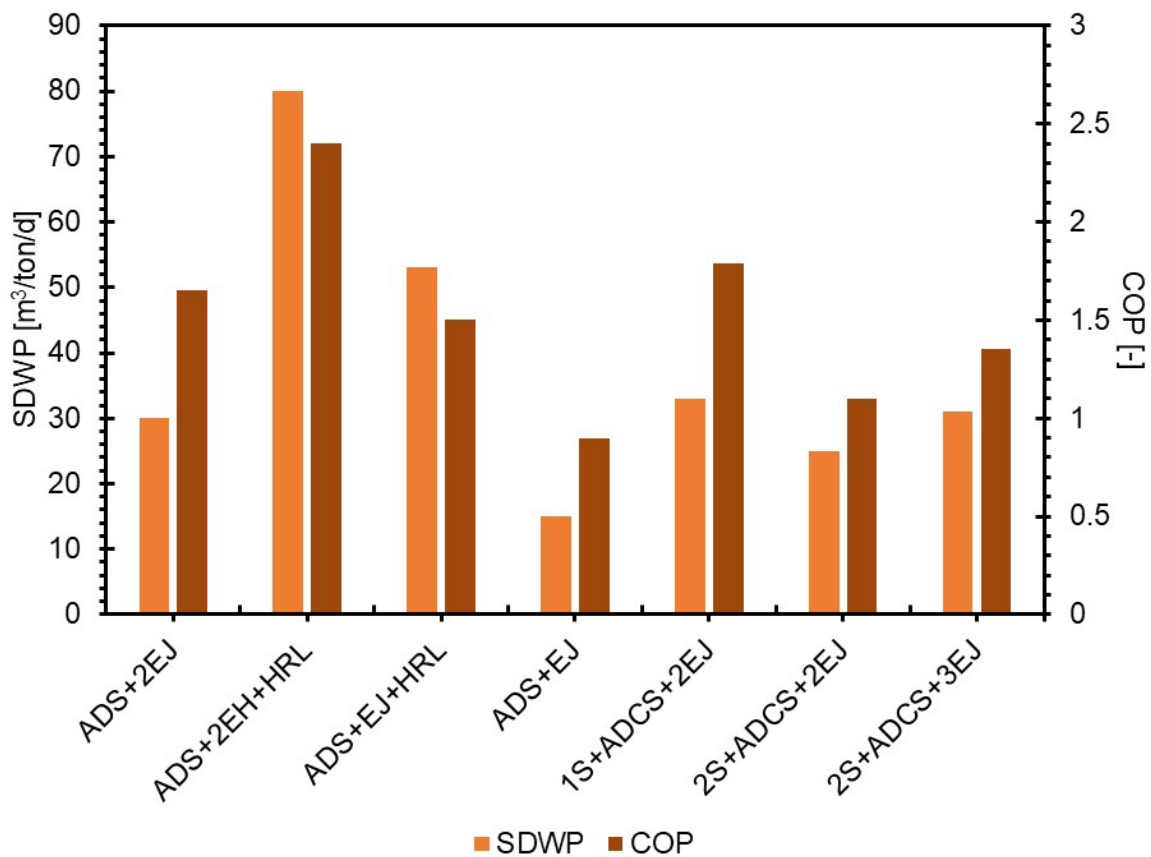


Fig. 30. Comparison between the reported ejector driven desalination based on the SDWP and COP.

From relevant literature survey, it has been realized that commercialized desalination technologies have massive footprint in desalination markets. However, these systems are equipped with thermodynamic boundaries and system level discrepancies that lowering the overall efficiency. The integration of the ADS/ADCS aided the commercialized desalination system in manner of capturing their waste heat and re-utilized for producing additional water from AD cycle. The contribution of freshwater production from the ADS/ADCS very minute as compared the studied integrated desalination technology. In addition, the cooling potential

of the ADCS was compromised because of its utilization for lowering the MED effects/stages temperature. Therefore, no remarkable improvement in AD cycle observed, however give benefits to the commercialized desalination technologies in a sense of extracting their thermal wastes. On the other hand, if focused on the integration of the ADS/ADCS with non-commercialized desalination technologies it has been explored, all the proposed schemes were investigated based on developing a numerical model. No experimental facilities are developed so far, that validate the feasibility of ejectors integration with ADS/ADCS. Therefore, a vast research avenue is still present in order to emphasize the system productivity.

4.4 Adsorbents Substituting Approaches

The AD Adsorbents Substituting Approach refers to the substitution of conventional silica-gels with the emerging adsorbents. In this context, compacted lab-scale prototypes were developed as shown in Fig. 31 in order investigate and compare the various adsorbent materials which belongs to different classes. Zeolites, MOFs, support ionic liquids are the potential adsorbents that has been extensively investigated for ADS/ADCS. For instance, the cited references explore the compatibility of zeotypes i.e., AQSOA-Z series [49,52,113,152–155] and FAM-Z series [50,51,70,156,157]. It has been reported that, for standalone adsorption cooling (AC), AQSOA-Z01 could be a promising adsorbent that improvised SCP even at low regeneration temperature ($T_{reg} < 60^{\circ}\text{C}$) [50,71]. The AQSOA-Z02 could be suitable candidate for ADCS however at low T_{evap} ($< 20^{\circ}\text{C}$) values comparative to RD-SG which utilizes high $T_{evap} > 20^{\circ}\text{C}$ [71,158]. On the other hand, AQSOA-Z05, found promising outputs for ADS due to sustaining high adsorption pressure and S-shape isotherm [50]. In case of FAM-Z series, FAM-Z05 is found relatively better than FAM-Z01/02 at low $T_{reg} < 55^{\circ}\text{C}$ [51]. Recent study reveals that synergy of CHA and AFI zeotypes doping with MOFs could mounting the adsorption capacity and faster the adsorption kinetics by 2 and 1.2 folds respectively [159]. Table 10 provide a comprehensive discussion on such reference studies that employ the zeolites in ADS/ADCS as an alternative adsorbent.

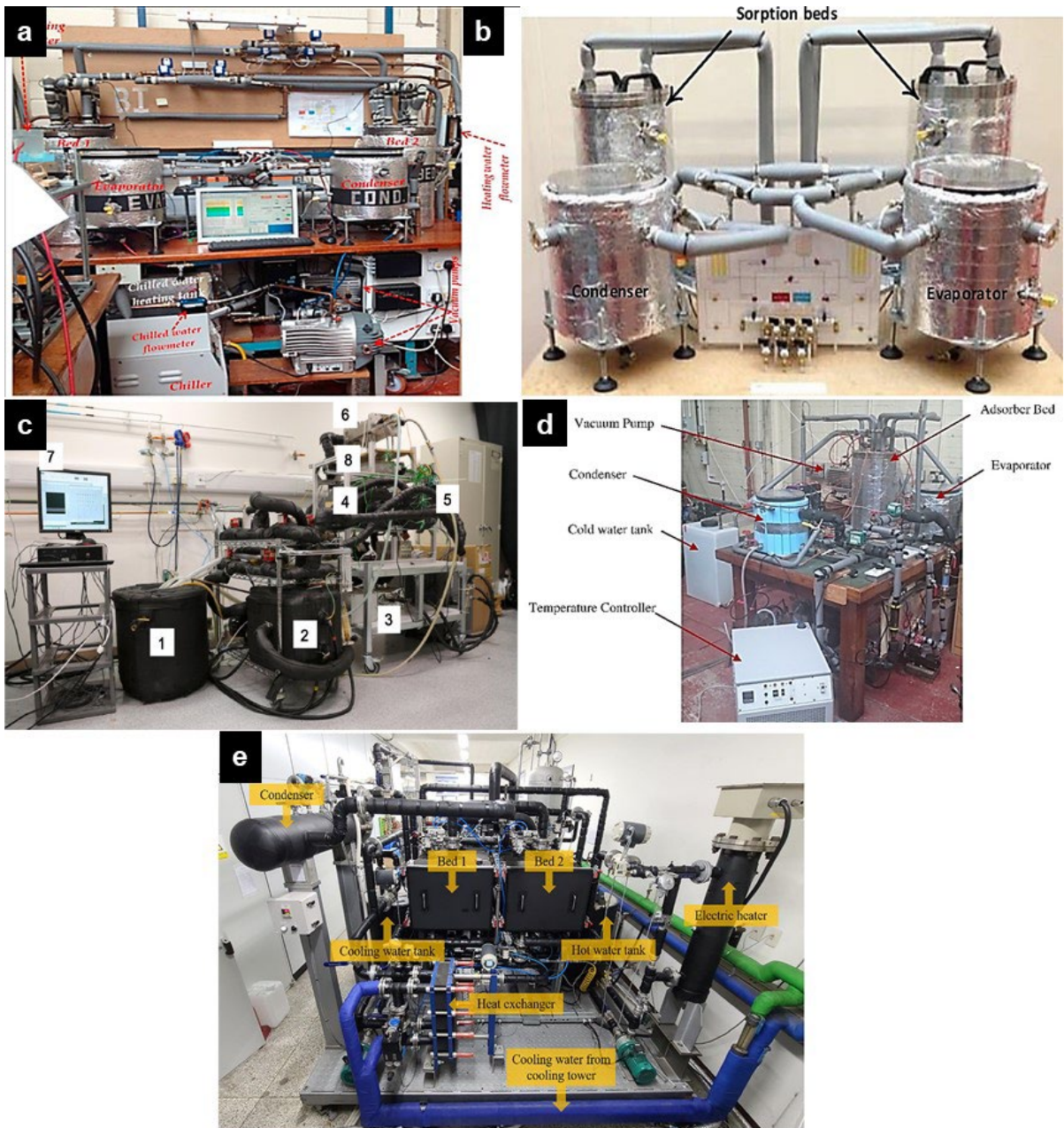


Fig. 31. Pictorial view small scale adsorption based desalinators employed for investigating the different adsorbent materials for ADCS installed in: (a) University of Birmingham, UK [79,80] (b) Sohag University, Egypt [160], (c) City University of Hong Kong, Hong Kong, China [161] (d) University of Birmingham, UK [162] (e) Hanyang University, Republic of Korea [51]

Table 10

Summarization of the studies reported on ADS/ADCS working on Adsorbents Substituting Approaches.

Year	Methodology	No. of beds	Operating conditions			SDWP m ³ /ton/d	COP -	PR -	SCP R-ton/ton	Ref.	
			Adsorbent	T _{hw-in} °C	T _{c-in} °C						T _{ch-in} °C
2015	M+Sim	4	AQSOA-Z02	85	25	20	7	N/A	N/A	53.7	Youssef et al. [71]
			RD-SG				6.8			15.0	
	Salient features of the work					Findings and concluding remarks					
<ul style="list-style-type: none"> The cited study focused to investigate AQSOA-Z02 adsorbent, manufactured by Mitsubishi plastics for ADCS. The effect of rating conditions were investigated corresponding to key performance indicators and compared with RD-SG adsorbent. 					<ul style="list-style-type: none"> For low T_{hw-in} (≤75°C) RD-SG found competent and respond more adsorption at high T_{evap} (≥20°C). RD-SG was recommended for systems having high T_{evap} (≥20°C). However, AQSOA-Z02, more favored for low T_{evap} (<20°C) with objectives of acquiring cooling and fresh water. 						
2016	M+Sim	2	MIL-101(Cr)	150	25	20	11	N/A	N/A	89.7	Elsayed et al. [73]
			Al-Fumarate	90			6.3			51.8	
			CPO-27(Ni)	150			4.6			38.1	
<ul style="list-style-type: none"> The cited study was focused to investigate the CPO-27(Ni) manufactured by Johnson Matthey and Al-fumarate manufactured by MOF technologies for ADCS. In addition, the authors synthesized another adsorbent MIL-101(Cr) which was also analyzed to emphasize the system productivity. The objective of the study was based on characterization of mentioned MOFs experimentally as well as material studio software. 					<ul style="list-style-type: none"> t_{h-cycle}/t_{sw} opted 700s/70s for CPO-27(Ni) and Al-Fumarate, while 300s/30s for MIL-101(Cr). CPO-27(Ni) imitates type-I isotherm, thereby appears an invariable rise in SDWP in response of high T_{evap}. Al-Fumarate and MIL-101(Cr) imitate type-IV, which reflects more adsorption at high T_{evap}. MIL-101(Cr) could be suitable for twin advantages only if a high heating source (90-150°C) were accessible. 						
2017	ES+M	1	CPO-27(Ni)	95	15	10	23	N/A	N/A	216	Youssef et al.

2016	M+Sim	2	CuSO ₄	80	25	25	8.2	0.57	N/A	227**	Ali et al. [163]
	<ul style="list-style-type: none"> The cited study determining the adsorption equilibrium and adsorption kinetics of CuSO₄ adsorbent for ADCS. The study performs modeling and analyze the material feasibility at assorted rating conditions. 					<ul style="list-style-type: none"> The dehydration reaction of CuSO₄ allow the material to adsorb and desorb the water vapors. The dehydration rate of CuSO₄ founds 97% at 25 °C temperature. Minimum T_{reg} required for desorption ranges between 70-75°C. t_{h-cycle} opted 450s. The CuSO₄ as a suitable candidate in comparison with SG for ADCS. 					
2019	ES	2	Emim-Ac/Syloid 72FP	60	30	25	25	N/A	N/A	N/A	Askalany et al. [164]
	<ul style="list-style-type: none"> The cited manufactured novel support ionic liquid composite material: (i) Syloid AL-1FP, (ii) Syloid 72FP are impregnated with Emim-Ac and Emim Oms. The study computes the thermophysical properties, adsorption equilibrium, perform modeling and analyze the optimistic adsorbent material for ADS. 					<ul style="list-style-type: none"> Authors, investigates Emim-Ac/Syloid 72FP (ionogel) for ADS. Due to high thermal conductivity, t_{h-cycle} reduces up to 5 folds (300s) comparative to reference studies [60,71]. The sorbent can be even regenerated at ambient temperature (25°C) with SDWP 6.5 m³/ton/d [165,166]. Emim-Ac/Syloid 72FP shows maximum uptake of 1.0 kg/kg. 					
2020	ES	2	Al-Fumarate	90	30	-	8.5	N/A	N/A	72.22	Elsayed et al. [79]
	<ul style="list-style-type: none"> The reference study aimed to experimentally investigate the Al-Fumarate for ADCS. The parametric study was conducted to evaluate the system performance corresponding to varying the rating conditions. In addition, the water quality and cost analysis are conducted and compared with the other commercialized desalination technologies. 					<ul style="list-style-type: none"> t_{h-cycle}/t_{sw} opted 900/70s, respectively. Higher T_{ch-in} reflects more SDWP and SCP due to increment of T_{evap}; thus more evaporation and cooling. Low T_{c-in} to adsorption-bed/condenser captures more adsorption-heat/latent-heat, thereby high fractional uptake/more condensate, respectively. Al-Fumarate could be a potential substitute for SG, especially for ADCS. Al-Fumarate integrated ADCS could be drivable even at 70 °C. 					
2020	ES	2	MIL-100(Fe)	95	30	20	19	N/A	N/A	226**	AL-
			CPO-27(Ni)	95			11			136**	
			Al-Fumarate	90			13				

	<ul style="list-style-type: none"> The cited study focused to investigate the characteristics of three MOFs and explore their thermophysical properties. The performance of the adsorbent material are compared based on SDWP and SCP. 				<ul style="list-style-type: none"> MIL-101(Cr) possesses low heat conductivity, reflecting more t_{sw} and $t_{h-cycle}$ hence more energy consumption. $t_{h-cycle}/t_{sw}$ opted as 700s/70s, respectively. MIL-101(Cr), MIL-100(Fe) and Al-Fumarate found suitable candidate for standalone ADS whereas, CPO-27(Ni) for AC. 						
2020	ES+M+Sim	2	Zeolite 13X/CaCl ₂	85	24	14	18	0.33	N/A	490**	Bai et al. [161]
	<ul style="list-style-type: none"> The cited study aimed to investigate the effect of seawater salinity of SDWP and SCP using a composite adsorbent. A comprehensive numerical model was developed that include the effect of mass recovery, preheating/precooling, and salinity as an influential aspects. 				<ul style="list-style-type: none"> During the static rating conditions the saltwater with high salinity degrade the system productivity both lowering SCP and SDWP. $t_{h-cycle}/t_{sw}/t_{pe}$ were opted 480s/40s/22s, respectively. 29%/49% reduction in SCP/SDWP was recorded as saline concentration varies from 0-100g/kg due to low evaporation rate. In addition, high saltwater mass flow rate decreases the COP (~46%), SCP (~43%) and increase the SDWP (~19%). 						
2021	ES	2	CPO-27(Ni)	95	25	N/A	9.5	0.43*	N/A	N/A	Askalany et al. [160]
	<ul style="list-style-type: none"> The cited study experimentally investigates the suitability of the CPO-27(Ni) adsorbent for ADS. In addition, two different condensing devices namely, (i) finned tube mesh shape and (ii) coil tube shape were evaluated. The effect of rating conditions were analyzed on the system productivity. Furthermore, the study investigated the HX coated with CPO-27(Ni) as an adsorption/desorption bed to improvise the heat transmission. 				<ul style="list-style-type: none"> CPO-27(Ni) possess high T_{reg} (95-120°C), comparatives of SG. $t_{h-cycle}$ and t_{sw} opted 360s and 30s, respectively. Average T_{evap}/T_{cond} recorded 35/40°C. Longer t_{sw} (30-45s) found sensitive to SDWP (5% reduction) and insensitive to GOR (0.4% reduction). Coiled condenser found suitable for lab-scale models as compared to fined tubes due to its blockage. 						
2021	ES+M	2	FAM-Z01	80	25	20	8.13	0.41	0.43	59.56	Woo et al. [51]
			FAM-Z02				10.27	0.40	0.40	75.87	
			FAM-Z05				7.89	0.47	0.49	58.33	
<ul style="list-style-type: none"> The cited study investigated FAM-Z series for ADCS in a manner of determining their adsorption equilibrium profiles and conduct its modeling using Modified Do-Do and hybrid Langmuir-Sips isotherm models. 				<ul style="list-style-type: none"> Step adsorption isotherms of FAM-Z series adsorbents were recorded. $t_{h-cycle}$ opted 636s. 							

						<ul style="list-style-type: none"> The study experimentally investigates the performance of FAM-Z series adsorbents using pilot scale ADCS installed in Hanyang University, Republic of Korea. 	<ul style="list-style-type: none"> FAM-Z01 is more appealing for T_{hw-in} range between 54-74°C comparative to FAM-Z02. FAM-Z02 found more optimistic in terms of SDWP compared to FAM-Z01 and FAM-Z05. FAM-Z05 is promising adsorbent for ADCS because it allows the system to operate below at 55°C. 			
2021	M+Sim	2	Al-Fumarate	70-50	25	20	2.35	0.70	N/A	185**
			RD-SG				1.8	0.74		160**
						<ul style="list-style-type: none"> The cited study aimed to investigate feasibility of the solar thermal driven ADCS using Al-Fumarate as an adsorbent. Overall system performance was explored corresponding to meteorological conditions. In addition, the effect of fin spacing was explored on the system productivity. 	<ul style="list-style-type: none"> The optimum $t_{h-cycle}$ for Al-Fumarate found 900 s, whereas 600 s are sufficient for RD-SG. The step shape adsorption isotherm of Al-Fumarate decrease the total number of desalination cycles per day. Optimum fin spacing observed 0.5 mm, further increment significantly reduces the throughput capacity, due to lag in maintaining requisite thermal inventories in adsorbent bed. In conclusion Al-Fumarate outperform comparative to conventional RD-SG. 	Elsheniti et al. [167]		

*Gross output ratio

**W/kg

MOFs triggers the performance of the ADS at higher levels due to its prominent features such as tunable structure design, high pore volume, entail with high adsorption capacity [168]. In this context a wide range of MOFs are available to configure with ADS. However, so far, few reputed MOFs such as CPO-27(Ni), MIL-100(Fe), MIL-101(Cr), and Al-Fumarate were investigated for ADS/ADCS. The CPO-27(Ni) was reported as an alternative adsorbent for ADCS [162,169] and produce SDWP of 23 m³/ton/d. Similarly, MIL-100(Fe) and MIL-101(Cr) outperforms from the conventional SG due to their water holding potential at high adsorption pressures [73,80]. The Al-Fumarate increases SDWP ~29% as compared to conventional SG due to its porous nature [73,79,170]. The amalgamation of graphene oxide with MOFs improves ~12% water holding capacity and significantly improves the thermal stability [80]. Whereas MIL-101(Cr) binding with CaCl₂ mounting the fractional uptake up to 2.174 kg/kg [171]. In addition, the hydro-thermal instability of the MOFs needs to be addressed by integrating with the emerging binders that strength its structure and ensure its durability [171–173].

From relevant literature review of adsorbent substitution approach, it has been realized that, for ADS/ADCS, very few MOFs adsorbents are investigated so far. Therefore, massive avenue of research gap available in this category that allows the researchers to investigate wide range of MOFs, determine their adsorption equilibrium profiles, and explore their thermodynamic behavior in accordance with the specific operating conditions. MOFs typically required high T_{reg} to desorb the water vapors from the adsorbent material which reflects a massive waste scavenging potential from the condenser that could improve the thermal efficiency. In addition, other adsorbents such as covalent organic frameworks (COFs), covalent triazine frameworks (CTF), porous organic polymers (POPs), carbon nanotubes (CNT) support ionic liquids (SIL) and composite adsorbents need to be explored from the perspectives of determining its feasibility for adsorption-based desalination. Furthermore, several heat and mass recovery schemes and multiple evaporator configuration are still needed to couple and explore their potential in the adsorbent substitution approach. For effective heat transfer between the HX and adsorbent material in the adsorption/desorption bed, synergy analysis needs to be conducted to identify the dead adsorbent spaces, and accordingly defines the fin spacing, and thickness of the adsorbents. The HXs coated with MOFs could be remarkable option that could further increase the COP. Due to employing MOF as an adsorbent media, MOFs integrated ADS/ADCS are expensive as compared to silica-gel based having same physical dimensions.

Thereby, cost-effective MOFs synthesis procedure to need to investigate that could be able to suppress the overall system capital and operation costs.

5. Factors affecting performance parameters

The performance of the ADS/ADCS are evaluated based on the SDWP, SCP and COP. The generalized relationships for measuring the performance of ADS are given by Eqs. (1)-(3), respectively:

$$SDWP = N \int_0^{t_{cycle}} \frac{Q_{cond}}{h_{fg}(T_{cond})M_{sg}} dt \quad (1)$$

$$SCP = \int_0^{t_{cycle}} \frac{Q_{evap}}{M_{sg}} dt \quad (2)$$

$$COP = \frac{Q_{evp}}{Q_{des}} \quad (3)$$

where, N is the number of operating cycles per day, Q_{cond} , Q_{evap} , and Q_{des} are the condensation energy, heat of evaporation, and amount of energy required to desorb the water vapors from the adsorbent material, respectively. Where M_{sg} is the mass of silica gel, h_{fg} is the latent heat of vaporization, t_{cycle} is the cycle time. The in-depth detail has been extensively available in literature. However, for this section, the influential parameters or rating conditions that substantially impacting the system productivity are discussed to explore the optimum operating regimes, that could be suitable for driving ADS/ADCS. The performance of the ADS/ADCS are super sensitive to T_{hw-in} , T_{evap} , T_{cond} , $t_{h-cycle}$ and seawater salinity. In this section, a generalized comparison is made by plotting the results of the relevant key performance indicators.

Fig. 32 shows the impact of T_{hw-in} on the SDWP and SCP in all pre-defined approaches. It can be analyzed that, higher T_{hw-in} is supportive for attaining maximum SDWP. It is because, high T_{hw-in} produce more hydrophobic conditions in adsorbent material which entails to desorb maximum water vapors from adsorbent material. In thermodynamic viewpoints it is not sustainable or energy efficient to operate ADS at higher temperatures, although it's scavenging low-grade waste heat. On the other hand, interconnecting of heat and mass recovery scheme not only upscaling the system productivity but also gives a noteworthy drop in regeneration temperature. A similar tendency has been found in hybrid configuration. However, it has been realized that the conventional ADS is not functional below 65 °C developed by the Wang and Ng. The optimum T_{hw-in} range for conventional ADS found between 75-85 °C in order to

acquire the maximum production with minimal compromising of COP. Similarly in case of heat and mass recovery approach, 2-bed integrated E-C capable to produce maximum SDWP even at 85 °C and capable to functionalize the system even at 50 °C. However, the experimental validation of integrated E-C device is still required. It is noteworthy that, all the heat and mass recovery approaches lacked to produce the cooling effect simultaneously except the dual stage multi evaporator and condenser configuration. The reason is that heat recovery schemes mainly increase the operating temperature of the evaporator, consequently high T_{ch-out} is produced which could not be utilized for air conditioning applications. In hybridization approach ejectors integrated configurations are compared. One can realized that, the COP of the all the configurations are very low from T_{hw-in} ranges between 45-55 °C, however can produce comparable SDWP with respect to conventional ADS. In adsorbent substitution the approach the effect of T_{hw-in} depends upon the type of the adsorbent employed in the adsorbent bed and correspondingly the COP values fluctuates.

Fig. 33 presents the impact of adsorption/desorption cycle ($t_{h-cycle}$) on system productivity. It has been observed that longer cycle time allows more time for adsorption/desorption. However, the gross impact on system productivity was diminished, due to decreasing the number of AD cycles per day. In addition, longer $t_{h-cycle}$ put adverse impact on COP, due to supplying energy for longer desorption period. On the other hand, shorter $t_{h-cycle}$ not favouring to achieve saturation limit of hydrophilic adsorbent. Thereby, diminishing the system productivity. A monotonical concave pattern has been observed in all approaches, having assorted optimum $t_{h-cycle}$ values which vary from configuration to configuration thus emphasizing the sensitivity of this influential parameters. Therefore, there is no deterministic $t_{h-cycle}$ value for ADS, one can adjust the optimistic values based on the configuration employed, conducting several experimentation and critical thinking/ analyzing output data. Also, machine learning algorithm (MLA) even found supportive to ascertain the requisite conditions. Approximately 70% enhancement in existing ADS/ADCS could be achieved by setting appropriate rating conditions [174].

Fig. 34 elucidate the impact of T_{evap} and T_{cond} on SDWP and SCP. It has been analyzed that high evaporator temperature increases seawater evaporation rate. Consequently, pressurized adsorption happen, entailing maximum SDWP and SCP. The T_{evap} below 20°C produce high-grade cooling whereas, T_{evap} above 25°C produce low-grade cooling [80,110,118,170]. Similarly, high T_{cond} drop the condensation rate. Therefore, low T_{cond} is more supportive to increase the SDWP. The concentration of saline in seawater is found insensitive to SDWP and

SCP as given in Fig. 35, thereby can be ignored [34,68]. Thus, rating conditions are supersensitive to key performance indicators. A hidden tradeoff among the cogeneration attributes of ADS is present which make the ADS sophisticated to operate. However, the optimistic values would be varied in a specified range as present in Fig. 32, Fig. 33, and Fig. 34 that can kind of benchmark for desalination facility optimization.

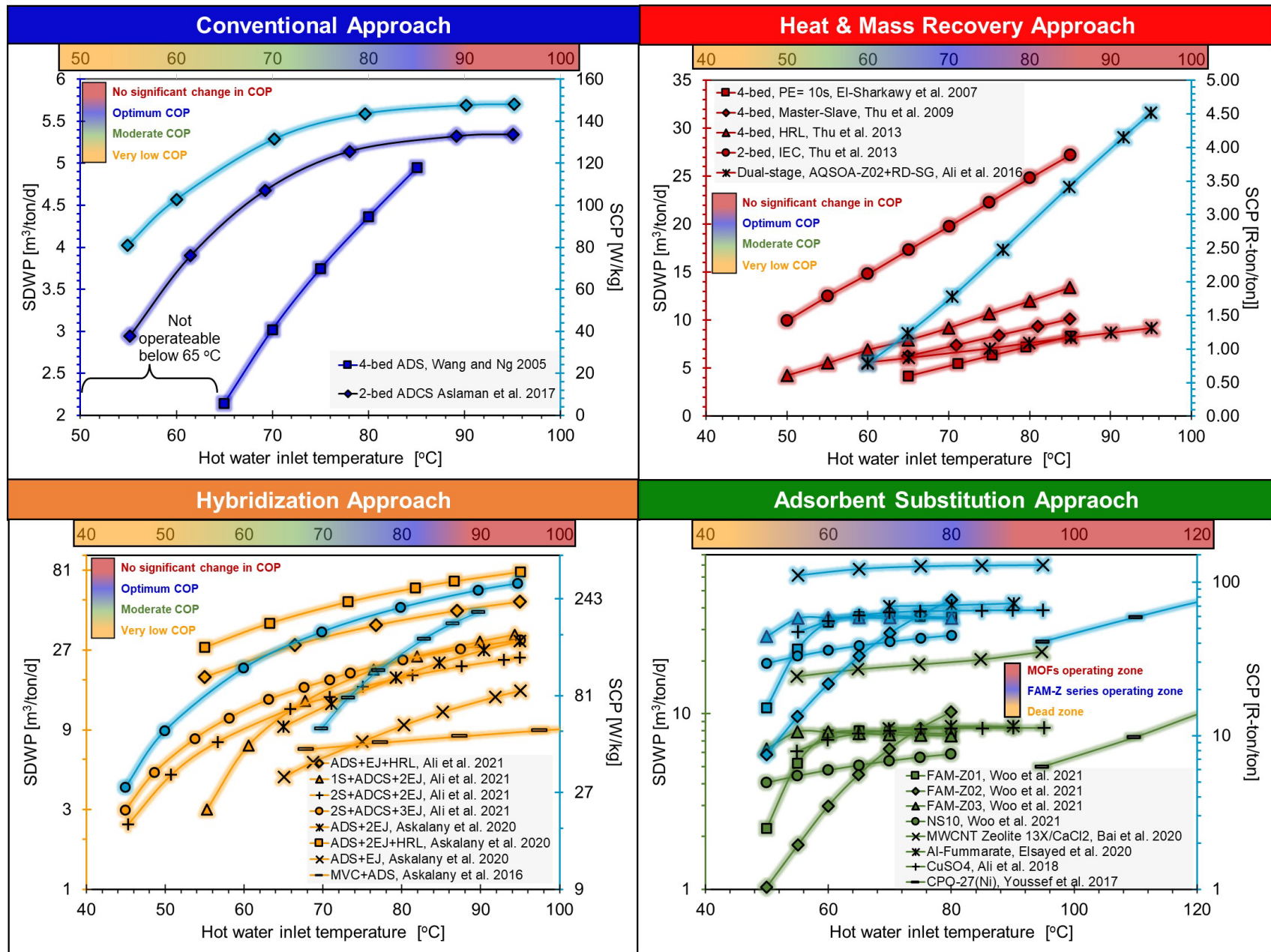


Fig. 32. Effect of hot water inlet temperature on SDWP and SCP reproduce here from the cited references.

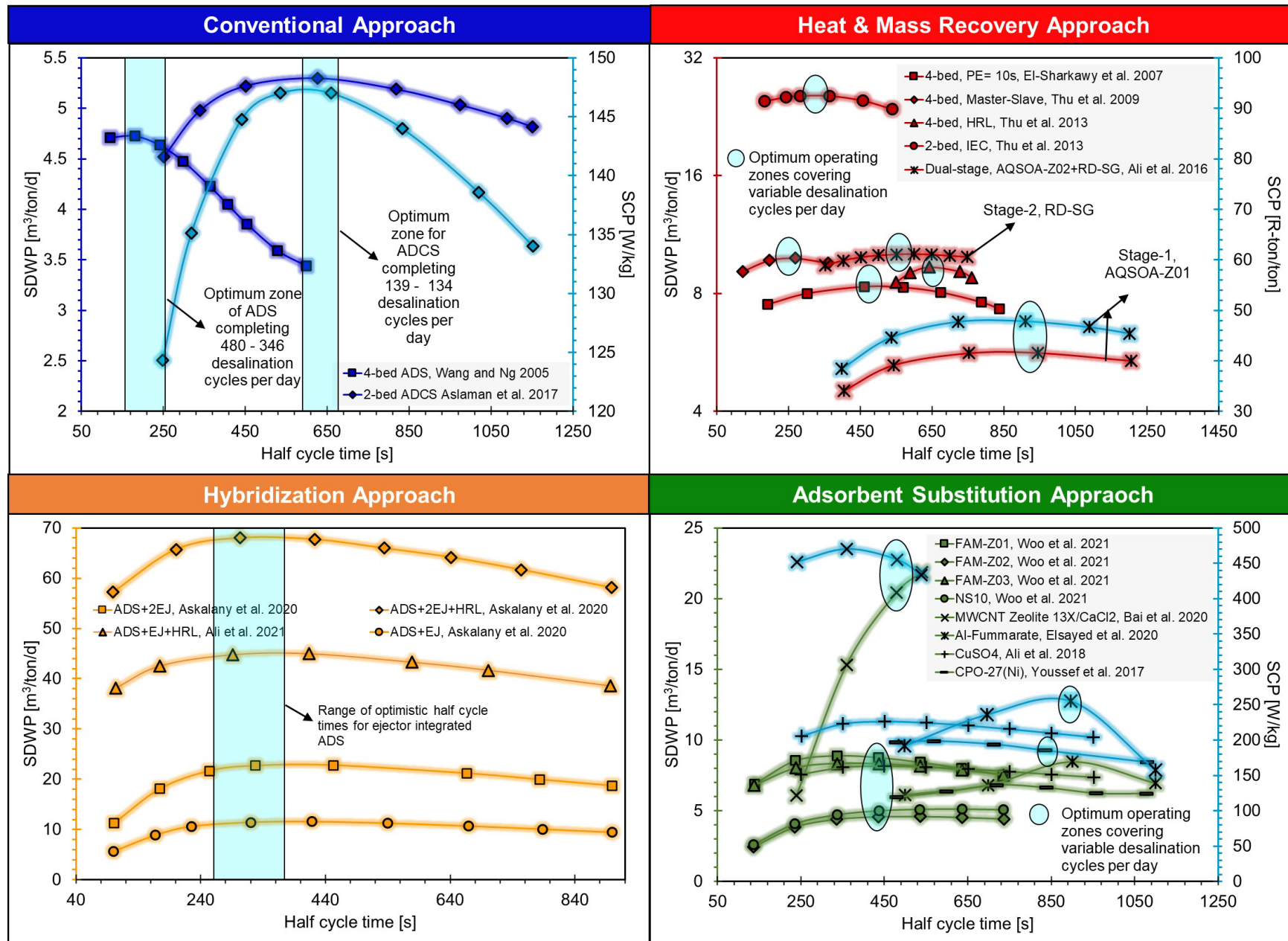


Fig. 33. Effect of cycle time/half cycle time of SDWP and SCP, reproduced here from the relevant previous publications.

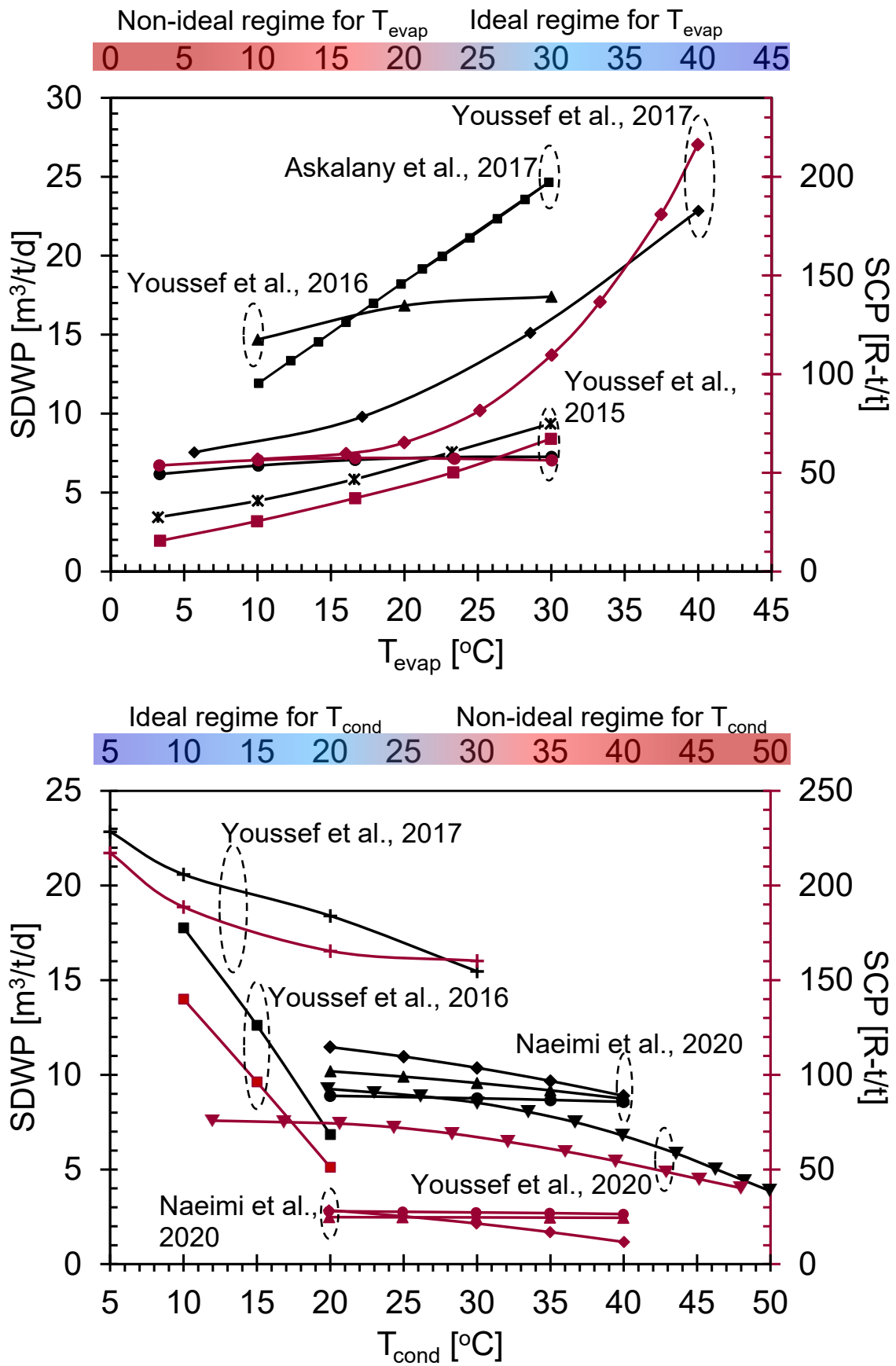


Fig. 34. Impact of evaporator and condenser temperature on SDWP and SCP, the data are reproduced from [80,110,118,170].

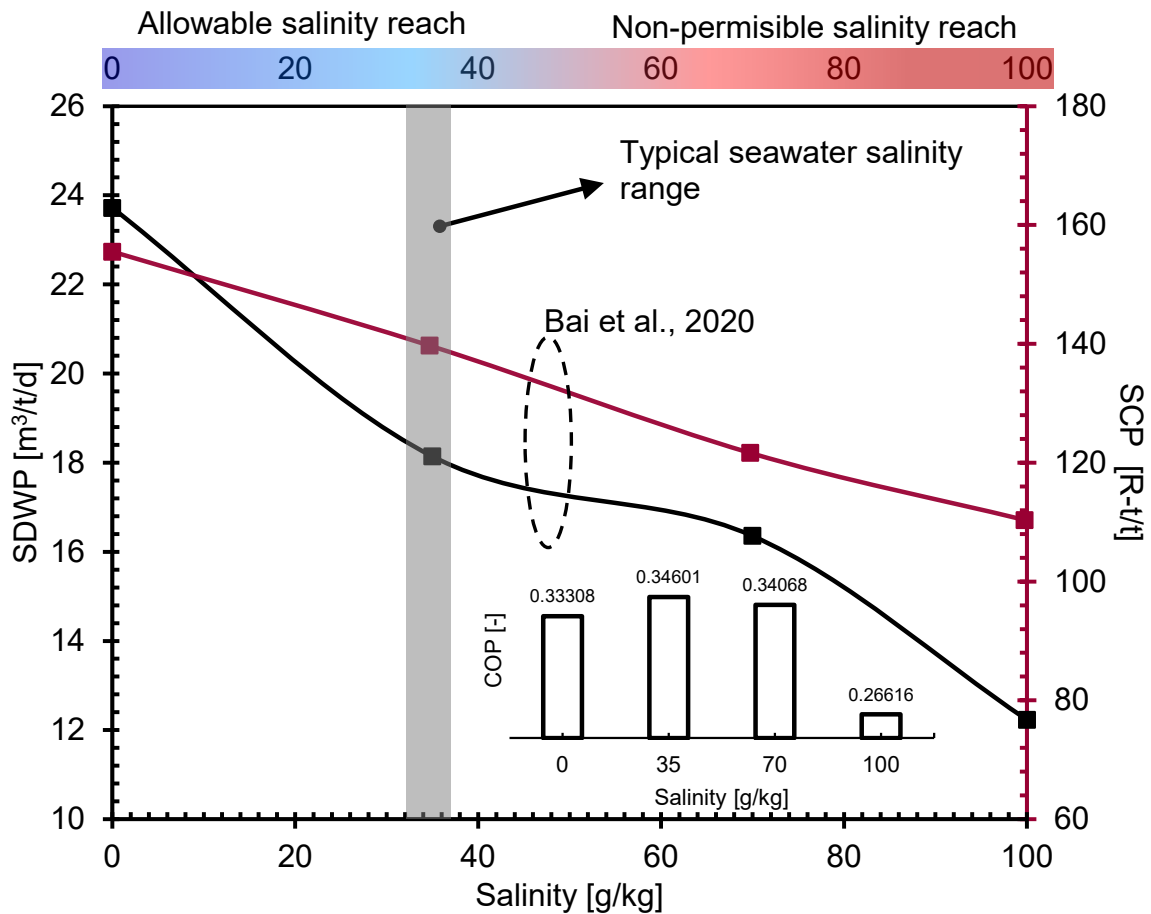


Fig. 35. Effect of salinity of SDWP, SCP and COP, the data are reproduced from [161].

The performance of the ADS/ADCS equipped with operational complexities and could be vary depending upon the type of the adsorbent and operating schemes. An intelligent optimization required in order to achieves the maximum throughput from the system. One can utilized the past experiences and contingent experiments of its own system in order to configure and drive the ADS/ADCS in the optimize state.

6. Market aspects, challenges and future perspectives

The desalination industry is intensifying with employing matured technologies. Globally more than 16,000 desalination facilities are being installed mainly employing MSF, MED, and RO modules [1,4]. It has been projected that, by the end of 2040, cumulative raise in primary energy consumption by the water sector would be manifested by two folds, occupying >75% contribution by the desalination industry [175]. The thermal energy consumed by MSF and MED were reported 69.44-83.33 kWh/m³ and 41.67-61.11 kWh/m³, while acquiring the desalination cost of 1.07 \$/m³ and 0.83 \$/m³, respectively [79,176]. Similarly, the RO

desalination mainly consumes electrical energy of 4-8 kWh/m³ by accounting desalination cost of 0.76 \$/m³ [177]. Few recent studies show a considerable reduction in the electrical energy used by RO systems (2.8 kWh/m³) due to advancements in membranes, however with a relatively poor recovery ratio.[178,179]. On the other hand, the non-payable thermal energy consumed by ADS was reported 39.8 kWh/m³ entail with payable electrical energy consumption varies between 0.92 to 1.38 kWh/m³ which significantly reduces the desalination cost even below 0.3 \$/m³ [30]. In addition, the water recovery ratio was identified >80% [30]. Despite of its promising aspects, the ADS are not well accepted in the desalination markets. The possible reasons may include: (i) non compactness in the system, (ii) requirement of additional water baths and run around circuits, (iii) non-continuous or batch process, (iv) slow adsorption/desorption cycles, and (v) low productivity as compared to other matured facilities. These issues/research gaps need to be address in order to develop a commercialized ADS.

Narrowing to technological advancements associated to ADS, some research gaps and future perspectives are indicated in the present work. Table 11 presents a qualitative scaling which focused to compare all the technological advancements based capital, and operational costs, thermal waste production, SDWP and SCP. In addition, future perspectives relevant to each classification are identified. To conclude it has been realized that the ADS, is a remarkable solution for the upcoming water challenges. However, so far, the technology is not mature and accomplished the standards of the technology readiness level [16]. Vast research avenue and contiguous efforts are still required which include efficient sizing of the evaporator and condenser, minimizing the heat and mass resistance between adsorber/desorber beds and heat exchangers, investigate the wide range of MOFs, COFs, CNT, and other potential adsorbents, and minimize the operational complexities by using smart controlling devices.

Table 11.

Cost comparison based on qualitative scaling for the technological advancements reported on ADS entail with future research perspectives.

ADS/ADCS classifications	Capital cost			Operational cost			Thermal waste production			SDWP			SCP			Future perspectives
	L	M	H	L	M	H	L	M	H	L	M	H	L	M	H	
Conventional Approach																
Conventional ADS/ADCS	x	x	✓	x	x	✓	x	x	✓	✓	x	x	✓	x	x	
Heat and Mass Recovery Approaches																
PE and VD scheme	x	✓	x	x	✓	x	x	✓	x	x	✓	x	✓	x	x	
Master-Slave scheme	x	x	✓	x	✓	x	x	✓	x	x	✓	x	✓	x	x	
HRL and Integrated E-C device	x	x	✓	x	✓	x	✓	x	x	x	✓	x	✓	x	x	
Dual-stage multi-evap. & cond.	x	x	✓	✓	x	x	✓	x	x	x	x	✓	x	✓	x	
Hybridization Approach																
MEDAD, RO+ADS, RO+MEDAD	x	x	✓	x	x	✓	✓	x	x	x	x	✓	x	✓	x	
ADS+EJs configurations	x	x	✓	x	✓	x	✓	x	x	x	x	✓	x	x	x	
Adsorbents Substituting Approaches																
MOFs integrated systems	x	x	✓	x	x	✓	x	x	✓	x	x	✓	x	✓	x	
FAM-Z series integrated systems	x	✓	x	x	✓	x	✓	x	x	x	✓	x	x	✓	x	

- Efficient designing/ sizing of evaporator and condenser is still required for ADS.
- Efforts are required to further minimize the heat & mass transfer resistances in the adsorbent bed.
- Need to identify the dead spaces and accordingly redesign adsorber reactor.
- Different types of heat exchangers need to employ and investigate for ADS.
- Optimize the thickness of an adsorbent layer on the heat exchangers.
- Experiments-based validation is required to explore the potential of ejector's integration with ADS.
- Reconsider the morphology of the adsorption/desorption layer specifically from the perspective of ADS.
- Investigate the wide range of MOFs, COFs, CTFs, POPs, CNT, SIL, and composite adsorbents

Note:- High (H), Moderate (M), and Low (L), ~The capital cost, and operational cost, are qualitatively compared based on the costs computed by the Thu et al. [180] for 10 R-ton/ton adsorption desalination plant.

7. Summary

Adsorption desalination is considered as a promising alternative to mitigate the water scarcity. Applicability and performance of the adsorption desalination system (ADS) are linked with nature of adsorbents, system design, operating conditions, and choice of low-grade thermal energy. Thereby, the present study aims to provide a state-of-the-art review on the recent developments of AD materials and system designs. The conventional (i.e., silica-gels and zeolites) and emerging adsorbents (i.e., metal-organic frameworks, MOFs) are investigated for their thermophysical properties and adsorption equilibrium/isotherms. Among the conventional adsorbents, the A⁺⁺ type silica-gel enables high porous properties (0.476-0.489 cm³/g), surface area (863.6 m²/g), and adsorption uptake (~0.45 kg/kg). Conversely, MOFs possess variety in structural layout, huge surface area, and high adsorption uptake. Comparing to conventional adsorbents, MOF of type MIL-101(Cr) possesses much higher adsorption equilibrium i.e., 1.45 kg/kg followed by MIL-100(Fe) (0.64 kg/kg), Al-Fumarate (0.56 kg/kg), and CPO-27(Ni) (0.47 kg/kg).

The study develops AD system classifications for the progressive modifications in the system designs from the viewpoint of conventional, heat/mass recovery, hybridization, and adsorbent substituting approaches. The conventional approach refers to silica-gel based AD system that produces specific daily water production (SDWP) of 4-4.7 m³/ton and low-grade cooling effect. The heat/mass recovery schemes refer to design modifications in conventional approach aiming to develop sustainable and energy-efficient AD system with high SDWP. For instance, pressure equalization and valve delay scheme has been applied for gaining ~5% additional adsorption/desorption of water-vapors on silica-gel and remove the thermal discrepancies which arises due to residency of coolant in piping circuit. Master-Slave configuration deduct ~50% heating/cooling requirements due to smart bed-operating mechanism. Evaporator-condenser amalgamation via heat recovery loop/ integrated vessel improvised the evaporator temperature/pressure from 30-42°C/9-12 kPa which led towards ~69% additional SDWP as compared to conventional approach, however with zero specific cooling power (SCP). Dual stage, multi evaporators/ condensers scheme employed multi evaporators/ condensers, operating at low and high pressures for acquiring cogenerating benefits from AD system. The scheme simultaneously produces SDWP of ~16 m³/ton/d and SCP of 47.8 R-ton/ton entail with a coefficient of performance (COP) of 0.53. The hybridization approach refers to the integration of commercialized multi-effect desalination

(MED) technology and/or individual components (i.e., ejectors and mechanical compressor) with AD system. The water production rate from MED+AD increases by 2.5-3 folds due to coupling of additional effects (ranges from 9-12 effects). The ejector integrated AD system produces SDWP of 80 m³/ton/d having COP of 2.22 by utilizing 0.92 kWh/m³ energy. The adsorbents substituting approach refers to the substitution adsorbent materials in contrast to the conventional silica-gels. The AD system coupled with CPO-27(Ni) produces SDWP and SCP of 23 m³/ton/d and 216 R-ton/ton, respectively. Similarly, MIL-100(Fe) produces additional 1.7 folds, and 3 folds SDWP and SCP compared to MIL-101(Cr) and AL-Fumarate, respectively. Ionogels produces SDWP of 25 m³/ton/d at regeneration temperature of 60°C and can be functional at ambient temperature.

Finally, the study analyzes the impact of influential factors i.e., hot water inlet temperature (T_{hw-in}), cycle time ($t_{h-cycle}/t_{cycle}$), evaporator temperature (T_{evap}), condenser temperature (T_{cond}) and seawater salinity affecting the performance of the AD system for all approaches and thereby explore the optimistic operating regimes. The T_{hw-in} found sensitive to the type of the approach and varied accordingly. For conventional approach, T_{hw-in} found between 75-85°C. The AD system coupled with heat and mass recovery approach found functional even below 55°C. In the hybridization approach, for instance MED+AD system and ejector integrated AD system found operative at T_{hw-in} of 20-35°C and 70-95°C, respectively. In adsorbents substituting approach, the T_{hw-in} depends upon the adsorbent type and can be varied between 80-150°C. It was analyzed that the maximum SDWP and SCP will be acquired at high T_{hw-in} despite of varying optimistic regimes. The COP of the AD system has been dramatically drops beyond the optimistic regimes. The $t_{h-cycle}/t_{cycle}$ found crucial to AD system designing aspects and manipulates the performance indicators accordingly. Shorter $t_{h-cycle}/t_{cycle}$ respond minimum SDWP due less water vapors uptake. Contrastingly, longer $t_{h-cycle}/t_{cycle}$ significantly reduces the number of desalination cycles per day. Thereby, optimum value needs to be selected appropriately by extensive experimentation. The T_{evap} and T_{cond} also influence the SDWP and SCP. High T_{evap} and low T_{cond} respond high evaporation rate and condensation rate, respectively. The optimistic operating regimes for T_{evap} found between 25-45°C, whereas as for T_{cond} it ranges between 5-20°C. The performance of AD system found unaffected by seawater salinity.

The performance of the AD system is limited in terms of producing SDWP and SCP. Possible future direction may include efficient designing/ sizing of evaporators/ condensers, minimizing the heat and mass transfer resistances in adsorber/desorber reactor, optimize the

thickness of the adsorbent layer in heat exchangers, and investigating wide range of adsorbent classes that can be driven with very low regeneration temperature.

CRedit authorship contribution statement

Hafiz M. Asfahan: Conceptualization, Methodology, Software, Formal analysis, Investigation, Writing - Original Draft. **Muhammad Sultan:** Conceptualization, Methodology, Validation, Resources, Writing - Original Draft, Visualization, Supervision, Project administration, Funding acquisition. **Takahiko Miyazaki:** Validation, Resources, Writing - Review & Editing, Supervision, Project administration. **Bidyut B. Saha:** Validation, Data Curation, Writing - Review & Editing, Visualization. **Ahmed A. Askalany:** Formal analysis, Validation, Writing - Review & Editing, Visualization. **Muhammad W. Shahzad:** Formal analysis, Validation, Writing - Review & Editing, Visualization. **William Worek:** Data Curation, Investigation, Validation, Writing - Review & Editing, Visualization.

Acknowledgements

This research was carried out in the Department of Agricultural Engineering, Bahauddin Zakariya University, Multan-Pakistan. The authors acknowledge the financial support from Bahauddin Zakariya University under the research grant of ORIC Project# 2020-21, awarded to Principal Investigator Dr. Muhammad Sultan.

Declaration of Competing Interest

The authors declare that they have no known competing financial interests or personal relationships that could have appeared to influence the work reported in this paper.

References

- [1] Connor R, Koncagül E. The United Nations World Water Development Report 2014: WATER AND ENERGY. vol. 1. 2014. <https://doi.org/10.46632/rmc/1>.
- [2] Miletto M. water and energy nexus: findings of the world water development report 2014. Proceedings of the International Association of Hydrological Sciences 2015;366:93–9.
- [3] Zapata-Sierra A, Cascajares M, Alcayde A, Manzano-Agugliaro F. Worldwide research trends on desalination. Desalination 2022;519:115305. <https://doi.org/10.1016/j.desal.2021.115305>.
- [4] UNESCO, UN-Water 2020. The United Nations World Water Development Report 2020: WATER AND CLIMATE CHANGE. Paris: 2020.

- [5] Gilbert F. Hounbo, Azoulay A. The United Nations World Water Development Report 2018: NATURE-BASED SOLUTIONS FOR WATER. 2018.
- [6] Shahzad MW, Burhan M, Ang L, Ng KC. Energy-water-environment nexus underpinning future desalination sustainability. *Desalination* 2017;413:52–64. <https://doi.org/10.1016/j.desal.2017.03.009>.
- [7] Boretti A, Rosa L. Reassessing the projections of the World Water Development Report. *NPJ Clean Water* 2019;2. <https://doi.org/10.1038/s41545-019-0039-9>.
- [8] Shahzad MW, Burhan M, Ang L, Ng KC. Energy-water-environment nexus underpinning future desalination sustainability. *Desalination* 2017. <https://doi.org/10.1016/j.desal.2017.03.009>.
- [9] United Nation. UN-Water Analytical Brief Unconventional Water Resources. 2020.
- [10] Dupont RR. *New Options for Water Desalination*. Water Resource Management Issues, CRC Press; 2019, p. 291–309.
- [11] Gassert F, Mandis M, Luck M, T. S. *Aqueduct Global Maps 2.1*. Washington, DC: World Resources Institute 2014. <http://www.wri.org/publication/aqueduct-metadata-global>.
- [12] Anand B, Shankar R, Murugavelh S, Rivera W, Midhun Prasad K, Nagarajan R. A review on solar photovoltaic thermal integrated desalination technologies. *Renewable and Sustainable Energy Reviews* 2021;141:110787. <https://doi.org/10.1016/j.rser.2021.110787>.
- [13] Curto D, Franzitta V, Guercio A. A review of the water desalination technologies. *Applied Sciences (Switzerland)* 2021;11:1–36. <https://doi.org/10.3390/app11020670>.
- [14] International Desalination Association n.d. <https://idadesal.org/> (accessed August 27, 2021).
- [15] Jones E, Qadir M, van Vliet MTH, Smakhtin V, Kang S. The state of desalination and brine production: A global outlook. *Science of the Total Environment* 2019;657:1343–56.
- [16] Alsaman AS, Askalany AA, Harby K, Ahmed MS. A state of the art of hybrid adsorption desalination-cooling systems. *Renewable and Sustainable Energy Reviews* 2016;58:692–703. <https://doi.org/10.1016/j.rser.2015.12.266>.
- [17] Fritzmann C, Löwenberg J, Wintgens T, Melin T. State-of-the-art of reverse osmosis desalination. *Desalination* 2007. <https://doi.org/10.1016/j.desal.2006.12.009>.
- [18] El-Dessouky HT, Ettouney HM. *Multi-Stage Flash Desalination*. Fundamentals of Salt Water Desalination, 2002. <https://doi.org/10.1016/b978-044450810-2/50008-7>.
- [19] El-Dessouky HT, Ettouney HM. Multiple-effect evaporation desalination systems: Thermal analysis. *Desalination*, 1999. [https://doi.org/10.1016/S0011-9164\(99\)00147-2](https://doi.org/10.1016/S0011-9164(99)00147-2).
- [20] Looney B. *Statistical Review of World Energy, 2020 | 69th Edition*. vol. 69. 2020.

- [21] Asif M. Sustainable energy options for Pakistan. *Renewable and Sustainable Energy Reviews* 2009;13:903–9. <https://doi.org/https://doi.org/10.1016/j.rser.2008.04.001>.
- [22] Mahmood MH, Sultan M, Miyazaki T, Koyama S, Maisotsenko VS. Overview of the Maisotsenko cycle – A way towards dew point evaporative cooling. *Renewable and Sustainable Energy Reviews* 2016. <https://doi.org/10.1016/j.rser.2016.08.022>.
- [23] Sultan M, Miyazaki T, Saha BB, Koyama S. Steady-state investigation of water vapor adsorption for thermally driven adsorption based greenhouse air-conditioning system. *Renew Energy* 2016;86:785–95. <https://doi.org/10.1016/j.renene.2015.09.015>.
- [24] Sultan M, Mahmood MH, Miyazaki T, Koyama S, Khan ZM. Close and open cycle adsorption kinetics: Development of correlation for desiccant air-conditioning. *Journal of Engineering and Applied Sciences* 2016;35:1–8.
- [25] Kalogirou SA. Seawater desalination using renewable energy sources. *Prog Energy Combust Sci* 2005. <https://doi.org/10.1016/j.pecs.2005.03.001>.
- [26] Amani M, Foroushani S, Sultan M, Bahrami M. Comprehensive review on dehumidification strategies for agricultural greenhouse applications. *Appl Therm Eng* 2020;181:115979. <https://doi.org/10.1016/J.APPLTHERMALENG.2020.115979>.
- [27] Sharon H, Reddy KS. A review of solar energy driven desalination technologies. *Renewable and Sustainable Energy Reviews* 2015;41:1080–118. <https://doi.org/https://doi.org/10.1016/j.rser.2014.09.002>.
- [28] Ng KC, Thu K, Oh SJ, Ang L, Shahzad MW, Ismail A Bin. Recent developments in thermally-driven seawater desalination: Energy efficiency improvement by hybridization of the MED and AD cycles. *Desalination* 2015;356:255–70. <https://doi.org/10.1016/j.desal.2014.10.025>.
- [29] Riaz N, Sultan M, Miyazaki T, Shahzad MW, Farooq M, Sajjad U, et al. A review of recent advances in adsorption desalination technologies. *International Communications in Heat and Mass Transfer* 2021;128:105594. <https://doi.org/10.1016/J.ICHEATMASSTRANSFER.2021.105594>.
- [30] Ng KC, Thu K, Kim Y, Chakraborty A, Amy G. Adsorption desalination: An emerging low-cost thermal desalination method. *Desalination* 2013;308:161–79. <https://doi.org/10.1016/j.desal.2012.07.030>.
- [31] Sultan M, El-Sharkawy II, Miyazaki T, Saha BB, Koyama S. An overview of solid desiccant dehumidification and air conditioning systems. *Renewable and Sustainable Energy Reviews* 2015;46:16–29. <https://doi.org/10.1016/j.rser.2015.02.038>.
- [32] Mohammed RH, Rezk A, Askalany A, Ali ES, Zohir AE, Sultan M, et al. Metal-organic frameworks in cooling and water desalination: Synthesis and application. *Renewable and Sustainable Energy Reviews* 2021;149:111362. <https://doi.org/10.1016/J.RSER.2021.111362>.
- [33] Aleem M, Hussain G, Sultan M, Miyazaki T, Mahmood MH, Sabir MI, et al. Experimental investigation of desiccant dehumidification cooling system for climatic

- conditions of multan (pakistan). *Energies* (Basel) 2020. <https://doi.org/10.3390/en13215530>.
- [34] Kim YD, Thu K, Masry ME, Ng KC. Water quality assessment of solar-assisted adsorption desalination cycle. *Desalination* 2014;344:144–51. <https://doi.org/10.1016/j.desal.2014.03.021>.
- [35] Hua WS, Xu HJ, Xie WH. Review on adsorption materials and system configurations of the adsorption desalination applications. *Appl Therm Eng* 2021:117958.
- [36] Qiu B, Gorgojo P, Fan X. Adsorption desalination: Advances in porous adsorbents. *中国化学工程学报* 2022;42:151–69.
- [37] Chauhan PR, Kaushik SC, Tyagi SK. Current status and technological advancements in adsorption refrigeration systems: A review. *Renewable and Sustainable Energy Reviews* 2022;154:111808.
- [38] Mohammed RH, Askalany AA. Productivity improvements of adsorption desalination systems. *Solar Desalination Technology*, Springer; 2019, p. 325–57.
- [39] Sultan M, El-Sharkawy II, Miyazaki T, Saha BB, Koyama S, Maruyama T, et al. Water vapor sorption kinetics of polymer based sorbents: Theory and experiments. *Appl Therm Eng* 2016. <https://doi.org/10.1016/j.applthermaleng.2016.05.192>.
- [40] Sultan M, Miyazaki T, Koyama S. Optimization of adsorption isotherm types for desiccant air-conditioning applications. *Renew Energy* 2018;121:441–50. <https://doi.org/10.1016/j.renene.2018.01.045>.
- [41] Ng KC, Thu K, Saha BB, Chakraborty A. Study on a waste heat-driven adsorption cooling cum desalination cycle. *International Journal of Refrigeration* 2012;35:685–93. <https://doi.org/10.1016/j.ijrefrig.2011.01.008>.
- [42] Thu K, Yanagi H, Saha BB, Ng KC. Performance analysis of a low-temperature waste heat-driven adsorption desalination prototype. *Int J Heat Mass Transf* 2013;65:662–9. <https://doi.org/10.1016/j.ijheatmasstransfer.2013.06.053>.
- [43] Shabir F, Sultan M, Miyazaki T, Saha BB, Askalany A, Ali I, et al. Recent updates on the adsorption capacities of adsorbent-adsorbate pairs for heat transformation applications. *Renewable and Sustainable Energy Reviews* 2020;119:109630. <https://doi.org/https://doi.org/10.1016/j.rser.2019.109630>.
- [44] Sultan M, Miyazaki T, Koyama S, Khan ZM. Performance evaluation of hydrophilic organic polymer sorbents for desiccant air-conditioning applications. *Adsorption Science & Technology* 2017;36:311–26. <https://doi.org/10.1177/0263617417692338>.
- [45] Sultan M, El-Sharkawy II, Miyazaki T, Saha BB, Koyama S, Maruyama T, et al. Insights of water vapor sorption onto polymer based sorbents. *Adsorption* 2015;21:205–15. <https://doi.org/10.1007/s10450-015-9663-y>.
- [46] Shabir F, Sultan M, Niaz EngrDrY, Ibrahim S, Feng Y, Bukke K, et al. Steady-State Investigation of Carbon-Based Adsorbent-Adsorbate Pairs for Heat Transformation Application. *Sustainability* 2020;12:7040. <https://doi.org/10.3390/su12177040>.

- [47] Hanif S, Sultan M, Miyazaki T. Effect of relative humidity on thermal conductivity of zeolite-based adsorbents: Theory and experiments. *Appl Therm Eng* 2019;150:11–8. <https://doi.org/10.1016/j.applthermaleng.2018.12.144>.
- [48] Alberti A, Armbruster T, Artioli G, Colella C, Galli E, Grice JD, et al. Recommended nomenclature for zeolite minerals: Report of the subcommittee on zeolites of the International Mineralogical Association, Commission on New Minerals and Mineral Names. *The Canadian Mineralogist* 1997;35:1571–606.
- [49] Fan W, Chakraborty A. Isosteric heat of adsorption at zero coverage for AQSOA-Z01/Z02/Z05 zeolites and water systems. *Microporous and Mesoporous Materials* 2018;260:201–7. <https://doi.org/https://doi.org/10.1016/j.micromeso.2017.10.039>.
- [50] Teo HWB, Chakraborty A, Han B. Water adsorption on CHA and AFI types zeolites: Modelling and investigation of adsorption chiller under static and dynamic conditions. *Appl Therm Eng* 2017;127:35–45. <https://doi.org/10.1016/J.APPLTHERMALENG.2017.08.014>.
- [51] Woo S-Y, Lee H-S, Kim J-S, Kim K-H, Ji H, Kim Y-D. Applicability assessment of functional adsorption zeolite materials in adsorption desalination cum cooling systems driven by low-grade heat source. *Chemical Engineering Journal* 2021:131375. <https://doi.org/10.1016/j.cej.2021.131375>.
- [52] Goldsworthy MJ. Measurements of water vapour sorption isotherms for RD silica gel, AQSOA-Z01, AQSOA-Z02, AQSOA-Z05 and CECA zeolite 3A. *Microporous and Mesoporous Materials* 2014;196:59–67. <https://doi.org/10.1016/J.MICROMESO.2014.04.046>.
- [53] Thu K, Saha BB, Chakraborty A, Chun WG, Ng KC. Study on an advanced adsorption desalination cycle with evaporator-condenser heat recovery circuit. *Int J Heat Mass Transf* 2011. <https://doi.org/10.1016/j.ijheatmasstransfer.2010.09.065>.
- [54] Sun B, Chakraborty A. Thermodynamic frameworks of adsorption kinetics modeling: Dynamic water uptakes on silica gel for adsorption cooling applications. *Energy* 2015;84:296–302. <https://doi.org/10.1016/j.energy.2015.02.101>.
- [55] Chua HT, Ng KC, Chakraborty A, Oo NM, Othman MA. Adsorption characteristics of silica gel + water systems. *J Chem Eng Data* 2002;47:1177–81. <https://doi.org/10.1021/je0255067>.
- [56] Wang X, Zimmermann W, Ng KC, Chakraborty A, Keller JU. INVESTIGATION ON THE ISOTHERM OF SILICA GEL+WATER SYSTEMS TG and volumetric methods. *J Therm Anal Calorim* 2004;76:659–69.
- [57] Mitra S, Thu K, Saha BB, Srinivasan K, Dutta P. Modeling study of two-stage, multi-bed air cooled silica gel + water adsorption cooling cum desalination system. *Appl Therm Eng* 2017;114:704–12. <https://doi.org/10.1016/j.applthermaleng.2016.12.011>.
- [58] Mitra S, Thu K, Baran B, Dutta P. Performance evaluation and determination of minimum desorption temperature of a two-stage air cooled silica gel/water adsorption system. *Appl Energy* 2017;206:507–18. <https://doi.org/10.1016/j.apenergy.2017.08.198>.

- [59] Wu JW, Biggs MJ, Pendleton P, Badalyan A, Hu EJ. Experimental implementation and validation of thermodynamic cycles of adsorption-based desalination. *Appl Energy* 2012;98:190–7. <https://doi.org/10.1016/j.apenergy.2012.03.022>.
- [60] Thu K, Ng KC, Saha BB, Chakraborty A, Koyama S. Operational strategy of adsorption desalination systems. *Int J Heat Mass Transf* 2009;52:1811–6. <https://doi.org/10.1016/j.ijheatmasstransfer.2008.10.012>.
- [61] Ali ES, Mohammed RH, Askalany A. A daily freshwater production of 50 m³/ton of silica gel using an adsorption-ejector combination powered by low-grade heat. *J Clean Prod* 2020:124494. <https://doi.org/10.1016/j.jclepro.2020.124494>.
- [62] Aristov YI, Tokarev MM, Freni A, Glaznev IS, Restuccia G. Kinetics of water adsorption on silica Fuji Davison RD. *Microporous and Mesoporous Materials* 2006;96:65–71. <https://doi.org/10.1016/j.micromeso.2006.06.008>.
- [63] Ma H, Zhang J, Liu C, Lin X, Sun Y. Experimental investigation on an adsorption desalination system with heat and mass recovery between adsorber and desorber beds. *Desalination* 2018;446:42–50. <https://doi.org/10.1016/j.desal.2018.08.022>.
- [64] Sapienza A, Velte A, Girnuk I, Frazzica A, Földner G, Schnabel L, et al. “Water - Silica Siogel” working pair for adsorption chillers: Adsorption equilibrium and dynamics. *Renew Energy* 2017;110:40–6. <https://doi.org/10.1016/J.RENENE.2016.09.065>.
- [65] Santori G, Frazzica A, Freni A, Galieni M, Bonaccorsi L, Polonara F, et al. Optimization and testing on an adsorption dishwasher. *Energy* 2013;50:170–6. <https://doi.org/10.1016/J.ENERGY.2012.11.031>.
- [66] Rezk A, Al-Dadah R, Mahmoud S, Elsayed A. Experimental investigation of metal organic frameworks characteristics for water adsorption chillers. *Proc Inst Mech Eng C J Mech Eng Sci* 2012;227:992–1005. <https://doi.org/10.1177/0954406212456469>.
- [67] Shi B, Al-Dadah R, Mahmoud S, Elsayed A, Elsayed E. CPO-27(Ni) metal-organic framework based adsorption system for automotive air conditioning. *Appl Therm Eng* 2016;106:325–33. <https://doi.org/10.1016/j.applthermaleng.2016.05.109>.
- [68] Woo S-Y, Lee H-S, Ji H, Moon D-S, Kim Y-D. Silica gel-based adsorption cooling cum desalination system: Focus on brine salinity, operating pressure, and its effect on performance. *Desalination* 2019;467:136–46. <https://doi.org/https://doi.org/10.1016/j.desal.2019.06.016>.
- [69] Alsaman AS, Askalany AA, Harby K, Ahmed MS. Performance evaluation of a solar-driven adsorption desalination-cooling system. *Energy* 2017;128:196–207. <https://doi.org/10.1016/j.energy.2017.04.010>.
- [70] Kim YD, Thu K, Ng KC. Adsorption characteristics of water vapor on ferroaluminophosphate for desalination cycle. *Desalination* 2014;344:350–6. <https://doi.org/10.1016/j.desal.2014.04.009>.

- [71] Youssef PG, Mahmoud SM, AL-Dadah RK. Performance analysis of four bed adsorption water desalination/refrigeration system, comparison of AQSOA-Z02 to silica-gel. *Desalination* 2015;375:100–7. <https://doi.org/10.1016/j.desal.2015.08.002>.
- [72] Moghadam PZ, Fairen-Jimenez D. Targeted classification of metal-organic frameworks in the Cambridge structural database (CSD). *Royal Society of Chemistry* 2020;11:8327–628. <https://doi.org/10.1039/d0sc01297a>.
- [73] Elsayed E, AL-Dadah R, Mahmoud S, Anderson PA, Elsayed A, Youssef PG. CPO-27(Ni), aluminium fumarate and MIL-101(Cr) MOF materials for adsorption water desalination. *Desalination* 2017;406:25–36. <https://doi.org/10.1016/j.desal.2016.07.030>.
- [74] Han X, Sun H, Liu L, Wang Y, He G, Li J. Improved desulfurization performance of polydimethylsiloxane membrane by incorporating metal organic framework CPO-27-Ni. *Sep Purif Technol* 2019;217. <https://doi.org/10.1016/j.seppur.2019.01.075>.
- [75] Zhang J, Sun L, Chen C, Liu M, Dong W, Guo W, et al. High performance humidity sensor based on metal organic framework MIL-101(Cr) nanoparticles. *J Alloys Compd* 2017;695:520–5. <https://doi.org/10.1016/j.jallcom.2016.11.129>.
- [76] Trung TK, Ramsahye NA, Trens P, Tanchoux N, Serre C, Fajula F, et al. Adsorption of C5-C9 hydrocarbons in microporous MOFs MIL-100(Cr) and MIL-101(Cr): A manometric study. *Microporous and Mesoporous Materials* 2010;134:134–40. <https://doi.org/10.1016/j.micromeso.2010.05.018>.
- [77] Rezk A, Al-Dadah R, Mahmoud S, Elsayed A. Characterisation of metal organic frameworks for adsorption cooling. *Int J Heat Mass Transf* 2012;55:7366–74. <https://doi.org/https://doi.org/10.1016/j.ijheatmasstransfer.2012.07.068>.
- [78] Fang Y, Yang Z, Li H, Liu X. MIL-100(Fe) and its derivatives: from synthesis to application for wastewater decontamination. *Environmental Science and Pollution Research* 2020;27:4703–24. <https://doi.org/10.1007/s11356-019-07318-w>.
- [79] Elsayed E, AL-Dadah R, Mahmoud S, Anderson P, Elsayed A. Experimental testing of aluminium fumarate MOF for adsorption desalination. *Desalination* 2020;475:114170. <https://doi.org/https://doi.org/10.1016/j.desal.2019.114170>.
- [80] AL-Dadah R, Mahmoud S, Elsayed E, Youssef P, Al-Mousawi F. Metal-organic framework materials for adsorption heat pumps. *Energy* 2020;190:116356. <https://doi.org/10.1016/j.energy.2019.116356>.
- [81] Shi B, Al-Dadah R, Mahmoud S, Elsayed A, Elsayed E. CPO-27(Ni) metal-organic framework based adsorption system for automotive air conditioning. *Appl Therm Eng* 2016;106:325–33. <https://doi.org/10.1016/j.applthermaleng.2016.05.109>.
- [82] Wang X, Ng KC. Experimental investigation of an adsorption desalination plant using low-temperature waste heat. *Appl Therm Eng* 2005;25:2780–9. <https://doi.org/10.1016/j.applthermaleng.2005.02.011>.
- [83] Ali ES, Harby K, Askalany AA, Diab MR, Alsaman AS. Weather effect on a solar powered hybrid adsorption desalination-cooling system: A case study of Egypt's

- climate. *Appl Therm Eng* 2017;124:663–72.
<https://doi.org/10.1016/j.applthermaleng.2017.06.048>.
- [84] Richter L. Seawater desalination process comprises using an adsorption exchanger in which water is adsorbed in a first phase and is then extracted in a second phase at higher pressure in a direct evaporator. *ICP C02F1/44*, July 2003;26.
- [85] Chua HT, Ng KC, Malek A, Kashiwagi T, Akisawa A, Saha BB. Multi-reactor regenerative adsorption chiller. Singapore Patent 1999.
- [86] Ng KC, Chu HT, Wang X. Prototype testing of a novel four-bed regenerative silica gel-water adsorption chiller. *International Congress of Refrigeration*, 2003, p. 0.
- [87] Wu JW, Hu EJ, Biggs MJ. Thermodynamic cycles of adsorption desalination system. *Appl Energy* 2012;90:316–22.
- [88] Wu JW, Biggs MJ, Hu EJ. Thermodynamic analysis of an adsorption-based desalination cycle. *Chemical Engineering Research and Design* 2010;88:1541–7.
<https://doi.org/10.1016/j.cherd.2010.04.004>.
- [89] Wu JW, Hu EJ, Biggs MJ. Thermodynamic analysis of an adsorption-based desalination cycle (part II): Effect of evaporator temperature on performance. *Chemical Engineering Research and Design* 2011;89:2168–75.
<https://doi.org/10.1016/j.cherd.2010.12.012>.
- [90] Wu JW, Biggs MJ, Hu EJ. Dynamic model for the optimisation of adsorption-based desalination processes. *Appl Therm Eng* 2014;66:464–73.
<https://doi.org/10.1016/j.applthermaleng.2014.02.045>.
- [91] Olkis C, Brandani S, Santori G. Design and experimental study of a small scale adsorption desalinator. *Appl Energy* 2019;253:113584.
<https://doi.org/10.1016/j.apenergy.2019.113584>.
- [92] Wang X, Chakarborty A, Ng KC, Saha BB. How heat and mass recovery strategies impact the performance of adsorption desalination plant: Theory and experiments. *Heat Transfer Engineering* 2007;28:147–53.
<https://doi.org/10.1080/01457630601023625>.
- [93] El-Sharkawy II, Thu K, Ng KC, Saha BB, Chakraborty A, Koyama S. Performance improvement of adsorption desalination plant: experimental investigation. *Int Rev Mech Eng* 2007;1:25–31.
- [94] Amirfakhraei A, Zarei T, Khorshidi J. Performance improvement of adsorption desalination system by applying mass and heat recovery processes. *Thermal Science and Engineering Progress* 2020;18:100516. <https://doi.org/10.1016/j.tsep.2020.100516>.
- [95] Ng KC, Wang X, Lim YS, Saha BB, Chakarborty A, Koyama S, et al. Experimental study on performance improvement of a four-bed adsorption chiller by using heat and mass recovery. *Int J Heat Mass Transf* 2006.
<https://doi.org/10.1016/j.ijheatmasstransfer.2006.01.053>.

- [96] Olkis C, AL-Hasni S, Brandani S, Vasta S, Santori G. Solar powered adsorption desalination for Northern and Southern Europe. *Energy* 2021;232:120942. <https://doi.org/10.1016/j.energy.2021.120942>.
- [97] Olkis C, Brandani S, Santori G. Cycle and performance analysis of a small-scale adsorption heat transformer for desalination and cooling applications. *Chemical Engineering Journal* 2019;378:122104. <https://doi.org/https://doi.org/10.1016/j.cej.2019.122104>.
- [98] Thu K, Yanagi H, Saha BB, Ng KC. Performance investigation on a 4-bed adsorption desalination cycle with internal heat recovery scheme. *Desalination* 2017;402:88–96. <https://doi.org/10.1016/j.desal.2016.09.027>.
- [99] Thu K, Kim YD, Myat A, Chakraborty A, Ng KC. Performance investigation of advanced adsorption desalination cycle with condenser-evaporator heat recovery scheme. *Desalination Water Treat* 2013;51:150–63. <https://doi.org/10.1080/19443994.2012.693659>.
- [100] Thu K, Chakraborty A, Kim Y-D, Myat A, Saha BB, Ng KC. Numerical simulation and performance investigation of an advanced adsorption desalination cycle. *Desalination* 2013;308:209–18. <https://doi.org/https://doi.org/10.1016/j.desal.2012.04.021>.
- [101] Alsaman AS, Ali ES, Harby K, Askalany AA, Ahmed MS. Performance Improvement of a Solar Driven Adsorption Desalination System By Heat Recovery Operation 2017:18–20.
- [102] Mitra S, Kumar P, Srinivasan K, Dutta P. Instrumentation and control of a two-stage 4-bed silica gel + water adsorption cooling cum desalination system. *Measurement (Lond)* 2016;79:29–43. <https://doi.org/10.1016/j.measurement.2015.10.014>.
- [103] Mitra S, Kumar P, Srinivasan K, Dutta P. Performance evaluation of a two-stage silica gel + water adsorption based cooling-cum-desalination system. *International Journal of Refrigeration* 2015;58:186–98. <https://doi.org/10.1016/j.ijrefrig.2015.06.018>.
- [104] Mitra S, Kumar P, Srinivasan K, Dutta P. Development and performance studies of an air cooled two-stage multi-bed silica-gel + water adsorption system. *International Journal of Refrigeration* 2016;67:174–89. <https://doi.org/10.1016/j.ijrefrig.2015.10.028>.
- [105] Mitra S, Kumar P, Srinivasan K, Dutta P. Simulation study of a two-stage adsorber system. *Appl Therm Eng* 2014;72:283–8. <https://doi.org/10.1016/j.applthermaleng.2014.04.023>.
- [106] Mitra S, Thu K, Saha BB, Dutta P. Modeling the Effect of Heat Source Temperature on the Performance of Two-stage Air Cooled Silica Gel + Water Adsorption System. *Energy Procedia* 2017;105:2010–5. <https://doi.org/10.1016/j.egypro.2017.03.575>.
- [107] Saha BB, Akisawa A, Kashiwagi T. Solar/waste heat driven two-stage adsorption chiller: The prototype. *Renew Energy* 2001;23:93–101. [https://doi.org/10.1016/S0960-1481\(00\)00107-5](https://doi.org/10.1016/S0960-1481(00)00107-5).

- [108] Saha BB, Akisawa A, Kashiwagi T. Silica gel water advanced adsorption refrigeration cycle. *Energy*, vol. 22, Elsevier Ltd; 1997, p. 437–47. [https://doi.org/10.1016/S0360-5442\(96\)00102-8](https://doi.org/10.1016/S0360-5442(96)00102-8).
- [109] Miyazaki T, Akisawa A, Saha BB, El-Sharkawy II, Chakraborty A. A new cycle time allocation for enhancing the performance of two-bed adsorption chillers. *International Journal of Refrigeration* 2009;32:846–53. <https://doi.org/10.1016/J.IJREFRIG.2008.12.002>.
- [110] Youssef PG, Mahmoud SM, AL-Dadah RK. Numerical simulation of combined adsorption desalination and cooling cycles with integrated evaporator/condenser. *Desalination* 2016;392:14–24. <https://doi.org/10.1016/j.desal.2016.04.011>.
- [111] Thu K, Kim YD, Myat A, Chun WG, Ng KC. Entropy generation analysis of an adsorption cooling cycle. *Int J Heat Mass Transf* 2013;60:143–55. <https://doi.org/10.1016/J.IJHEATMASSTRANSFER.2012.12.055>.
- [112] Chua HT, Ng KC, Malek A, Kashiwagi T, Akisawa A, Saha BB. Entropy generation analysis of two-bed, silica gel-water, non-regenerative adsorption chillers. *J Phys D Appl Phys* 1998;31:1471–7. <https://doi.org/10.1088/0022-3727/31/12/011>.
- [113] Ali SM, Chakraborty A. Adsorption assisted double stage cooling and desalination employing silica gel + water and AQSOA-Z02 + water systems. *Energy Convers Manag* 2016;117:193–205. <https://doi.org/10.1016/j.enconman.2016.03.007>.
- [114] Thu K, Saha BB, Chua KJ, Ng KC. Performance investigation of a waste heat-driven 3-bed 2-evaporator adsorption cycle for cooling and desalination. *Int J Heat Mass Transf* 2016;101:1111–22. <https://doi.org/10.1016/j.ijheatmasstransfer.2016.05.127>.
- [115] Ali SM, Haider P, Sidhu DS, Chakraborty A. Thermally driven adsorption cooling and desalination employing multi-bed dual-evaporator system. *Appl Therm Eng* 2016;106:1136–47. <https://doi.org/10.1016/j.applthermaleng.2016.06.045>.
- [116] Chakraborty A, Thu K, Saha BB, Ng C. Adsorption – Desalination Cycle 2013:377–451.
- [117] Ali ES, Askalany AA, Zohir AE. Innovative employing of salt hydration with adsorption to enhance performance of desalination and heat transformation systems. *Appl Therm Eng* 2020;179:115614. <https://doi.org/10.1016/j.applthermaleng.2020.115614>.
- [118] Naeimi A, Nowee SM, Akhlaghi Amiri HA. Numerical simulation and theoretical investigation of a multi-cycle dual-evaporator adsorption desalination and cooling system. *Chemical Engineering Research and Design* 2020;156:402–13. <https://doi.org/10.1016/j.cherd.2020.02.016>.
- [119] Chen Q, Thu K, Bui TD, Li Y, Ng KC, Chua KJ. Development of a model for spray evaporation based on droplet analysis. *Desalination* 2016;399:69–77. <https://doi.org/10.1016/J.DESAL.2016.08.017>.

- [120] Rezk ARM, Al-Dadah RK. Physical and operating conditions effects on silica gel/water adsorption chiller performance. *Appl Energy* 2012;89:142–9. <https://doi.org/10.1016/J.APENERGY.2010.11.021>.
- [121] Chen Q, M KJ, Li Y, Chua KJ. Experimental and mathematical study of the spray flash evaporation phenomena. *Appl Therm Eng* 2018;130:598–610. <https://doi.org/10.1016/J.APPLTHERMALENG.2017.11.018>.
- [122] Li M, Zhao Y, Long R, Liu Z, Liu W. Computational fluid dynamic study on adsorption-based desalination and cooling systems with stepwise porosity distribution. *Desalination* 2021;508:115048. <https://doi.org/10.1016/j.desal.2021.115048>.
- [123] Li M, Zhao Y, Long R, Liu Z, Liu W. Field synergy analysis for heat and mass transfer characteristics in adsorption-based desalination and cooling systems. *Desalination* 2021;517:115244. <https://doi.org/10.1016/j.desal.2021.115244>.
- [124] Albaik I, Al-Dadah R, Mahmoud S, Solmaz İ. Non-equilibrium numerical modelling of finned tube heat exchanger for adsorption desalination/cooling system using segregated solution approach. *Appl Therm Eng* 2021;183:116171. <https://doi.org/10.1016/j.applthermaleng.2020.116171>.
- [125] Thu K, Kim YD, Amy G, Chun WG, Ng KC. A hybrid multi-effect distillation and adsorption cycle. *Appl Energy* 2013;104:810–21. <https://doi.org/10.1016/j.apenergy.2012.12.007>.
- [126] Ophir A, Lokiec F. Advanced MED process for most economical sea water desalination. *Desalination* 2005;182:187–98.
- [127] Thu K, Kim YD, Amy G, Chun WG, Ng KC. A synergetic hybridization of adsorption cycle with the multi-effect distillation (MED). *Appl Therm Eng* 2014;62:245–55. <https://doi.org/10.1016/j.applthermaleng.2013.09.023>.
- [128] Shahzad MW, Ng KC. An Improved Multi-evaporator Adsorption Desalination Cycle for Gulf Cooperation Council Countries. *Energy Technology* 2017. <https://doi.org/10.1002/ente.201700061>.
- [129] Shahzad MW, Thu K, Saththasivam J, Chun WG, Ng KC. Waste heat operated hybrid (MEDAD) desalination plant: An experimental investigation. *ACRA 2014 - Proceedings of the 7th Asian Conference on Refrigeration and Air Conditioning, 2014*.
- [130] Shahzad MW, Ng KC, Thu K, Saha BB, Chun WG. Multi effect desalination and adsorption desalination (MEDAD): A hybrid desalination method. *Appl Therm Eng* 2014. <https://doi.org/10.1016/j.applthermaleng.2014.03.064>.
- [131] Shahzad MW, Thu K, Kim Y deuk, Ng KC. An experimental investigation on MEDAD hybrid desalination cycle. *Appl Energy* 2015. <https://doi.org/10.1016/j.apenergy.2015.03.062>.
- [132] Son HS, Shahzad MW, Ghaffour N, Ng KC. Pilot studies on synergetic impacts of energy utilization in hybrid desalination system: Multi-effect distillation and adsorption cycle (MED-AD). *Desalination* 2020;477:114266. <https://doi.org/10.1016/j.desal.2019.114266>.

- [133] Shahzad MW, Burhan M, Ng KC. Pushing desalination recovery to the maximum limit: Membrane and thermal processes integration. *Desalination* 2017. <https://doi.org/10.1016/j.desal.2017.04.024>.
- [134] Sarai Atab M, Smallbone AJ, Roskilly AP. A hybrid reverse osmosis/adsorption desalination plant for irrigation and drinking water. *Desalination* 2018;444:44–52. <https://doi.org/10.1016/j.desal.2018.07.008>.
- [135] Thu K, Kim YD, Shahzad MW, Saththasivam J, Ng KC. Performance investigation of an advanced multi-effect adsorption desalination (MEAD) cycle. *Appl Energy* 2015. <https://doi.org/10.1016/j.apenergy.2015.09.035>.
- [136] Ghenai C, Kabakebji D, Douba I, Yassin A. Performance analysis and optimization of hybrid multi-effect distillation adsorption desalination system powered with solar thermal energy for high salinity sea water. *Energy* 2021;215:119212. <https://doi.org/10.1016/j.energy.2020.119212>.
- [137] Thu K, Kim YD, Shahzad MW, Saththasivam J, Ng KC. Performance investigation of an advanced multi-effect adsorption desalination (MEAD) cycle. *Appl Energy* 2015;159:469–77. <https://doi.org/10.1016/j.apenergy.2015.09.035>.
- [138] Ng KC, Shahzad MW, Son HS, Hamed OA. An exergy approach to efficiency evaluation of desalination. *Appl Phys Lett* 2017;110:184101.
- [139] Ng KC, Shahzad MW. Sustainable desalination using ocean thermocline energy. *Renewable and Sustainable Energy Reviews* 2018;82:240–6. <https://doi.org/10.1016/j.rser.2017.08.087>.
- [140] Shahzad MW, Burhan M, Son HS, Oh SJ, Ng KC. Desalination processes evaluation at common platform: a universal performance ratio (UPR) method. *Appl Therm Eng* 2018;134:62–7.
- [141] Shahzad MW, Ng KC. An Improved Multi-Evaporator Adsorption Desalination Cycle for Gulf Cooperation Council Countries. *Energy Technology* 2017;5:1663–9. <https://doi.org/10.1002/ente.201700061>.
- [142] Shahzad MW, Ng KC. Sustainable Desalination Approach for GCC Region. Noor Publisher; 2017.
- [143] Askalany AA. Innovative mechanical vapor compression adsorption desalination (MVC-AD) system. *Appl Therm Eng* 2016;106:286–92. <https://doi.org/10.1016/j.applthermaleng.2016.05.144>.
- [144] Varga S, Lebre PS, Oliveira AC. Readdressing working fluid selection with a view to designing a variable geometry ejector. *International Journal of Low-Carbon Technologies* 2013. <https://doi.org/10.1093/ijlct/ctt026>.
- [145] Askalany AA, Ali ES. A new approach integration of ejector within adsorption desalination cycle reaching COP higher than one. *Sustainable Energy Technologies and Assessments* 2020;41:100766. <https://doi.org/10.1016/j.seta.2020.100766>.

- [146] Sanaye S, Emadi M, Refahi A. Thermal and economic modeling and optimization of a novel combined ejector refrigeration cycle. *International Journal of Refrigeration* 2019. <https://doi.org/10.1016/j.ijrefrig.2018.11.007>.
- [147] Dai Y, Wang J, Gao L. Exergy analysis, parametric analysis and optimization for a novel combined power and ejector refrigeration cycle. *Appl Therm Eng* 2009;29:1983–90. <https://doi.org/10.1016/J.APPLTHERMALENG.2008.09.016>.
- [148] Saito Y, Ito T, Matsuo A, Sato H. Ejector configuration for designing a simple and high performance solar cooling system. *Energy Procedia*, 2014. <https://doi.org/10.1016/j.egypro.2014.10.267>.
- [149] Vincenzo L, Mads Pagh N, Søren Knudsen K. Ejector design and performance evaluation for recirculation of anode gas in a micro combined heat and power systems based on solid oxide fuel cell. *Appl Therm Eng* 2013. <https://doi.org/10.1016/j.applthermaleng.2013.01.021>.
- [150] Ali ES, Asfahan HM, Sultan M, Askalany AA. A novel ejectors integration with two-stages adsorption desalination: A way to scavenge the ambient energy. *Sustainable Energy Technologies and Assessments* 2021;48:101658.
- [151] Askalany A, Ali ES, Mohammed RH. A novel cycle for adsorption desalination system with two stages-ejector for higher water production and efficiency. *Desalination* 2020;496:114753. <https://doi.org/10.1016/j.desal.2020.114753>.
- [152] Kakiuchi H, Shimooka S, Iwade M, Oshima K, Yamazaki M, Terada S, et al. Novel water vapor adsorbent FAM-Z01 and its applicability to an adsorption heat pump. *Kagaku Kogaku Ronbunshu* 2005;31:361–4.
- [153] Youssef PG, Mahmoud SM, Al-Dadah RK. Effect of evaporator temperature on the performance of water desalination/refrigeration adsorption system using AQSOA-ZO2. *World Academy of Science, Engineering and Technology, International Journal of Environmental, Chemical, Ecological, Geological and Geophysical Engineering* 2015;9:701–5.
- [154] Teo HWB, Chakraborty A, Fan W. Improved adsorption characteristics data for AQSOA types zeolites and water systems under static and dynamic conditions. *Microporous and Mesoporous Materials* 2017;242:109–17.
- [155] Kayal S, Baichuan S, Saha BB. Adsorption characteristics of AQSOA zeolites and water for adsorption a. *Int J Heat Mass Transf* 2016;92:1120–7. <https://doi.org/10.1016/J.IJHEATMASSTRANSFER.2015.09.060>.
- [156] Li A, Ismail A Bin, Thu K, Ng KC, Loh WS. Performance evaluation of a zeolite–water adsorption chiller with entropy analysis of thermodynamic insight. *Appl Energy* 2014;130:702–11. <https://doi.org/10.1016/J.APENERGY.2014.01.086>.
- [157] He Z, Bai Y, Huang H, Li J, Huhetaoli, Kobayashi N, et al. Study on the performance of compact adsorption chiller with vapor valves. *Appl Therm Eng* 2017;126:37–42. <https://doi.org/10.1016/J.APPLTHERMALENG.2017.07.130>.

- [158] Kayal S, Baichuan S, Saha BB. Adsorption characteristics of AQSOA zeolites and water for adsorption chillers. *Int J Heat Mass Transf* 2016;92:1120–7. <https://doi.org/https://doi.org/10.1016/j.ijheatmasstransfer.2015.09.060>.
- [159] Han B, Chakraborty A. Water adsorption studies on synthesized alkali-ions doped Al-fumarate MOFs and Al-fumarate + zeolite composites for higher water uptakes and faster kinetics. *Microporous and Mesoporous Materials* 2019;288:109590. <https://doi.org/10.1016/j.micromeso.2019.109590>.
- [160] Askalany A, Alsaman AS, Ghazy M, Mohammed RH, AL-Dadah R, Mahmoud S. Experimental optimization of the cycle time and switching time of a metal organic framework adsorption desalination cycle. *Energy Convers Manag* 2021;245:114558. <https://doi.org/10.1016/j.enconman.2021.114558>.
- [161] Bai S, Ho TC, Ha J, An AK, Tso CY. Study of the salinity effects on the cooling and desalination performance of an adsorption cooling cum desalination system with a novel composite adsorbent. *Appl Therm Eng* 2020;181:115879. <https://doi.org/https://doi.org/10.1016/j.applthermaleng.2020.115879>.
- [162] Youssef PG, Dakkama H, Mahmoud SM, AL-Dadah RK. Experimental investigation of adsorption water desalination/cooling system using CPO-27Ni MOF. *Desalination* 2017;404:192–9. <https://doi.org/10.1016/j.desal.2016.11.008>.
- [163] Ali ES, Askalany AA, Harby K, Diab MR, Alsaman AS. Adsorption desalination-cooling system employing copper sulfate driven by low grade heat sources. *Appl Therm Eng* 2018;136:169–76. <https://doi.org/10.1016/j.applthermaleng.2018.03.014>.
- [164] Askalany A, Olkis C, Bramanti E, Lapshin D, Calabrese L, Proverbio E, et al. Silica-Supported Ionic Liquids for Heat-Powered Sorption Desalination. *ACS Appl Mater Interfaces* 2019;11:36497–505. <https://doi.org/10.1021/acsami.9b07602>.
- [165] Olkis C, Dong H, Brandani S, Santori G. Ionogels at the Water-Energy Nexus for Desalination Powered by Ultralow-Grade Heat. *Environ Sci Technol* 2020;54:3591–8. <https://doi.org/10.1021/acs.est.9b06037>.
- [166] Dong H, Askalany AA, Olkis C, Zhao J, Santori G. Hydrothermal stability of water sorption ionogels. *Energy* 2019;189:116186. <https://doi.org/10.1016/j.energy.2019.116186>.
- [167] Elsheniti MB, Rezk A, Shaaban M, Roshdy M, Nagib YM, Elsamni OA, et al. Performance of a solar adsorption cooling and desalination system using aluminum fumarate and silica gel. *Appl Therm Eng* 2021;194:117116. <https://doi.org/10.1016/j.applthermaleng.2021.117116>.
- [168] Li H, Eddaoudi M, O’Keeffe M, Yaghi OM. Design and synthesis of an exceptionally stable and highly porous metal-organic framework. *Nature* 1999;402:276–9. <https://doi.org/10.1038/46248>.
- [169] Dakkama HJ, Youssef PG, Al-Dadah RK, Mahmoud S. Adsorption ice making and water desalination system using metal organic frameworks/water pair. *Energy Convers Manag* 2017;142:53–61. <https://doi.org/10.1016/j.enconman.2017.03.036>.

- [170] Youssef P, Mahmoud S, Al-Dadah R, Elsayed E, El-Samni O. Numerical Investigation of Aluminum Fumarate MOF adsorbent material for adsorption desalination/cooling application. *Energy Procedia* 2017;142:1693–8. <https://doi.org/10.1016/j.egypro.2017.12.551>.
- [171] Elsayed E, Anderson P, AL-Dadah R, Mahmoud S, Elsayed A. MIL-101(Cr)/calcium chloride composites for enhanced adsorption cooling and water desalination. *J Solid State Chem* 2019;277:123–32. <https://doi.org/10.1016/j.jssc.2019.05.026>.
- [172] Yang J, Zhao Q, Li J, Dong J. Synthesis of metal-organic framework MIL-101 in TMAOH-Cr(NO₃)₃-H₂BDC-H₂O and its hydrogen-storage behavior. *Microporous and Mesoporous Materials* 2010;130:174–9. <https://doi.org/10.1016/j.micromeso.2009.11.001>.
- [173] Elsayed E, AL-Dadah R, Mahmoud S, Anderson P, Elsayed A. Adsorption cooling system employing novel MIL-101(Cr)/CaCl₂ composites: Numerical study. *International Journal of Refrigeration* 2019;107:246–61. <https://doi.org/10.1016/j.ijrefrig.2019.08.004>.
- [174] Rezk H, Alsaman AS, Al-Dhaifallah M, Askalany AA, Abdelkareem MA, Nassef AM. Identifying optimal operating conditions of solar-driven silica gel based adsorption desalination cooling system via modern optimization. *Solar Energy* 2019;181:475–89. <https://doi.org/10.1016/j.solener.2019.02.024>.
- [175] Zarzo D, Prats D. Desalination and energy consumption. What can we expect in the near future? *Desalination* 2018;427:1–9.
- [176] Mezher T, Fath H, Abbas Z, Khaled A. Techno-economic assessment and environmental impacts of desalination technologies. *Desalination* 2011;266:263–73.
- [177] Gude VG. Desalination and sustainability—an appraisal and current perspective. *Water Res* 2016;89:87–106.
- [178] Atab MS, Smallbone AJ, Roskilly AP. An operational and economic study of a reverse osmosis desalination system for potable water and land irrigation. *Desalination* 2016;397:174–84.
- [179] Edalat A, Hoek EMV. Techno-Economic analysis of RO desalination of produced water for beneficial reuse in California. *Water (Switzerland)* 2020;12. <https://doi.org/10.3390/W12071850>.
- [180] Thu K. Adsorption desalination: theory & experiments 2010.